

POLITECNICO DI TORINO

Facoltà di Ingegneria

**Corso di Laurea Magistrale
in Ingegneria Meccanica**

Tesi di Laurea Magistrale

**Techno-economic analysis of solar-PV-battery
systems for the residential sector in Scotland**



Relatori

Prof. Marco Carlo Masoero

Prof. Michele Angelo Pastorelli

Dr. Edward Owens

Candidato

Alessandro Cristofaro

Anno Accademico 2017-2018

To my mother and my father

To my sister Ludovica

To my cousin Genny

Acknowledgements

I would like to express my gratitude to Prof. Marco Carlo Masoero of the Energy Department of the Polytechnic University of Turin, for giving me the opportunity to live a unique life experience abroad in a beautiful country like Scotland.

I would like to thank Prof. Michele Pastorelli for the didactic support and for the huge availability during all the didactic talks.

I would like to thank my external supervisor, Dr. Edward Owens, for choosing me among all the candidates to do this work of thesis in Edinburgh and for welcoming me to Heriot-Watt University.

I would like to thank Dr. Andrew Peacock for leading me during my stay at Heriot-Watt University and for accepting all my teaching needs.

I would like to thank Dr. Giulio Cerino Abdin for giving me all the support necessary to conclude in the best possible way what has been done in Scotland, showing a lot of patience and competence.

I thank all my friends, especially Giuseppe, Antonio, Demetrio, Emanuele, Vittorio, Gianmarco, Manuel, Vincenzo, Luca, Chiara, Beatrice, Silvia, Assunta, who represent a second family for me.

I thank my friends Angelo, Raffaele, Manuel, Domenico and Emilio not only as great friends but also and mostly for helping me during my thesis work, even when my needs became claims.

The most grateful thanks is for my family and especially to my beloved parents and to my sister Ludovica to whom I dedicate this work of thesis. Their support and their closeness has never been interrupted, even in my moments of greatest difficulty. Because there is no support greater than that received by the most important people in their lives.

Finally I dedicate a sweet thought to my cousin Genny, with the awareness that living in the heart of those who remain means never dying.

Contents

1. INTRODUCTION.....	5
2. REVIEW OF STATE OF THE ART AND EXISTING KNOWLEDGE.....	6
3. METODOLOGY.....	22
4. PRESENTATION OF DATA.....	26
4.1 Associated weather	26
4.2 PV generation	28
4.3 Household demand	30
5. DATA MODELING.....	37
5.1 Solar-PV system.....	37
5.1.1 Fintry Sports and Recreation Club	41
5.1.2 PVUSA model	44
5.1.3 Critical issues	49
5.1.4 Assignment of the PV system size.....	55
5.1.5 Results	62
5.2 Solar-PV-battery system	68
5.2.1 Battery model	71
5.2.2 Assignment of battery size	78
5.2.3 Choice of the battery	81
5.2.4 Results	84
6. ECONOMIC ANALYSIS	91
6.1 Market Review	91
6.2 Results.....	96
7. CONCLUSIONS.....	112

8. REFERENCES.....	123
9. WEBSITES.....	128

1. INTRODUCTION

The work in question concerns a technical and economic analysis of photovoltaic systems and PV-battery systems in the residential context of a village in central-northern Scotland. In particular, a photovoltaic system and a PV-battery system were assigned to each village house considering the input data related to the energy consumption of the previous year.

Knowing the climatic data of Fintry for the year 2017 and the power data produced by a 50 kWp photovoltaic system of a sports center of the village, a regression model was applied from which the regression coefficients were obtained for this system.

Using the same regression model it was possible to assign a photovoltaic system to each of the houses considered and obtain a dataset of the demand, net of the energy produced by the photovoltaic panels.

Subsequently, a battery was selected to be combined with the PV systems assigned to each house and a battery model was constructed to obtain a demand dataset in case a part of the excess energy produced by the PV system is stored and used. when the panels are not able to generate energy.

Finally, an economic analysis was conducted to evaluate the payback of the systems considered and to find out if the investments are convenient based on the costs and energy tariffs in Scotland.

2. REVIEW OF STATE OF THE ART AND EXISTING KNOWLEDGE

Today, the majority of the world's energy is produced by burning fossil fuels such as petroleum, coal and methane. At the same time, global energy demand is growing steadily, so it is necessary to cope with their possible shortage. Moreover, it is now established that excessive use of fossil fuels creates harmful pollutant gases for the entire environment.

An important classification of energy is given by the subdivision into renewable energies, that is, those forms of energy that have the ability to regenerate in relatively short time and non-renewable energies.

However, renewable energies are not all the same and are therefore split into traditional renewable energies (such as hydroelectric power) and new renewable energies (including wind power, biomass, solar photovoltaic energy, solar energy thermal, tide energy, geothermal and hydroelectric micro-systems).

The focus of this paper is on the analysis of the latter. Wind energy is the mechanical energy that can be obtained from the kinetic energy of moving air particles and can be used directly as such or transformed to generate electricity. There are several ways to exploit wind energy, some ancient and now obsolete and other more modern and advanced. An example might be sailing, an ancient navigational system that exploits the kinetic energy of the wind to travel through the seas; or the windmill, the most representative element of this type of energy, who used the wind energy to activate a grinder. Nowadays, a wind turbine system is characterized by a support pole, which must be capable of being high enough to absorb better the kinetic energy of the wind, a rotating blade system and a rotor connected to a dynamo transforming mechanical energy into electricity.

Solar energy is the energy produced by the sun's rays that can be captured and transformed into thermal and electrical energy. It is obviously a source of inexhaustible energy in relation to man's life: the power with which the Sun radiates our planet is about 174000 million gigawatts, some of which is reflected and an absorbed part (<http://www.enea.it/it/seguici/le-parole-dellenergia/radiazione-solare/quanta-energia-solare-arriva-sulla-terra>). This type of energy is considered inexhaustible as it does not decrease over time in terms of flow, so in theory it is the perfect energy type in terms of respect for the environment, renewability and economic savings.

Geothermal energy is the thermal energy derived from the Earth's core. It is well-known since ancient times that it digs deeper and the Earth's temperature rises: examples that confirm all this are volcanoes, thermal springs, fumaroles and other surface phenomena of this type. Earth, therefore, thanks to the natural nuclear decay processes of natural radioactive elements such as uranium, thorium and potassium, is used as a heat engine that can feed a heat stream from its core, whose temperature is around to 6000 °C, to the outside (<http://www.esrf.eu/news/general/Earth-Center-Hotter>). In fact, the geothermal gradient varies from area to area: there are in fact areas where the gradient is far greater than its average value. This type of energy, if evaluated in a short time, can be considered alternative and renewable.

Biomass refers to a set of biological origin materials such as agricultural waste, wood, marine algae or vegetable waste, which can be modified to generate fuels or directly from electrical and thermal energy. This technology, therefore, uses vegeta-

ble of vegetable or organic origin to run an electric power generator. It is considered a renewable energy source because fuel can be produced from short-term crops and green because the carbon dioxide produced by the combustion of biomass is balanced by the carbon dioxide absorbed by the plantations during the period of growth (Andreotti et al., 2010).

The development and implementation of so-called new renewable energies is indispensable for the EU to achieve two main objectives: reducing dependence on oil and reducing greenhouse gas (GHG) emissions. Abdallah et al. (2013) state that about 40% of the global CO₂ emissions are emitted by the thermoelectric power systems, whose production is through the transformation of thermal energy generated by combustion of fossils in mechanical energy thanks to the motion of the turbine blades, the latter then transformed into electricity by an alternator. The authors report worrying data for the year 2010, with CO₂ emissions of 30 Gt, of which 12 Gt generated exclusively from the fossil fuel power generation sector.

The increase in CO₂ concentration in the atmosphere over the last two centuries has already caused a significant increase in the average temperature of the planet, and this can lead to other catastrophic consequences such as rising sea levels, droughts, floods, intense storms, forest fires, cardiovascular diseases, but also the progressive melting of polar ice, a gradual collapse of the Amazon Forest, acidification of the oceans and other irreversible climate change (Abdallah et al., 2013).

The EU has decided to stem this harsh environmental pollution phenomenon, aiming to reduce 80-95% of CO₂ emissions by 2050, given that the most polluting sectors are in descending order of responsibility, the electricity production sector, the transport sector and industry (Seixas et al., 2015)

As mentioned, the diffusion of new renewable energies, and in particular wind and photovoltaics, is steadily growing.

However, this growth is limited and conditioned by the main problem related to these types of energy: intermittent generation. This intermittent characteristic is mainly due to the weather, weather conditions, cloud motion and wind speed, and this is why they are still considered not reliable enough when they are to be integrated into the power grid.

The real challenge for the future is to search solutions that can smooth the fluctuation of output power from intermittent sources, in order to increase the presence of these renewable energies within the power grid. Shivashankar et al. (2016) state that by the end of 2014, RES (Renewable Energetic Sources) contributed 22,8% to world electricity generation and PV capacity installed increased by 27% between 2013 and 2014 (Fig 2.1).

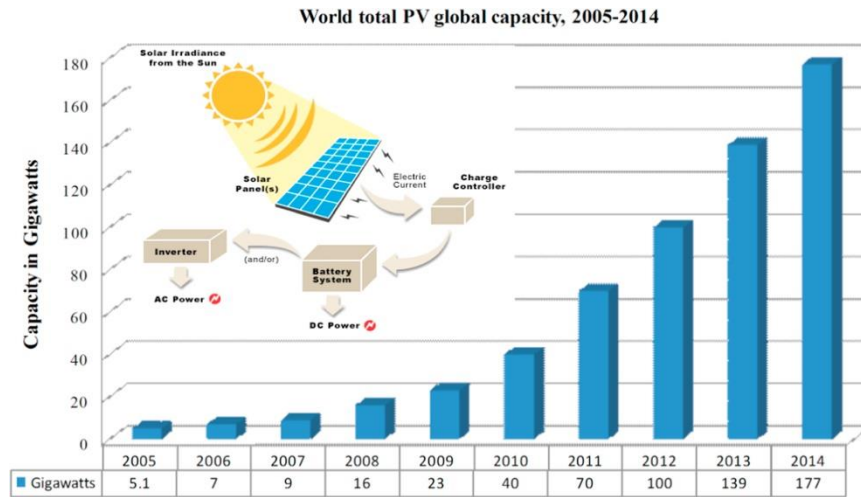


Fig 2.1: Global PV capacity between 2005-2014 (Shivashankar et al., 2016).

Nowadays, PV is one of the first sources of renewable energy in order of importance and use, second only to hydroelectric and wind energy. The amount of electricity that can be produced by PV is directly proportional to the intensity of sunlight, so a photovoltaic system can produce electricity according to the solar cycle, both daily and annually. This implies that more energy may be produced at certain times and may be defective in others.

It is therefore necessary to make a prediction of solar radiation, which can be obtained by mathematical models based on the artificial neural network (ANN), or by regression models, empirical regression models, empirical coefficient models, angstrom model and models based on fuzzy logic (Shivashankar et al., 2016).

The difficulty of performing accurate solar radiation forecasts and the intermittent characteristic of this source of energy hinder the full penetration of PV into the power grid.

The main limits of PV penetration within the power grid emerge in the form of voltage and disequilibrium variations, current and voltage harmonics and other power quality issues, such as flicker and stress on the distribution transformer. These impacts can be summarized as either steady-state or dynamic in nature: voltage fluctuation in feeder, consist of voltage rise or fall and unbalanced voltage; malfunction operation of voltage regulation equipment such as on load tap changer, line voltage regulators and capacitor banks; possibility of overload in distribution feeders; variation of reactive power flow due to malfunction operation of capacitor bank devices; malfunction operation of overcurrent and overvoltage protection devices; islanding operation and islanding detection in case of grid disconnection; reliability and security of the distribution system (Karimi et al., 2016).

One of the main causes of the fluctuation of output power in PV reported in the same document is the movement of the clouds. The problems arising from it are different: when PV penetration increases, it is not easy for conventional generators in the system to track the quick change in PV generation; when PV output power changes rapidly, the area control error of two more interconnected areas may exceed its prescribed limit; large uncontrolled PV penetration may change dispatch of regulating units in the utility causing a violation in dispatch regulating margins; frequent

changes in PV output caused by changes in cloud pattern increases overall operating cost of the system (Shivashankar et al., 2016).

Fig 2.2 (Denholm et al., 2007) shows the options for using the photovoltaic solar generation in excess. Here is explained that the amount of PV generated energy is subtracted from the normal load, with any generation that reduces the load so as to make it smaller compared to the minimum overload load considered and discarded by the system. In the case considered by the authors, the photovoltaic system provides 8% of the annual load of the system and the minimum load is set at 35% of the annual peak demand, corresponding to a 65% flexibility factor. The dark area represents generation of surplus PV.

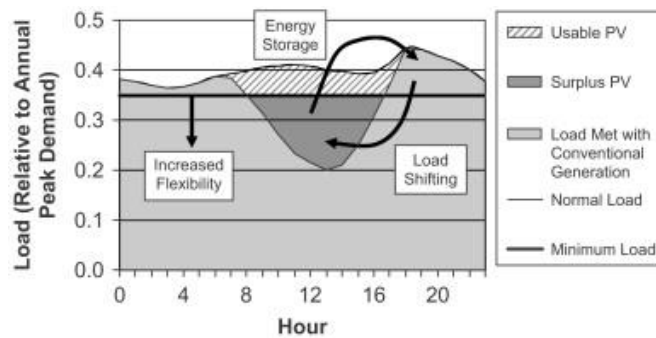


Fig 2.2: Options for using surplus solar PV generation (Denholm et al., 2007).

As a result, problems related to a hypothetical high PV penetration can be multiple: voltage fluctuations in grid, increased voltage and reverse power flow, power fluctuation in grid, frequency variation, and various grounding issues. In addition, PV penetration in low voltage distribution network also causes harmonic distortion in current and voltage waveforms (Shivashankar et al., 2016).

Voltage fluctuation compared to the prescribed value represents one of the most common problems as any power injection in a distribution system causes a voltage increase at the connection point and locally in the surrounding network. Rising the penetration generates an inverse flow in the distribution network, which also induces an increase of the voltage level to the substation: when a PV group is connected to the low voltage distribution network, the voltage increases with the reverse power flow from the intermittent source to the substation. When the voltage increases, it is necessary to limit the output power, and in the extreme case, disconnect the intermittent power source from the network (Shivashankar et al., 2016). Fig 2.3 (Shivashankar et al., 2016) shows how “the voltage across the distribution line decreases from the sub-station until it reaches the point of PV connection”: it suddenly increases at points A and B until it reaches the limit value, which is why at points C and D the PVs are disconnected.

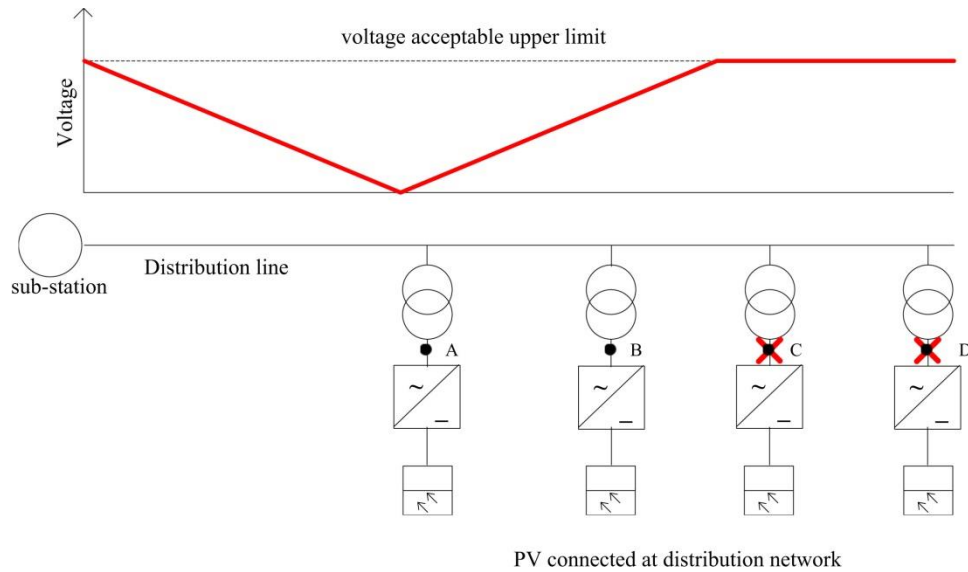


Fig 2.3: Problem of voltage rise at distribution network (Shivashankar et al., 2016).

A study carried out by Thomson et al. (2017) shows how the increase in voltage depends on PV penetration levels. The authors have found that as with a 50% PV penetration, the voltage has risen up to 5V on low voltage (LV) distribution network in both summer and winter season at midday with 50% PV penetration which exceeds the limitation of 250 V; however, decreasing penetration to 30% increase in voltage is limited proportionally.

Shivashankar et al. (2016) explain that reverse power generation can also create other issues about voltage rise in distribution feeder, protection desensitization and potential break of protection synchronization, increase of short circuit current which tends to reach harmful level.

Another issue related to PV intermittence is voltage flicker due to the movement of the clouds, particularly as shown in Fig 2.4 (Shivashankar et al., 2016).

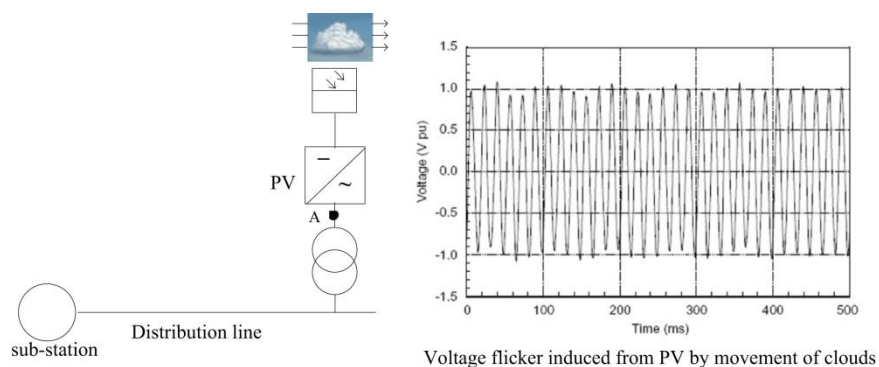


Fig 2.4: Problem of cloud induced voltage flicker (Shivashankar et al., 2016).

On the other hand, unintentional islanding “occurs when a fault occurs in distribution level, during which the power generated from PV is equal to load demand. The power interruption from the grid side cannot be sensed by the PV system and PV continues to generate power to the load. However for safety concerns PV system has

to stop generating power. This state is called Unintentional Islanding” (Shivashankar et al., 2016).

Frequency variation is another possible dangerous consequence of the continuous fluctuation of output power from PV. During grid interconnection frequency must be kept constant: it can be adjusted by installing energy storage devices. Currently the frequency deviation due to PV penetration is lower than wind turbines since the installed capacity of wind units is higher than PV (Shivashankar et al., 2016).

Ultimately, PV output fluctuations can not be predicted. However, there are methods used to limit fluctuations.

Denholm et al. (2007) discuss three general methods to increase the utility of excess PV generation. The first concerns more flexibility, that is to reduce the system's minimum to get more normal PV load. In a previous study by the same authors (Denholm et al., 2007), the low flexibility of traditional electrical systems potentially limited the penetration of intermittent renewable energies. Fig 2.5 (Denholm et al., 2007) shows a load duration curve for Electric Reliability Council of Texas (ERCOT) for the year 2000.

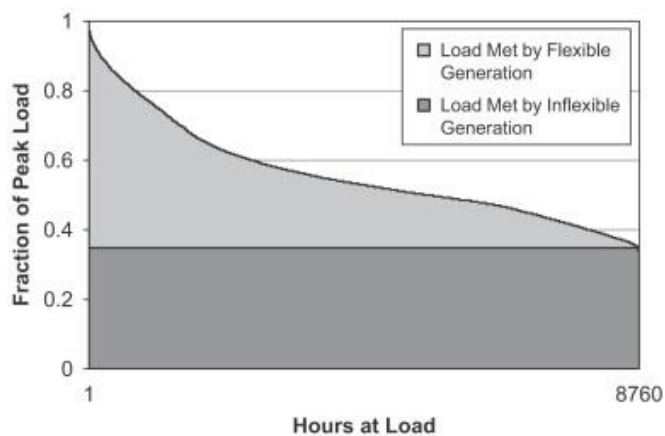


Fig 2.5: Load duration curve for the ERCOT system in 2000 (Denholm et al., 2007).

The second method described relates shifting normal load to times of greater PV output. Peak-load shifting is the process of mitigating the effects of large energy load blocks during a period of time by advancing or delaying their effects until the power supply system can readily accept additional load. The traditional intent behind this process is to minimize generation capacity requirements by regulating load flow (https://m.csemag.com/index.php?id=9575&tx_ttnews%5Btt_news%5D=117807&cHash=95b3d2a5db6725428142c5a605ac6d89).

The third and last method concerns energy storage technologies, that is storing solar generated electricity and releasing this stored energy at times of reduced or zero solar output.

Shivashankar et al. (2016) discuss widely a number of methods of resolving intermittent generation problems. One of these is the reduction of energy fluctuation by geographical dispersion. This method is normally used to “mitigate short-term output power fluctuations for PV clusters installed in wide area”. It is also observed that the

protection issue caused by large PV penetration can also be solved by dispersing PV generation. Fig 2.6 (Shivashankar et al., 2016) shows the location of six geographically dispersed photovoltaic systems over 1000 square kilometres in Spain on the left (a), and their outputs on the right (b).

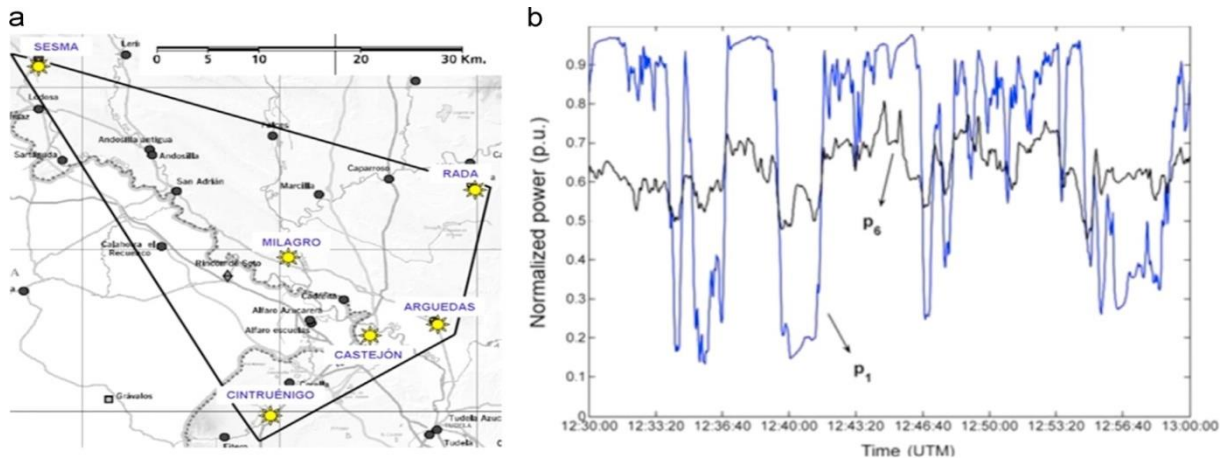


Fig 2.6: (a) Six PV systems geographically spread over 1000 km², (b) Output power from Cintruenigo, PV system (P1) and combined output of six PV systems (P6) (Shivashankar et al., 2016).

From this study emerged that smoothing depends on the pooling of photovoltaic installations and the corresponding distance between them.

In this study is also cited the output of one hundred PVs distributed in Germany studied to calculate the long-term stability and predictability of the dispersed photovoltaic energy generation. The result was positive in smoothing power fluctuations, while short-term fluctuations remained roughly unchanged. In conclusion, the decrease in the number of photovoltaic systems increases the instability of the output power.

Hoff et al. (2010) introduced a model to calculate the output variability of PV group by computing the standard deviation of change in fleet output power, relative output variability and dispersion factor (the fleet computation is valid but difficult to implement practically since the multiple system calculation involves heavy mathematical calculations and insufficient data on solar irradiance). In conclusion, increased dispersion reduces variability indicated by standard deviation and Pearson correlation coefficient analysis.

Energy storage represents perhaps the ultimate solution to the problem of intermittent generation. Storage devices help to accomplish one or more important tasks such as smoothing power fluctuation, shifting peak generation period, protection during outages when installed along with large PV generation.

An example of storage technology is battery. A battery is a genuine electrochemical accumulator that allows you to store a good amount of excess energy during the most hours of sunlight, and then reuse it for the needs during the night.

Battery energy storage (BES) is characterized by the presence of a series and parallel connected battery system that produces the required power for the application.

The operation of a battery-powered photovoltaic system consists in taking away from the rays the energy required to power the electrical loads in self-consumption, while the excess energy that is not used is accumulated by the battery to be exploited later.

Energy storage in BES occurs through an electrochemical process and also have quick response in charging and discharging mode (<http://www.energyhunters.it/content/sistemi-di-accumulo-di-energia-elettrica-%E2%80%93-classificazione-caratteristiche-vantaggi-e-svanta>). There are many types of batteries used for BES applications, such as flooded lead acid (LA) batteries, valve regulated lead acid (VRLA) batteries, nickel cadmium (NiCd) batteries, lithium ion (Li-ion) batteries, sodium sulfur (NaS) batteries and vanadium redox (VRB) batteries (Shivashankar et al., 2016).

LA batteries are very much used in this area as they are very cheap and available on the market, although maintenance costs have increased. VRLAs are the best alternative because they do not need maintenance, the lifespan is longer than normal LA and achieves an efficiency of 70-80%. Sodium sulfide batteries, on the other hand, are used for large power applications. Fig 2.7 (Shivashankar et al., 2016) shows an PV and battery source connected through separate voltage source converter.

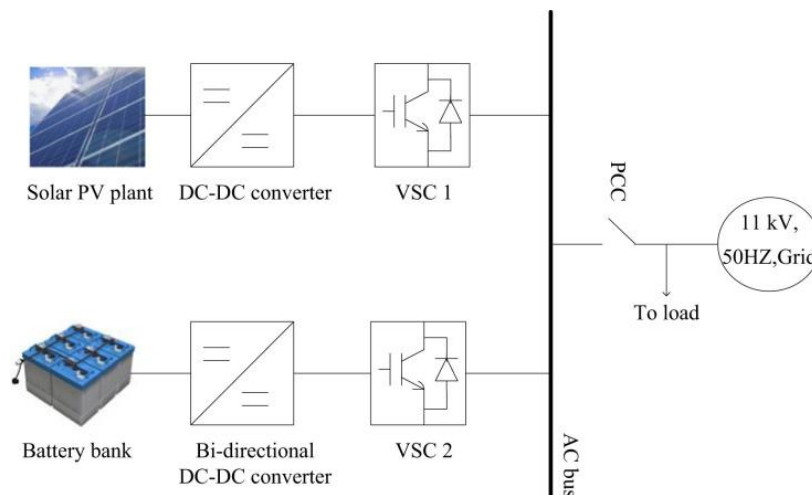


Fig 2.7: Battery station for smoothing PV output connected with grid (Shivashankar et al., 2016).

Shivashankar et al. (2016) affirm that the BES act as a centralized storage installed in distribution feeder since the control of battery in centralized storage is easy.

With regard to the implementation of BES technologies within the power grid, Hill et al. (2012) affirm that there are two possible ways to use, which share views on it. The first is to provide centralized storage at the MW level at the distribution substation; the second is to use smaller energy storage systems distributed on the distribution feeders, networked together and remotely controlled at the substation. The advantages of centralized storage are easy access to substation electrical and SCADA (Supervisory Control and Data acquisition) equipment, simplified control schemes, economies of scale, and the fact that there is already utility-owned land available behind the substation fence.

In summary, photovoltaic systems do not have inertial components and output power can change very quickly in relation to the quality of sunlight reception. It is the BES task to level the sudden output power variations to ensure a reasonable ramp rate (kW/min) value for the system operator (Shivashankar et al., 2016).

Another example of alternative battery storage technology is capacitors and superconductive magnetic energy storage (SMES).

The supercapacitors are a technology derived from that of the classic electrolytic capacitors, but unlike they have a higher capacity and therefore can store much more energy. A capacitor is generally an element consisting of two armatures called anode and cathode that can lead. An insulating material is inserted between them. As soon as a voltage is generated between the two armatures, the capacitor deposits electrically charged charges on the armor, thereby triggering the charging process (<http://www.energyhunters.it/content/sistemi-di-accumulo-di-energia-elettrica-%E2%80%93-classificazione-caratteristiche-vantaggi-e-svanta>).

SMES, or electromagnetic batteries, are devices capable of exploiting a particular property of the materials, which can be explained by quantum mechanics, called superconductivity. In practice, some materials have, among other properties, the ability to enter superconducting state when subjected to particular temperatures, usually close to absolute zero. The temperature under which each material enters the superconducting stage is known as the critical temperature. Below this temperature, the magnetic permeability and electrical resistance to the current flow of the material are reset (<http://www.energyhunters.it/content/sistemi-di-accumulo-di-energia-elettrica-%E2%80%93-classificazione-caratteristiche-vantaggi-e-svanta>).

The superconductors are able to control the ramp rate of the PV generators connected to the network by absorbing the power difference between PV and inverter output. The problem of voltage shake due to PV variation is mitigated by installing this kind of devices, as reported by Woyte et al. (2003). The use of SMES is effective in maintaining the value of the frequency within the limits set. The experimental results under various weather conditions discussed by Jung et al. (2009) show how SMES use better PV output.

A third example of storage technology is the diesel generator. However, Shivashankar et al. (2016) affirm that there are several difficulties regarding the use of such systems, in particular slow response during continuously changing PV and decrease in operational efficiency when it is made to run at low output levels during high level of oscillation in PV. In a paper Datta et al. (2011) developed a fuzzy controller for PV generator to control the frequency of a PV-diesel hybrid system. The PV generator controlled the output produced and effectively maintained the frequency deviation within ± 0.2 Hz. The results were satisfactory when compared with PV with MPPT (Maximum Power Point Tracking) control. The diesel generator acted as a backup source which will follow the changes caused by variation in PV output and load. Fig 2.8 (Shivashankar et al., 2016) shows a hybrid system of the diesel generator.

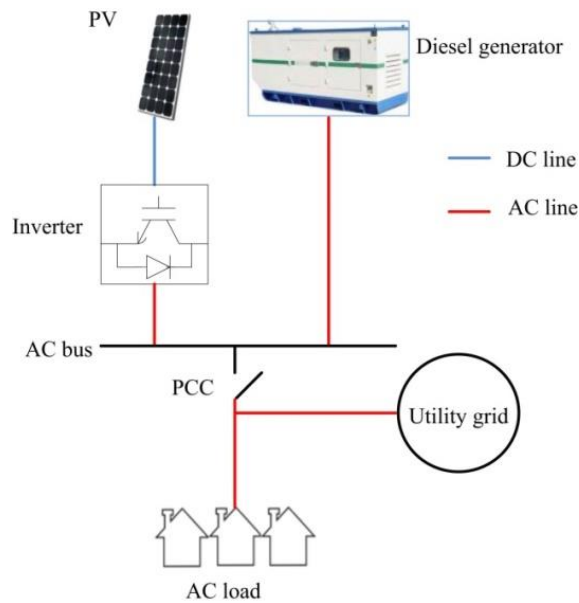


Fig 2.8: PV, diesel generator hybrid system (Shivashankar et al., 2016).

However, problems with previously mentioned diesel generators have driven users to focus on fast response technologies with greater operational flexibility, such as battery power buildup, capacitors, and fuel cell.

An additional example of storage technology is the fuel cell. They are electrochemical systems capable of converting chemical energy derived from a fuel (usually hydrogen) directly into electrical energy, without an intermediate transformation passage into thermal energy. This feature makes these elements free from the Carnot cycle limitations and allows high conversion returns. Other features that are causing its development are high reliability and low maintenance cost, fast response, and the ability to install fuel cells close to the car with noise and reduced missions (Ronchetti, 2008). Fig 2.9 (Shivashankar et al., 2016) shows a PV system connected to the fuel cell.

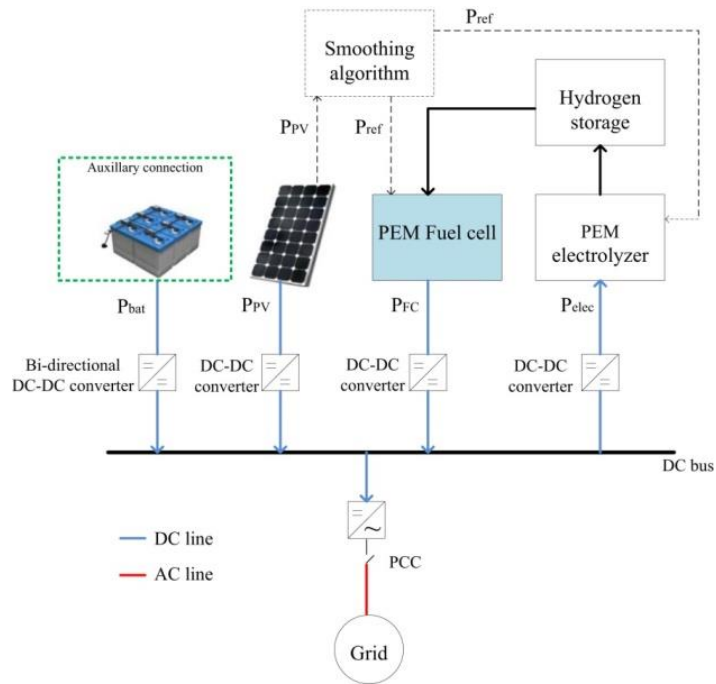


Fig 2.9: PV connected to fuel cell (Shivashankar et al., 2016).

Wind energy, together with solar energy stored through the use of PV, is one of the most widely used energy sources. The use of wind power has undergone considerable growth in recent years, as shown in Fig 2.10 (Ayodele et al., 2015). As reported by T. R. Ayodele et al. (2015), the progressive increase in the presence of wind power in Europe alone reached a value of 106 GW in 2012, which is an increase of 12,6% annually. In addition, world wind capacity reached 318 GW at the end of 2013 as shown in Fig 2.11 (Ayodele et al., 2015).

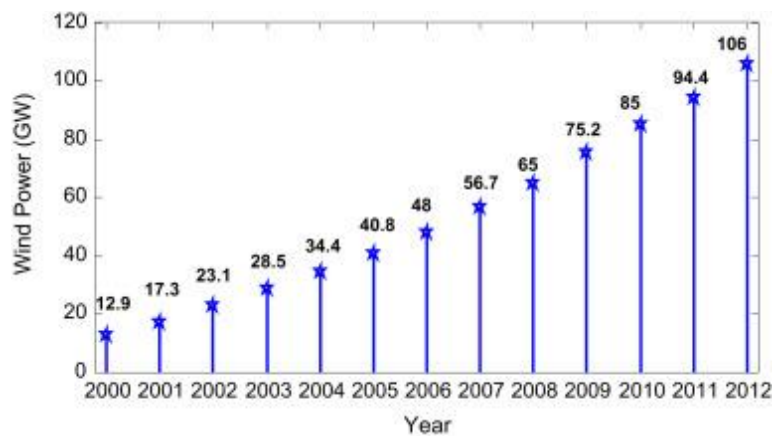


Fig 2.10: Cumulative installed wind power in the European Union between 2000 and 2012 (Ayodele et al., 2000).

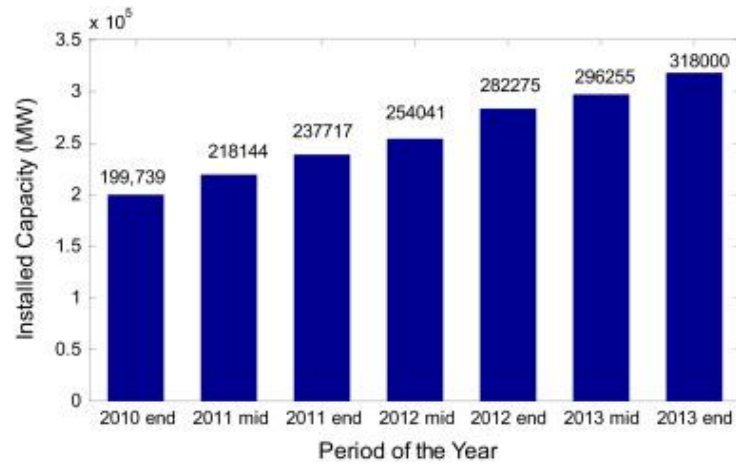


Fig 2.11: Total installed wind capacity in the world between 2010 and 2013 (Ayodele et al., 2000).

According with what is said for solar energy, wind energy is also an example of intermittent energy generation. In particular, the parameter that most influences the reliability of a wind system is the wind speed, which varies from day to day, hourly or even during even smaller intervals. The wind forecast is also more complicated than the sun. M. Jabir et al. (2017) briefly describe some of the most commonly used methods for predicting time, such as artificial intelligence (AI) and machining learning (ML). Other widespread applications described include multi-layer perceptrons (MPL), radial basis function neural network (RBFNN), recurrent neural networks (RNN), and support vector regression (SVR).

As is the case with solar one, wind power penetration also creates a disagreement between energy generation and demand, and this forces operators to face a number of difficulties to fully meet the demand for electricity. Ayodele et al. (2015) describe three methods used to balance different demand and supply. The regulation technique is the technique for which it is supplied more or less power depending on the signal sent by the control system that monitors both load and generation and is used in case of fast and unpredictable loading that occurs in time slots between the second and the minute. Wind speed variation is not usually instantaneous, so this technique is poorly used and the cost is rather low. The load following balancing technique, however, is used when the variation takes place in periods of time between 10 minutes and several hours. In this case, there is enough time to plan load and generation based on time-based variation, so system operators use different types of generation to meet up energy demand at the lowest cost. In the case of unit commitment, the generators that will be needed for each day's operation will be selected by the utility operator (Ayodele et al., 2015).

Finally, even wind power penetration within the power grid causes energy quality issues such as voltage variation, unintentional islanding from the grid, reverse power flow, and power fluctuations in grid connected systems, already described above.

In particular, voltage fluctuation is the biggest problem for the use of wind energy. As stated by M. Jabir et al. (2017), the voltage of a wind connected grid depends on the wind output power and the wind power depends on various parameters including air density, wind speed and the characteristics of the wind turbine. The rash of volt-

age is due to the sudden increase in wind speed. On the contrary, a sudden drop in speed causes a voltage drop in the connected network.

Ultimately, wind power alone is not able to feed a network continually, as is the case with wind power. The storage devices used to mitigate wind intermittent issues are several, and some common ones to those used in the PV case.

In addition to the methods already described for PV such as batteries, SMES and supercapacitors, other methods are employed including the use of the flywheel. It is a device capable of accumulating kinetic energy in a spinning mass, drawing electricity from the primary source and storing it in a high-density spinning flywheel. It can be a low speed flywheel (up to 6'000 rpm) and a high speed flywheel (up to 60'000 rpm). The flywheel represents an excellent excess energy storage system produced by a wind system, and is able to return it by transforming kinetic energy into electricity by exploiting the inertia of the rotor. Fig 2.12 shows how the flywheel is connected to the wind turbine while the electrical part is connected to the grid via back to back electronic converter (Ayodele et al., 2015).

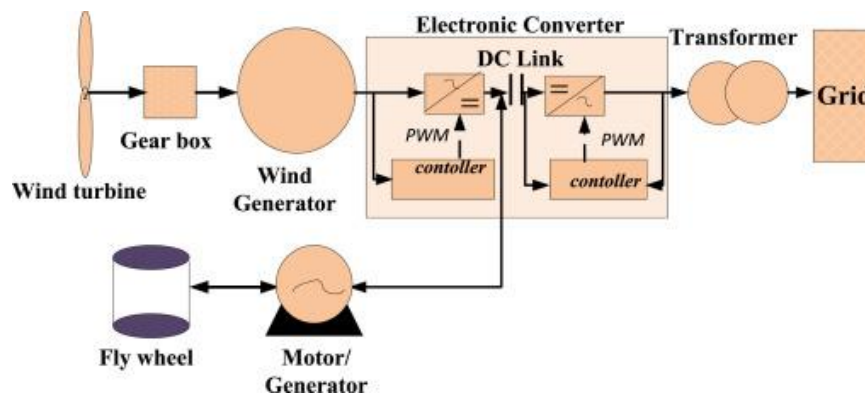


Fig 2.12: Wind energy conversion system and fly wheel energy storage system (Ayodele et al., 2015).

An alternative method is pumped hydroelectric storage (PHS) technology. As stated by Ayodele et al. (2015), in these systems the water is pumped in the time of excess wind power into the upper reservoir and then released through a generator in the lower reservoir during the low wind power production. It is a highly developed system, with a total installed capacity of about 127 GW up to 2009 and this value is expected to grow steadily. The limits of this technology are identified by the fact that it can only be used in specific topological areas and large enough to contain the two types of reservoir, it has a high cost of capital and a high construction time (Ayodele et al., 2015).

Compressed air energy storage (CAES), instead, is able to store mechanical energy through compression of air into a container located underground when excess wind energy is generated. Compressed air is used and expanded to get electricity when wind power is unable to satisfy demand and power the power grid. According with Ayodele et al. (2015), the advantages of CAES consist of a high capacity and long lifetime of energy storage, as well as ease of use and startup. The limit that most influences its performance is the dispersion of heat generated during compression when the compressed air is held for too long.

One of the most interesting technologies that is progressively developing in the field of renewable energies as a smoothing system of intermittent generation is hydrogen storage. Hydrogen is not present in nature as a free molecule and this is the reason because it is necessary to produce it from the substances that contain it, as is produced by electrolysis to obtain it from the water. From the point of view of energy application, hydrogen can be used theoretically as fuel through chemical conversion, that is, by utilizing its combustion when combined with pure oxygen. On the other hand, it can be used through electrochemical conversion, that is, for the direct generation of electricity (http://orizzontenergia.it/testi.php?id_testi=137#null).

Excess energy from a wind power system can be used to produce low pressure hydrogen (207-2068 kPa) then compress and preserve it at high pressure (20684 kPa). It can then be converted into electricity during the low wind speed period directly into a fuel cell using a non-toxic product, that is the water (Ayodele et al., 2015).

Thanks to all the positive aspects of the use of hydrogen, such as its versatility, ease to storage, ease to transport and its "clean" nature, it is considered a potential alternative to automotive applications and is being studied by some of the world's most famous automakers.

The use of hydrogen in the future will require storage onboard vehicles and at hydrogen production sites, hydrogen refueling stations, and stationary power sites.

The main limit for spreading this method is the need to find a reliable and effective way to store hydrogen. Hydrogen has a very high energy content by weight (about three times more than gasoline), but it has a very low energy content by volume (liquid hydrogen is about four times lower than gasoline) (Ayodele et al., 2015).

A possible method of hydrogen storage is the compression of hydrogen gas in high pressure reservoirs. As stated by Gray et al. (2011), hydrogen storage in the form of pressurized gas is theoretically simple. However, it is necessary to apply a compression to increase the volumetric energy density and to achieve acceptable values, and this is not easy for several reasons. An alternative method of hydrogen storage is the physical storage of cryogenic liquid hydrogen (cooled to 253 °C, at pressures of 6-350 bar) in insulated tanks. Liquid H₂ has a better volumetric density than the compressed H₂ at 700 bar (Ayodele et al., 2015). However, the liquefaction process is energy intensive. In addition, evaporation losses are important whose the liquid state has been achieved. Consequently, this represents an impractical solution onboard a road vehicle.

Due to limitations in the application of the above methods, a third storage method is being considered which involves the use of some solid state materials to be combined with hydrogen to obtain benefits during storage. The solid state storage option is actually a very large topic as it could be exploited by various H₂-solid physical interactions. One of the most commonly used solutions is to reversibly combine H₂ with a metal. The advantages of hydrogen storage in the form of metal-hydride (MH) consist to achieve much higher volumetric energy density and, therefore, compatible with the electrolyser output pressure, and greater safety compared to compressed gas (Ayodele et al., 2015). However, this technology is still in the process of being studied and it takes more years before it can actually be implemented.

Very important is the use of Phase Change Materials (PCM) for thermal energy storage. Generally, thermal energy storage can be obtained by imposing phase transfor-

mations on a material and by exploiting the thermal energy exchanged during transformations. The efficiency of the method used is directly proportional to the specific thermal capacity and volume of the material.

These materials are latent heat thermal energy storage (LHTES), that is accumulators of that amount of energy that is exchanged during phase transitions in the form of heat, and are able to store a high amount of constant temperature energy. PCMs have a high fusion enthalpy and are able to store or release large amounts of energy as latent heat during liquid-solid phase transformations and vice versa, in a relatively small volume (Pielichowska et al., 2014).

The ideal PCM must meet certain specific properties such as thermal properties, such as having a melting temperature in the desired operating range, a high phase transition latent heat per unit volume, a high specific heat and a high thermal conductivity of both phases. It should also meet physical properties such as a small volume change on phase transformation, a low vapor pressure at the operating temperature, a balance to make favorable and high density. Last but not least, the PCM should meet kinetic properties, such as no super-cooling, high nucleation rate and an appropriate rate of crystallization, and chemical properties such as long-term chemical stability, a completely reversible freeze/melt cycle, compatibility with the construction materials, no corrosion influence on the construction materials and should be non-toxic, non-flammable and non-explosive to ensure safety (Pielichowska et al., 2014).

PCMs can be classified in different ways, depending on the temperature ranges on which the phase transition occurs or according to the phase transition mode. Based on this latter classification, there are gas-liquid, solid-gas, solid-liquid and solid-solid systems. Applications of gas-solid and liquid-gas systems are limited due to the large volume variations that come into play (Pielichowska et al., 2014).

Among the different application areas of the PCM, the most recent is surely the storage of solar energy. Hammou et al. (2006) achieved positive results from the study of a Hybrid Heat Accumulation System (HTESS) for the simultaneous management of solar and electrical heat storage, noting that the system reduced energy consumption for heating almost 32%.

One possible application of PCMs is that of vehicles. From a study carried out by Chau et al. (2007), vehicles deliver about 65-75% of the fuel energy in the form of heat through the drain or radiator, so it is necessary to focus the analysis on the possible improvement of the overall thermal efficiency of the vehicle. In particular, vehicle components can undergo different thermal conditions in relation to the surrounding environment, so vehicles must be able to operate between temperatures below zero and very high temperatures. PCMs may be able to buffer thermal transients and allow the system to be designed for medium heat loads rather than peak (Jankowski et al., 2014).

Electric Vehicle (EV) batteries are also used as energy storage devices to mitigate the intermittence of renewable energies. EVs are alternative vehicles to traditional vehicles with internal combustion engine (ICV) and, thanks to their energy efficiency, are able to contribute massively to reducing CO₂ emissions.

As reported by Sexias et al. (2015), the use of EVs is currently limited because it is linked to several factors such as costs, social status, and driving habits. However, the

authors argue that Europe decided to intervene heavily on the issue of CO₂ emissions by imposing a reduction in GHG emissions and dependence on oil by 2050 by 80-95% compared to 1990 levels. All this will help the gradual entry into the market of electric vehicles such as battery electric vehicles (BEV) and plug-in hybrid vehicles (PHEV). BEV and PHEV are very different from traditional hybrid vehicles. Traditional hybrid vehicles are called because of their ability to be powered by both an electric motor and an internal combustion engine, cannot be recharged by connecting to an electrical outlet and their batteries are recharged using the exploitation of the kinetic energy produced during braking and transformed into electricity.

PHEV is similar to traditional hybrid vehicle because they both have electric motors and internal combustion, but the main difference is that they can be recharged by plugging into an electrical outlet. BEV, on the other hand, only has an electric motor and works using the energy input of the batteries, which can be recharged by an electrical outlet. The most important advantage of BEV is the lack of polluting gases (Goldman, 2014).

These vehicles use their batteries to store excess energy produced by a wind turbine or PV so that they can be used later in case of power shortages. This is a way to mitigate the problem of the amount of unnecessary energy if it causes overvoltage.

In addition, as stated by Ayodele et al. (2015), vehicles remain steady and unused for 90% of the time. The idea is to take parked vehicles and put them in the power grid so that the batteries can be made available to give or store energy. This model is known as the Vehicle to Grid (VTG) and would provide useful services to the power grid, replacement of energy storage systems and improve the efficiency of the entire system. Aguero et al.(2012) discuss the integration of EV and PV from a technical point of view. Positive results point out how Distributed Energy Storage (DES) system can really be a great way to mitigate intermittent problems.

In conclusion, the penetration of PV and, in general, all the sources of energy that possess the characteristic of interference, within the power grid, finds many obstacles. Above all, there is the problem of the disagreement between electricity supply and demand for electricity, and the lack of appropriate tools to overcome the problem of rapid changes in the load. For this reason there is a progressive step towards the so-called "smart grid", understood as an evolution of traditional electrical networks. This innovation allows you to manage your electricity and respond promptly to the demand for greater or lower consumption of one or more users by increasing connectivity, automation, and co-ordination between suppliers, consumers and the network to optimize transmission and distribution of energy.

3. METODOLOGY

The analysis carried out in this thesis work refers to a project under way in the *Stirlingshire* village of Fintry (population of about 700 people) already launched in 2016 called *Smart Fintry*, which would last two years ending in 2018. This project aims to develop a system enabling UK consumers to purchase energy directly from nearby renewable energy generators, so as to reduce electricity costs and reduce carbon emissions for consumers located near such renewable electricity generators.

The project is divided into four main phases. The first phase concerned the preparation of the project to start delivery.

The second phase involved the preparation of everything necessary for the installation of smart meters and heat pumps, as well as the inclusion of a new local tariff designed by the project partner *Good Energy*. The target of this phase was to register 100 families at this new rate by the end of October 2016. The result is very close to the target, in fact 83 families are currently able to take part.

The third phase consisted of the installation of smart meters capable of providing almost real-time data and of all communication links necessary to make data collection feasible. This goal was achieved at the end of March 2017, although there are still a few meters to be installed.

The fourth phase is underway and would last until March 2018. It concerns the expansion of the project to include a larger number of participating families. The aim is to develop methodologies and tools that increase the replicability of the project taking into account the forecast risks associated with the generation of intermittent renewable energy, such as wind, hydro and solar PV energy (<http://smartfintry.org.uk/>).

So the implementation of this project and the analysis carried out in this thesis work concern the town of Fintry, a small village located in the central part of Scotland about 19 miles north of Glasgow (Fig 3.1).



Fig 3.1: Fintry, Scotland, UK (www.google.com/maps).

The goal of the project is to create a replicable local energy economy that can expand and be adopted by other communities in UK.

Therefore, this thesis work focuses on the analysis of a certain number of houses. Among these houses, only a small part already owns a PV system while the remaining part is without a PV system. The study carried out has as its aim the economic analysis resulting from the application of a solar-PV system or a combined solar-PV-battery system for each house of this analyzed village. It is necessary to understand if it is reasonable to adopt such systems or is inconvenient from an economic point of view. In particular, this thesis work evaluates whether investments in a PV system and a combined PV-battery system can be considered satisfactory on the basis of the relative payback, considering the energy tariffs and the incentives applied in Scotland.

The work done can be briefly described in five basic steps. The first step consists in the construction of a PV model applying a regression analysis starting from the data relative to a 50 kWp PV system installed in a sports center in Fintry.

As a regression model, it was decided to use the *PVUSA* (Photovoltaics for Utility Scale Applications), a very simple model based on data collection of solar, meteorological and power output data for a certain period of time and regresses the output of the system against a combination of solar radiation and temperature.

Knowing the meteorological data, the second step starts assigning a PV system of acceptable size for domestic use to each considered houses. Having calculated the regression coefficients for a 50 kWp system, it is easy to obtain the new coefficients for a different known size of PV system.

In this way it is immediate to obtain a dataset of the demand in the absence of a PV system and a dataset of the demand when a PV system of a certain size suitably chosen is installed.

From the comparison between the trend of the energy required to the network from any house without PV and the trend of the net energy required to the network after the installation of appropriate solar panels given by the difference between the required energy and the produced solar energy, it is immediately to observe that the quantity of solar energy of a generic house is sufficient to require less energy from the network and, in some case, higher than the demand to be able to feed a battery for the energy storage to reuse it at a later time or to sell it and profit from it. However, if the house needs additional energy it can be imported from the network at any time (Fig 3.2).

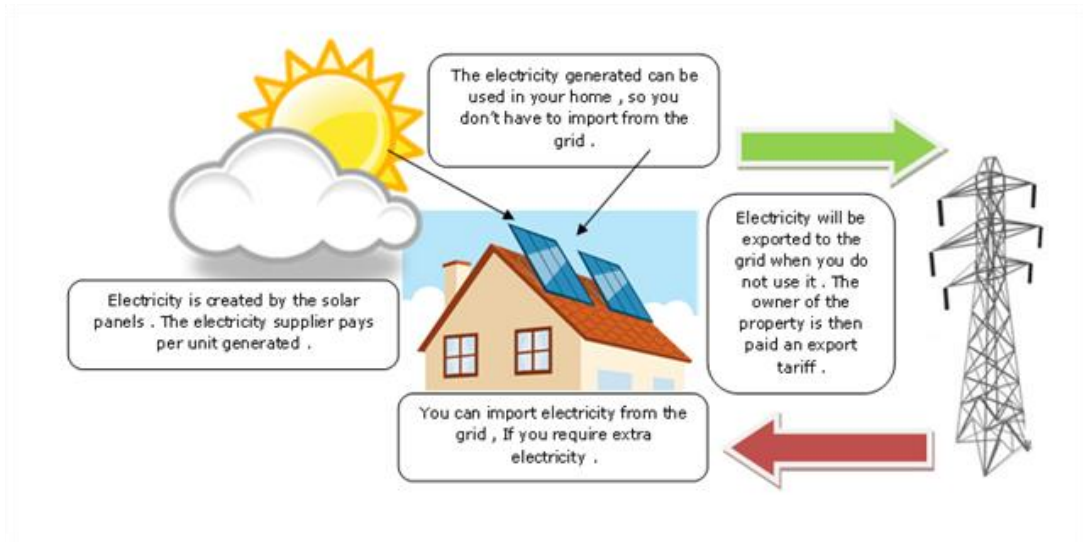


Fig 3.2: PV system generic scheme (<https://www.rbgrant.co.uk/renewables/solar-pv-panels/>).

In Fig 3.3 the generic trend of the energy required by a house is shown in blue, while the quantity of energy produced by a PV system is shown in red. The peak demand is reached during the evening time when all the residents are usually at home. On the other side the peak of solar production is obviously reached during the daytime hours. The portion of space between the red curve and the blue curve represents a surplus of energy that can be used to store reserve energy in a battery or can be fed into the network.

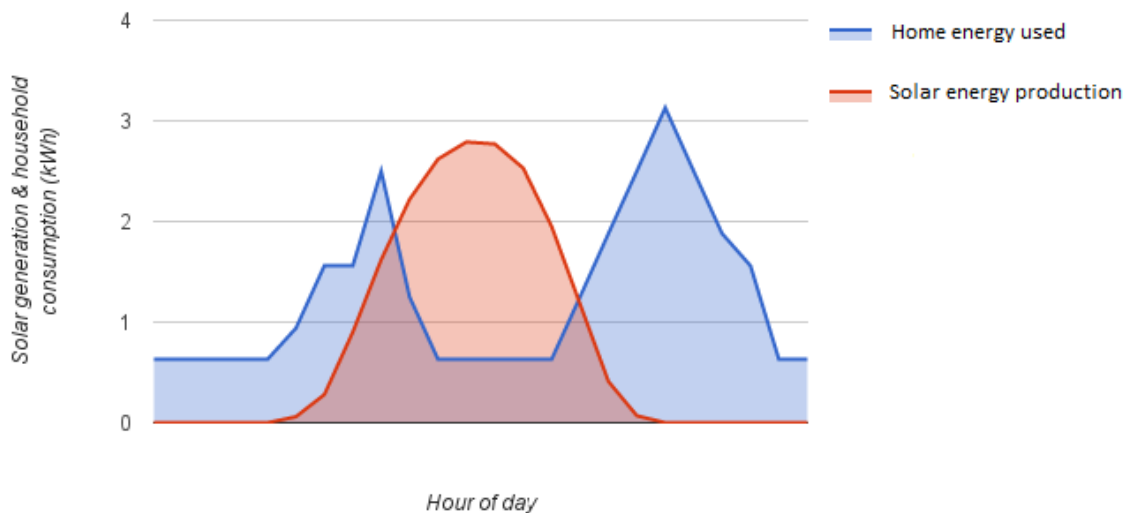


Fig 3.3: House energy demand and solar energy produced for a generic house during the day .

The third step consists in carrying out a research on the BESS market in Europe, in order to verify which brands are prominent and choose an appropriate type of bat-

tery that guarantees the correct functioning of a hypothetical combined PV-battery system installed on the houses (Fig 3.4).

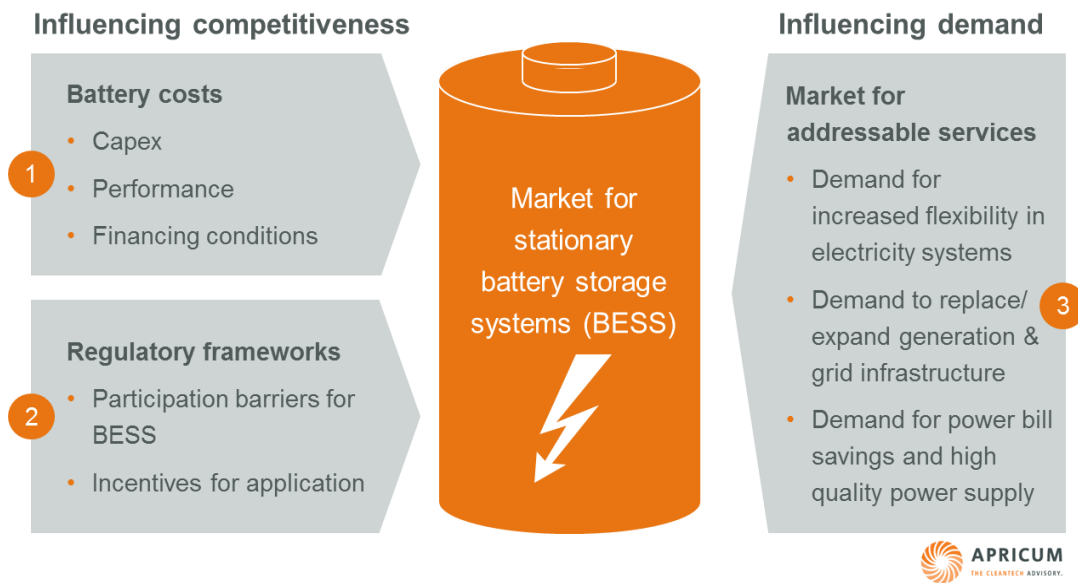


Fig 3.4: Market for a stationary battery storage system (<http://planetsave.com/2015/10/08/stationary-battery-energy-storage-systems-what-will-drive-their-growth/>).

After choosing the appropriate battery, the BESS model was built considering the technical data (capacity, discharge rate, charge rate, round-trip efficiency, lifetime) of the model considered.

Assuming to apply a combined PV-BESS system to all the houses, in the fifth step an economic analysis was made. This analysis involved the economic study of a PV system installed on each house to understand how long it would be able to payback. The same analysis was done about the installation of a PV-BESS system, where the initial expenditure and consumption change significantly.

4. PRESENTATION OF DATA

The starting data for the analysis carried out in this thesis work were provided in the form of Microsoft Excel files, and can be subdivided respectively into three sectors.

4.1 Associated weather

The folder called "Associated weather" contains twelve files, each of which contains the values of the reference climate parameters for each month of the year 2017. In particular, the data concern the temperature T measured in degrees Celsius ($^{\circ}\text{C}$), the wind speed w measured in miles per hour (mph) and the solar radiation I measured in watts per square meter (Wm^{-2}).

Fig 4.1, Fig 4.2 and Fig 4.3 show respectively the temperature, the solar radiation and the wind speed average values trends for each month related to the year 2017.

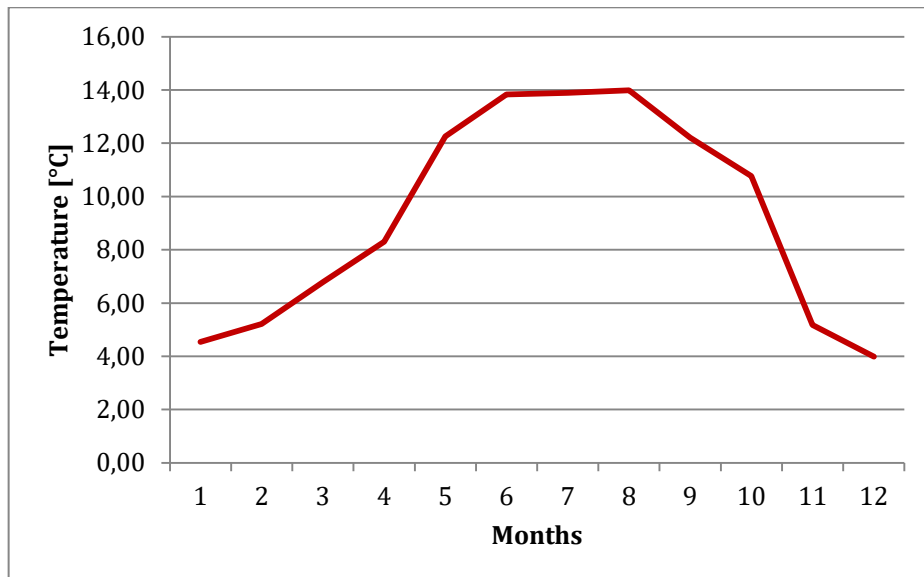


Fig 4.1: Average temperature values of Fintry in 2017.

The average temperature curve shows a slow increasing trend during the first months of the year, then a quicker increasing trend until reaching the absolute maximum value between the end of May and the beginning of August, then starts to decrease relatively slowly until the beginning of October. Subsequently the curve continues to decrease but in a more sudden manner.

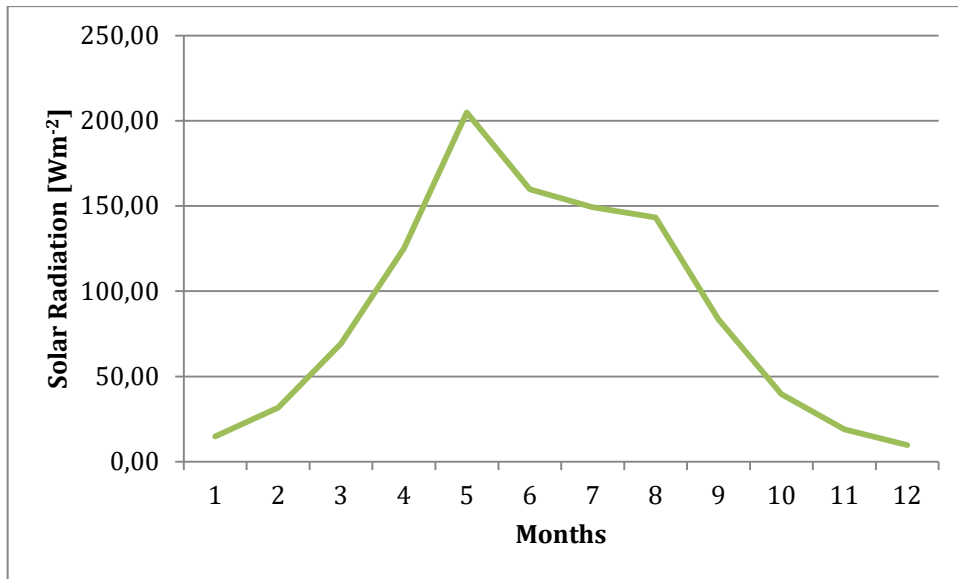


Fig 4.2: Average solar radiation values of Fintry in 2017.

The curve of the average trend of the solar radiation starts from a relative minimum value during the first months of the year and grows until it reaches its peak value towards the first half of May. From then on it decreases slightly until reaching a relative maximum value during June and another one during August, then decreasing inexorably in the following autumn and winter months.

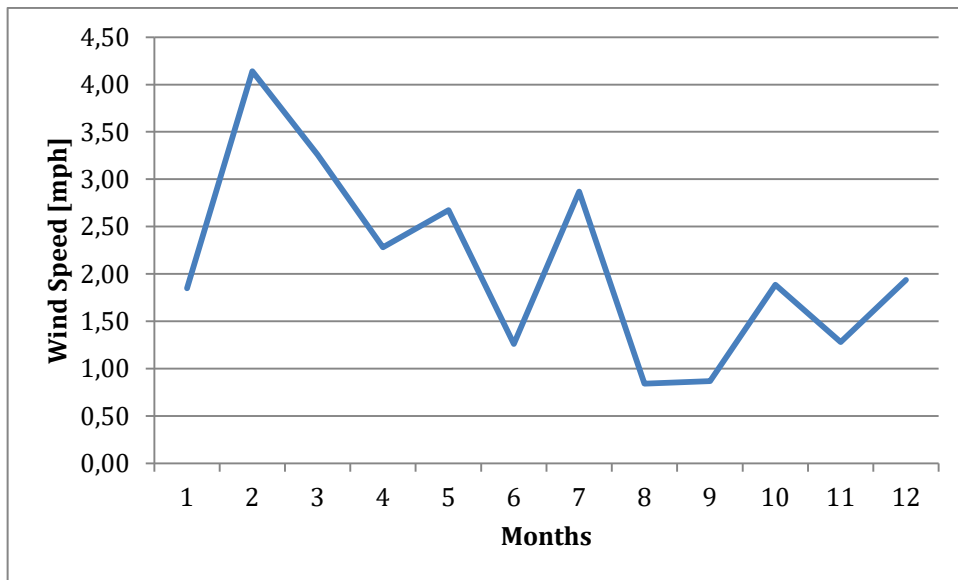


Fig 4.3: Average wind speed values of Fintry in 2017.

The trend of the mean wind speed values shown in the last figure is understandably undulating, considering that Scotland is subject to relatively high wind speeds. The average value during the course of the year 2017 was approximately 2,50 mph.

The provided weather data show information for each reference month of the year 2017 with a time interval of 5 minutes (Fig 4.4).

	A	B	C	D	E	F	G
1	Timestamp	Month	Temperature [°C]	Wind Speed [kph]	Solar [W/m ²]		
2	01/01/2017 00:03	1	3,40	0,00	0,00		
3	01/01/2017 00:08	1	3,40	0,00	0,00		
4	01/01/2017 00:13	1	3,30	0,00	0,00		
5	01/01/2017 00:18	1	3,20	0,00	0,00		
6	01/01/2017 00:23	1	3,10	0,00	0,00		
7	01/01/2017 00:28	1	3,00	0,00	0,00		
8	01/01/2017 00:33	1	2,90	0,00	0,00		
9	01/01/2017 00:38	1	2,70	0,00	0,00		
10	01/01/2017 00:43	1	2,50	0,00	0,00		
11	01/01/2017 00:49	1	2,40	0,00	0,00		
12	01/01/2017 00:54	1	2,30	0,00	0,00		
13	01/01/2017 00:59	1	2,10	0,00	0,00		
14	01/01/2017 01:04	1	2,00	0,00	0,00		
15	01/01/2017 01:09	1	2,00	0,00	0,00		
16	01/01/2017 01:14	1	1,90	0,00	0,00		
17	01/01/2017 01:19	1	1,80	0,00	0,00		
18	01/01/2017 01:24	1	1,70	0,00	0,00		
19	01/01/2017 01:29	1	1,70	0,00	0,00		
20	01/01/2017 01:34	1	1,70	0,00	0,00		
21	01/01/2017 01:39	1	1,70	0,00	0,00		
22	01/01/2017 01:45	1	1,70	0,00	0,00		
23	01/01/2017 01:50	1	1,80	0,00	0,00		
24	01/01/2017 01:55	1	1,70	0,00	0,00		
25	01/01/2017 02:00	1	1,60	0,00	0,00		
26	01/01/2017 02:05	1	1,60	0,00	0,00		
27	01/01/2017 02:10	1	1,50	0,00	0,00		
28	01/01/2017 02:15	1	1,40	0,00	0,00		

Fig 4.4: Extract of the weather data of May showed in Microsoft Excel.

4.2 PV generation

The folder named "PV generation" contains seven files, each of which contains the power data relative to the 50 kWp PV system installed on the roof of the Fintry Sports Club. The power data provide the values of the used power measured in kilo-

watt peak (kWp) and discretized every 10 minutes starting from 26th April 2017 at about 12:10 pm until 31st October 2017 at about 11:50 pm (Fig 4.5).

	A	B	C	D	E	F	G
1	Timestamp	Total [kWh]	Power [kW]				
2	2017-05-01 06:20:28.000	55230,83	0,36				
3	2017-05-01 06:30:33.000	55230,95	0,72				
4	2017-05-01 06:40:48.000	55231,17	1,32				
5	2017-05-01 06:51:13.000	55231,45	1,68				
6	2017-05-01 07:00:28.000	55231,76	1,86				
7	2017-05-01 07:10:55.000	55232,11	2,10				
8	2017-05-01 07:20:33.000	55232,38	1,62				
9	2017-05-01 07:30:34.000	55232,52	0,84				
10	2017-05-01 07:40:28.000	55232,63	0,66				
11	2017-05-01 07:50:35.000	55232,74	0,66				
12	2017-05-01 08:00:53.000	55232,89	0,90				
13	2017-05-01 08:10:54.000	55233,16	1,62				
14	2017-05-01 08:20:28.000	55233,49	1,98				
15	2017-05-01 08:30:33.000	55233,92	2,58				
16	2017-05-01 08:40:33.000	55234,57	3,90				
17	2017-05-01 08:50:31.000	55235,48	5,46				
18	2017-05-01 09:00:48.000	55236,71	7,38				
19	2017-05-01 09:11:50.000	55238,20	8,94				
20	2017-05-01 09:20:48.000	55239,57	8,22				
21	2017-05-01 09:31:18.000	55240,63	6,36				
22	2017-05-01 09:40:33.000	55241,79	6,96				
23	2017-05-01 09:51:24.000	55243,46	10,02				
24	2017-05-01 10:00:40.000	55245,95	14,94				
25	2017-05-01 10:10:33.000	55248,68	16,38				
26	2017-05-01 10:20:35.000	55250,82	12,84				
27	2017-05-01 10:30:37.000	55254,15	19,98				
28	2017-05-01 10:40:33.000	55258,33	25,08				
29	2017-05-01 10:50:28.000	55263,30	29,82				
30	2017-05-01 11:00:28.000	55267,64	26,04				
31	2017-05-01 11:10:55.000	55272,15	27,06				

Fig 4.5: Extract of the power data of the Fintry Sports Club in May showed in Microsoft Excel.

The Fig 4.6 shows the trend of the produced power during the period between on 26th April and 31st October 2017 from the 50 kWp PV system of Fintry Sports Club.

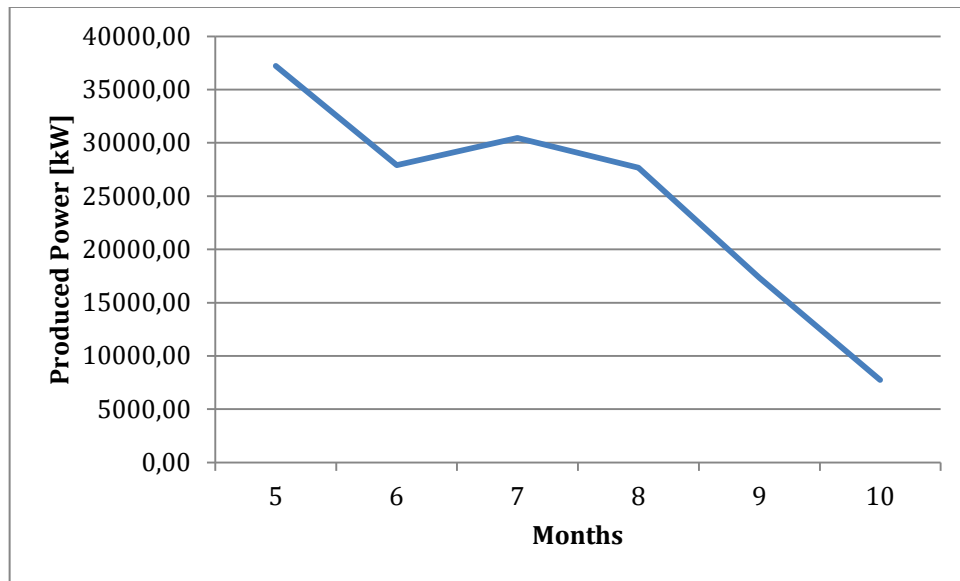


Fig 4.6: Produced power trend of the 50 kWp PV system of the Fintry Spots Club in 2017 (real data).

4.3 Household demand

The folder called "Household demand" contains twelve files, each of which contains the energy used and the energy exported data of each house starting from 00:30 on 1st January 2017 until 11:30 pm on 31st December 2017. The data are discretized every 30 minutes, the houses are named through numbers and the energy values provided are measured in watt hours (Wh) (Fig 4.7).

	A	B	C	D	E	F
1	NodeID	Timestamp	E_Used [Wh]	E_Exported [Wh]		
2	110	01/01/2017 00:30	121	0		
3	110	01/01/2017 01:00	107	0		
4	110	01/01/2017 01:30	110	0		
5	110	01/01/2017 02:00	131	0		
6	110	01/01/2017 02:30	92	0		
7	110	01/01/2017 03:00	109	0		
8	110	01/01/2017 03:30	133	0		
9	110	01/01/2017 04:00	104	0		
10	110	01/01/2017 04:30	92	0		
11	110	01/01/2017 05:00	135	0		
12	110	01/01/2017 05:30	103	0		
13	110	01/01/2017 06:00	133	0		
14	110	01/01/2017 06:30	246	0		
15	110	01/01/2017 07:00	192	0		
16	110	01/01/2017 07:30	130	0		
17	110	01/01/2017 08:00	108	0		
18	110	01/01/2017 08:30	103	0		
19	110	01/01/2017 09:00	114	0		
20	110	01/01/2017 09:30	117	0		
21	110	01/01/2017 10:00	102	0		
22	110	01/01/2017 10:30	99	0		
23	110	01/01/2017 11:00	128	0		
24	110	01/01/2017 11:30	102	0		
25	110	01/01/2017 12:00	90	0		
26	110	01/01/2017 12:30	133	0		
27	110	01/01/2017 13:00	103	0		
28	110	01/01/2017 13:30	90	0		
29	110	01/01/2017 14:00	122	0		
30	110	01/01/2017 14:30	114	0		

Fig 4.7: Extract of the energy data of the analyzed houses of Fintry in May showed in Microsoft Excel.

At the beginning the houses to be examined were 89 but afterwards some were eliminated from the analysis due to the lack of a sufficient number of data for which the number has dropped down. Discarding even the houses with a previous installed PV system, the number has dropped to 42.

Moreover, the column “C” (Fig 4.7) shows the values of energy used, that is, the amount of energy that the house needs and that must be taken from the grid in the absence of a PV system, while the column “D” (Fig 4.7) shows the values of energy

exported, ie that surplus of energy that would occur at some hours of the day if the house was equipped with a PV system. It is evident that if the values relating to the exported energy of a given house (or node) in exams were different from zero, then the house would already have a previously installed PV system.

It is convenient to consider the normal distribution of the average daily energy values required by each node to show the energy values used by the houses and get an idea of the actual consumption.

In probability theory, the normal or Gaussian distribution is a continuous probability distribution that is often used as a first approximation to describe random variables to real values that tend to focus around a single mean value. The validity of this theory is ascertained by the *central limit theorem* which states that assuming certain conditions, the sum of n random variables with finite mean and variance tends to a normal distribution when n tends to infinity (www.unife.it).

The normal distribution depends on two parameters: the mean (usually indicated by the symbol μ) and the square of the standard deviation σ^2 . Using *Microsoft Excel* it is possible to apply the normal distribution using the mean μ and standard deviation σ^2 values related to the average energy values of each node reported in the Tab 4.1.

Mean μ	Standard Deviation σ^2
20,38	14,26

Tab 4.1: Standard deviation and mean values referring to the average daily energy demand of each node.

Tab 4.2 shows the values of the normal distribution of the average daily energy $\bar{E}_{DEMAND|day}$ used by each node (or house). It is calculated with reference to the mean and the standard deviation.

Node	$\bar{E}_{DEMAND day}$ [kWh]	Normal Distribution
110	10,46	0,022
80	7,33	0,018
78	8,48	0,020
77	10,08	0,022
76	9,85	0,021
67	9,85	0,021
41	10,35	0,022
31	5,70	0,016
27	10,77	0,022
25	8,40	0,020
12	9,01	0,020
10	5,11	0,016
2	10,75	0,022
79	14,43	0,026
73	14,13	0,025
70	14,73	0,026
68	18,24	0,028

64	15,69	0,027
62	18,89	0,028
59	16,43	0,027
49	17,72	0,027
47	11,09	0,023
42	16,50	0,027
39	13,13	0,025
36	14,06	0,025
32	16,05	0,027
24	12,69	0,024
13	13,08	0,025
9	16,78	0,027
4	16,22	0,027
96	52,51	0,002
82	39,43	0,011
75	42,78	0,008
65	28,17	0,024
63	27,24	0,025
57	33,60	0,018
53	33,93	0,018
44	25,33	0,026
37	41,31	0,010
23	26,72	0,025
11	22,79	0,028
7	19,22	0,028
6	69,87	0,000
5	20,83	0,028
3	57,36	0,001

Tab 4.2: Normal distribution values referring to the average daily energy used in 2017 of each node.

Fig 4.8 shows the trend of the normal distribution of the average daily energy of the nodes.

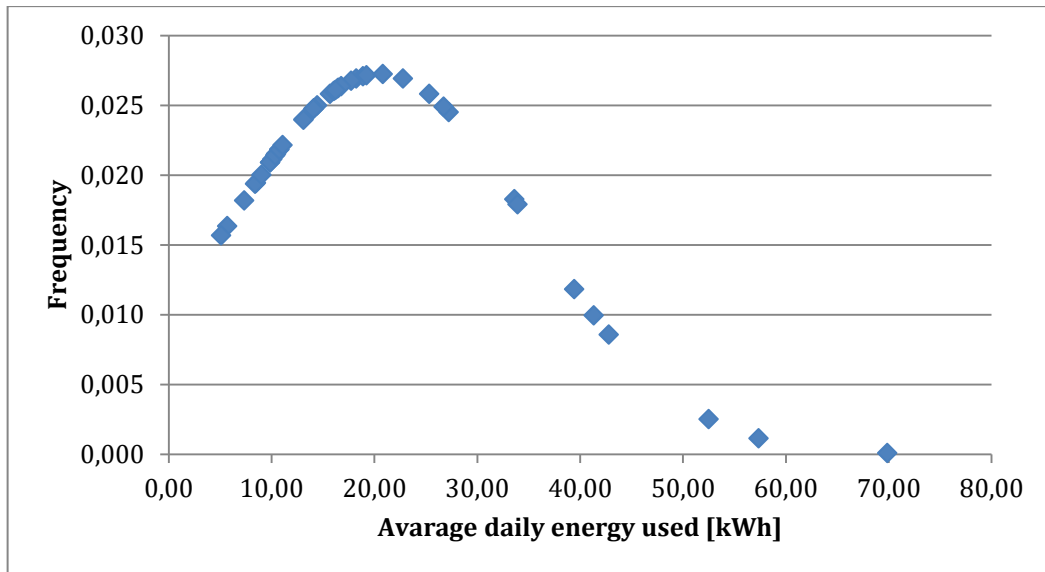


Fig 4.8: Frequency of nodes depending on the average daily energy used in 2017.

The graph has the classic "bell" shape. A certain symmetry is evident with respect to the mean value μ , in which the graph reaches its maximum. The equation (4.1) describes the curve:

$$f(x) = \frac{1}{\sigma\sqrt{2\pi}} e^{-\frac{(x-\mu)^2}{2\sigma^2}} \quad (4.1)$$

Where e represents the Napier constant approximately equal to 2,71. The random variables characterized by an exponential function of this type are briefly indicated with $N(\mu, \sigma)$, the letter N indicates that there is a normal probability distribution with parameters μ and σ .

It is known that by randomly sampling among the normally distributed values there is a probability equal to 68,27% to obtain a value between $\mu - \sigma$ and $\mu + \sigma$ (www.unife.it).

As a result, three areas can be identified in the graph: the first area between 0 kWh and 12 kWh contains nodes with lowest values of average daily energy used; the second area between 12 kWh and 25 kWh contains the nodes with middle values of average daily energy used; the third area that starts from 25 kWh contains nodes with highest values of average daily energy used.

For convenience, only the data of a representative node for each area of the normal distribution curve are shown. The followings show the energy trends used by representative *node 41*, *node 44* and *node 57* (Fig 4.9, Fig 4.10 and Fig 4.11).

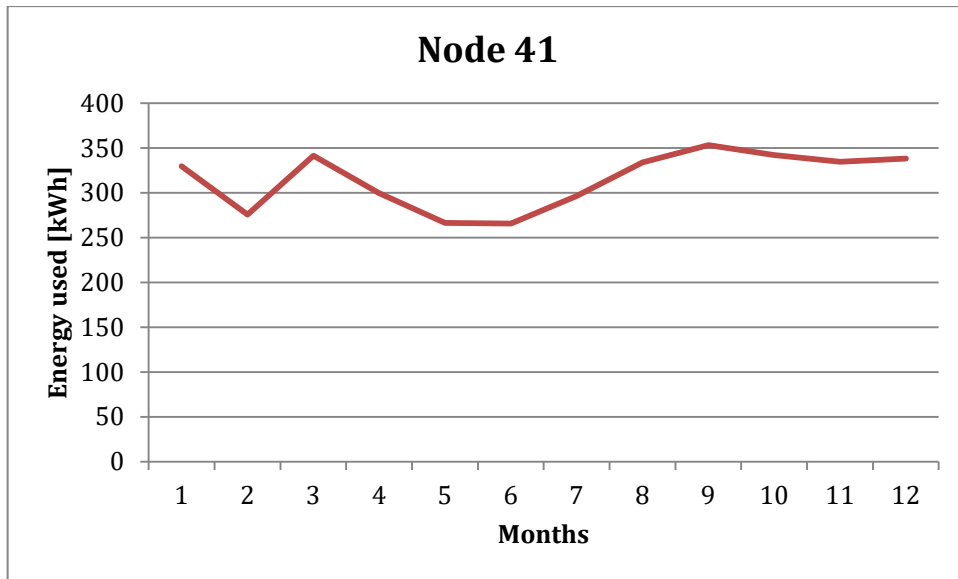


Fig 4.9: Energy used trend in 2017 of node 41.

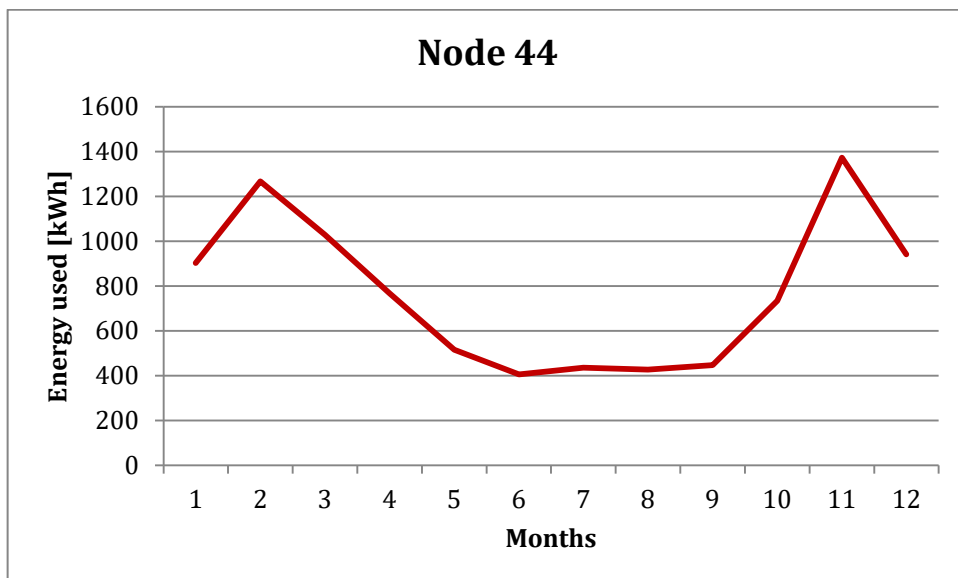


Fig 4.10: Energy used trend in 2017 of node 44.

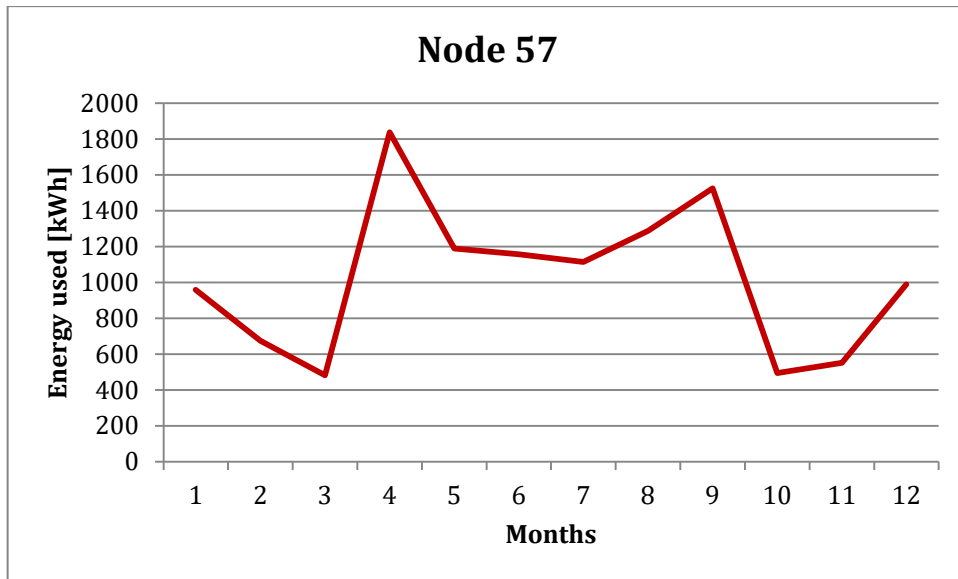


Fig 4.11: Energy used trend in 2017 of node 57.

5. DATA MODELING

As briefly anticipated, the study carried out aims to assign a PV system in a first case and a combined PV-battery system in a second case for all the analyzed houses located in Fintry, starting from the actual data provided for a 50 kWp PV system installed in the Fintry Sports Club.

5.1 Solar-PV system

Photovoltaic systems are classified according to two main types: *stand-alone* PV systems and *grid-connected* PV systems.

Stand-alone systems work without being connected to the network. They are widespread in buildings distant from the electricity grid, in buildings located in hardly accessible areas or buildings with low energy consumption that do not make the connection to the public network convenient. This type of system is usually combined with BESS to allow the use of solar energy even during the nighttime when the panels do not produce energy.

Grid-connected systems are electrically connected to the national grid in a bidirectional way, ie the power flow can be directed from the system to the grid and vice-versa. It is usually installed in buildings whose energy consumption is relatively high in order to save on expenses or, if there is a large area for the installation of the system and well exposed to the sun rays, for the purpose to sell energy and produce a certain gain.

In the examined case, it is assumed to install a PV system of the second type, ie with connection to the electricity grid. The grid-connected PV systems work in an exchange regime with the local electricity grid. In summary, during the day the user consumes the electricity produced by their solar system while during the nighttime when the solar radiation is not enough to produce the amount of energy required or if the user requires more than the system PV is able to supply, the electricity grid guarantees the supply of electricity. However, when the system produces more energy than required by the user it can be exported to the network.

A system of this type is characterized by a set of fundamental components interconnected with each other and which interfaces with the electricity grid, as mentioned.

Photovoltaic panels represent all the photovoltaic units, are exposed to the sun and produce electricity in direct current form (DC). They are made up of hundreds of photovoltaic cells which make it possible to directly transform the solar radiation into electrical energy by exploiting the so-called *photovoltaic effect*. This effect is based on the properties of some conducting materials suitably treated such as *silicon (Si)* to generate electricity directly when they are hit by solar radiation. The behavior of a photovoltaic cell exposed to solar radiation is similar to a power generator with a characteristic voltage/electric current curve that depends basically on the intensity of solar radiation, temperature and surface (<https://www.docsity.com/it/panel-PV-composition/705450/>).

A photovoltaic cell is generally a square-shaped element with a surface of about 100 cm² whose behavior is similar to a battery. Nowadays the most common types of

photovoltaic cell are (<https://www.fotovoltaiconorditalia.it/idee/dimensioni-pannelli-fotovoltai-ci-2>):

- *Monocrystalline silicon cells.* Monocrystalline silicon is the most common semiconductor material used for photovoltaic cells because it allows the highest possible efficiency (14-17%) thanks to the high degree of purity it possesses.
- *Amorphous silicon cells.* The structure is segmented and particularly dark. It is a real deposition of thin semiconductor wires on flexible surfaces, very light and very large (efficiency equal to 5-7%).
- *Polycrystalline silicon cells* (efficiency of 12-16%).

The Fig 5.1 shows the typical composition of a photovoltaic panel.

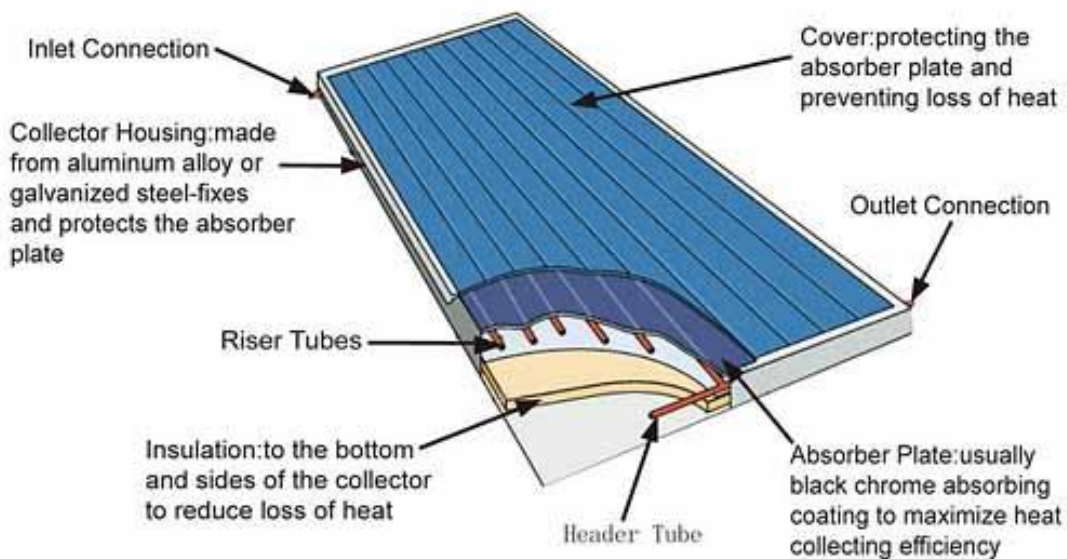


Fig 5.1: PV panel composition scheme (<http://www.consulente-energia.com>).

Their size varies according to the material. They usually have the following sizes (<https://www.fotovoltaiconorditalia.it/idee/dimensioni-pannelli-fotovoltai-ci-2>):

- For polycrystalline and monocrystalline panels with peak powers between 230 and 245 Wp the height varies between 160 and 170 cm, the width between 90 and 100 cm and the thickness between 4 and 5 cm.
- For compact monocrystalline panels with peak powers between 190 and 200 Wp the height varies between 130 and 140 cm, the width between 90 and 100 cm and the thickness between 4 and 5 cm.
- For thin film panels with peak powers of between 77,5 and 87,5 Wp the height is 120 cm, the width of 60 cm and the thickness is between 0,6 and 0,7 cm.

The phenomenon that underlies the photovoltaic effect was discovered many years ago, when it was observed that if two identical electrodes immersed in a weakly conducting solution were illuminated, a small electric current between them would be automatically generated (<https://www.doccity.com/en/alternator-and-transformer/624227/>).

A set of photovoltaic cells connected to each other forms a photovoltaic module, thus succeeding in supplying an electric power per module of a value between 50 W and 100 W on average. It is possible to increase the electric power by creating a panel formed by several modules, or more creating a string consisting of a set of panels. Photovoltaic modules are able to convert light energy almost instantly into direct current electricity.

In order to obtain a PV system all the photovoltaic modules must first be connected together to obtain the required voltage (the string voltage is given by the sum of the voltages of the different modules) and then the different strings are connected in parallel to an inverter.

The *inverter* is a component capable of transforming the electricity produced by panels from direct current (DC) to alternating current (AC). This component is particularly important since it is known that the form of the electricity used in domestic field is AC, so that the solar energy produced must be converted to be used. At the same time, if the solar energy produced is greater than the user demand, it must be fed into the grid and therefore also converted in AC (<http://www.mpptsolar.com/it/schema-funzionamento-inverter.html>).

The inverter is an electronic device able to transform DC electricity into AC electricity and vice-versa at a certain voltage and frequency. In UK and in Italy the electrical standards provide for a domestic voltage of 230 V and a frequency of 50 Hz. It is used not only in the photovoltaic field but also in the speed controllers of electric motors, switching power supplies or lighting (<http://www.mpptsolar.com/it/schema-funzionamento-inverter.html>).

The inverters are used in stand-alone PV systems to power electrical devices of isolated houses, mountain huts, campers, boats or in grid-connected PV systems to introduce the electricity produced by the PV system directly into the electricity grid distribution.

It is necessary to mention the definitions of *alternator* and *transformer* to better understand the operation of an inverter. The alternator is a rotating electric machine that transforms mechanical energy into AC electricity through the natural phenomenon of *electromagnetic induction*. A simple functional scheme could be represented by a coil placed near a rotating magnet which will induce the generation of a current induced in the coil with direction of motion opposite to the rotation of the magnet as soon as it approaches one of its poles to the coil. The AC electricity produced by a transformer has a very low intensity and a very high potential difference (<http://www.mpptsolar.com/it/schema-funzionamento-inverter.html>).

A transformer is similar to an alternator but has another coil (*primary coil*) having AC flowing in it instead of the magnet close to the other coil (*secondary coil*) on which the electric current will be induced. Each coil crossed by AC electricity behaves like a magnet and produces a magnetic field. The goal of the transformer is to obtain lower and safer potentials and higher current intensities, allowing domestic energy use. However, if the primary coil is crossed by AC instead of DC of a battery, a magnetic field will no longer be generated and consequently no induced current. But if the current direction is continuously and quickly changed, this exactly represents the operation of a very simple inverter (Fig 5.2). This inverter produces a square wave output whose frequency depends on the time taken to change the direction of

DC circulating in the primary coil (<https://www.docsity.com/en/alternator-and-transformer/624227/>).

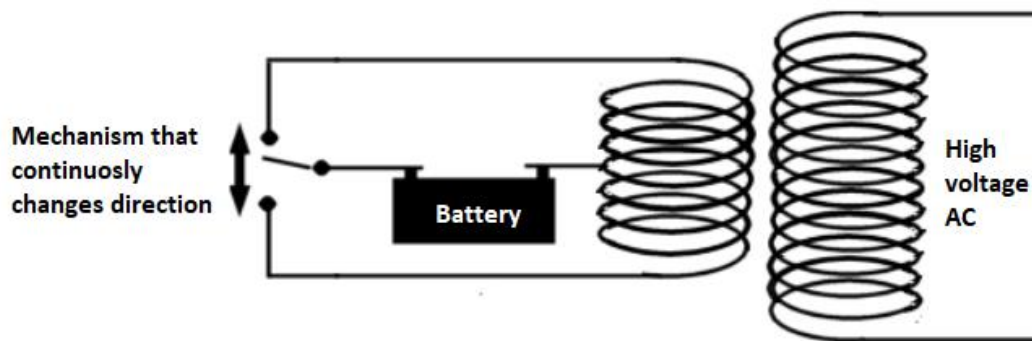


Fig 5.2: Functional scheme of a simple inverter.

The inverter for grid-connected PV systems must have some important characteristics to do the best (<https://residenziale.viessmannitalia.it/cosa-e-come-funziona-inverter-fotovoltaico>):

- Ability to work as close as possible to the point of maximum power on the voltage-current curve of the photovoltaic generator, even in the case of partial shading and rapid variations of solar radiation on the modules.
- High conversion efficiency even at low power levels.
- Ability to synchronize with the electricity grid and to transfer all the available power to it in compliance with the existing connection rules.
- Detection of any insulation losses of the photovoltaic generator.
- Detachment from the network in case of failure or anomalies detected on the latter.
- Protection against direct current input in the event of a fault.

Finally, the *meter* is the component that measures all the energy produced by the photovoltaic system. Depending on the amount of energy produced, there are two different tariffs that respectively represent the remuneration of energy produced and consumed directly by the producer, and the energy not consumed and fed into the grid.

Fig 5.3 shows the simplified functional scheme of a grid-connected PV system.

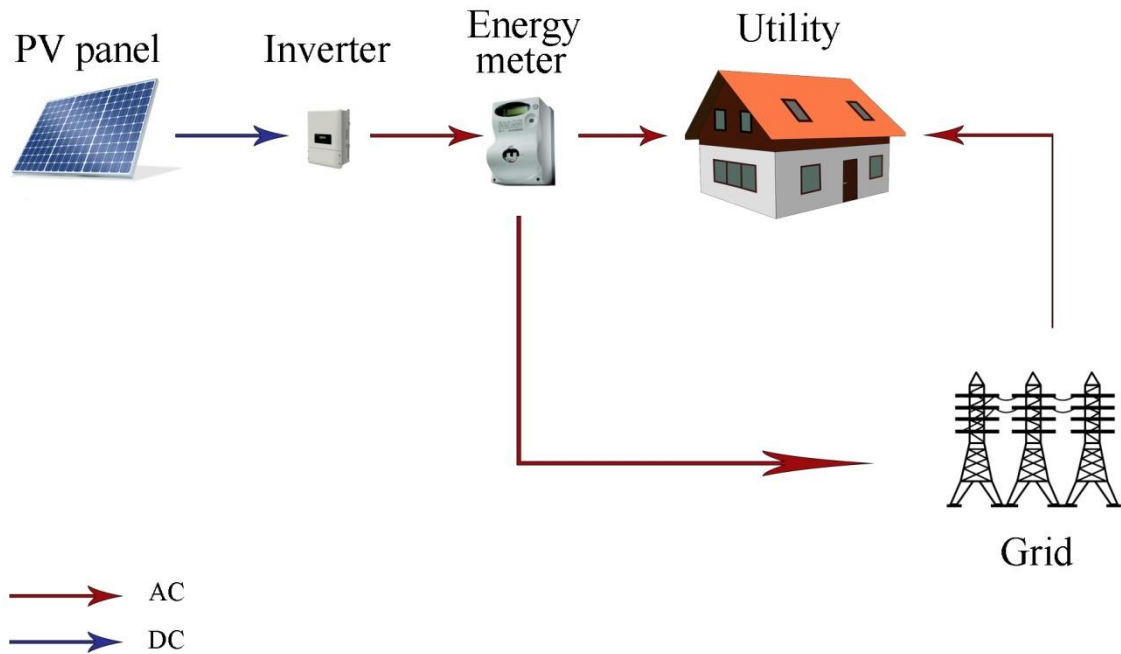


Fig 5.3: Grid-connected PV system scheme.

From an electrical point of view, the PV system must guarantee the correct connection with the network and the correct use of the energy produced by the system. Indeed not all the electricity produced should be fed into the network but part of it is consumed inside the house at the same time as it is produced without going through the meter and being counted. It will therefore be a direct saving on the electricity costs of the operator.

Finally, the correct scheme of the system must include the precise measurement of the total amount of energy produced by the system, the total amount of energy fed into the grid and the total amount of energy taken from the grid.

5.1.1 Fintry Sports and Recreation Club

Fintry Sports Center and Recreation Club was established in 1979 and currently has about 750 members. It is a modern club with excellent facilities located between the Campsie Fells to the North and the Fintry Hills to the South (Fig 5.4, latitude 56.056650; longitude - 4.227280).



Fig 5.4: Fintry Sports Club, Scotland, UK (www.google.com/maps).

In 2015, a work was carried out on the roof of the sports center building to install a PV system with a rated output of 50 kWp. The system is characterized by 200 modules of 250 V (Volt) each of them in monocrystalline silicon *Solon Black 220/16*. The Fig 5.5 shows the technical data relating to a panel of the type described.

SOLON 220/16

SOLON Black 220/16 (monocrystalline)



Electrical data – typical (STC)

STC (Standard Test Conditions): 1,000 W/m², (25 ± 2)°C, AM 1.5 in accordance with EN 60904-3

Power rating	P _{max}	265 Wp ¹⁾	260 Wp ¹⁾	255 Wp	250 Wp	245 Wp	240 Wp
Module efficiency		16,16%	15,85%	15,55%	15,24%	14,94%	14,63%
Rated voltage	U _{mpp}	30,7 V	30,5 V	30,2 V	30,0 V	29,8 V	29,6 V
Rated current	I _{mpp}	8,67 A	8,57 A	8,45 A	8,34 A	8,22 A	8,11 A
Open circuit voltage	U _{oc}	38,1 V	37,8 V	37,5 V	37,3 V	37,0 V	36,8 V
Short circuit current	I _{sc}	9,01 A	8,92 A	8,83 A	8,74 A	8,65 A	8,56 A
Maximum reverse current	I _r	20 A	20 A	20 A	20 A	20 A	20 A
Maximum system voltage		1.000 V	1.000 V	1.000 V	1.000 V	1.000 V	1.000 V

Measuring tolerance for P_{max}: ± 3%

Reduction of module efficiency from 1,000 W/m² to 200 W/m²: < 4 %

Electrical data – typical (NOCT)

NOCT (Nominal Operating Cell Temperature): 800 W/m², NOCT, AM 1.5

Power rating	P _{max}	190 Wp	186 Wp	183 Wp	179 Wp	176 Wp	172 Wp
Rated voltage	U _{mpp}	27,5 V	27,3 V	27,1 V	26,9 V	26,7 V	26,6 V
Rated current	I _{mpp}	6,92 A	6,83 A	6,75 A	6,66 A	6,57 A	6,48 A
Open circuit voltage	U _{oc}	34,4 V	34,2 V	33,9 V	33,7 V	33,5 V	33,2 V
Short circuit current	I _{sc}	7,27 A	7,20 A	7,13 A	7,06 A	6,98 A	6,91 A

Thermal data

T_c of open circuit voltage -0,33% /K

T_c of short circuit current 0,04% /K

T_c of power -0,43% /K

NOCT (according to IEC 61215) 48°C ± 2°C

Measuring tolerance for all final data: ± 10 % (except P_{max} (STC) and NOCT)

Fig 5.5: Technical specifications of Solon 220/16 monocrystalline panels.

This PV system is installed on a roof with an isolated metallic corrugated sheets similar to the one shown in the example in Fig 5.6 (www.puntoenergiashop.it).



Fig 5.6: Example of PV panels on corrugated sheets (www.puntoenergiashop.it).

The modules are installed on the roof (maximum height of 5 metres), which has an inclination equal to 25° (slope angle) in relation to the horizontal plane of the ground and the collecting surface has an angle equal to 23° (azimuth angle) with respect to

the North-South axis. Fig 5.7 and Fig 5.8 show respectively all the sizes, the slope angle and the azimuth angle previously described.



Fig 5.7: Views of the Fintry Sports Club (www.google.com/maps).

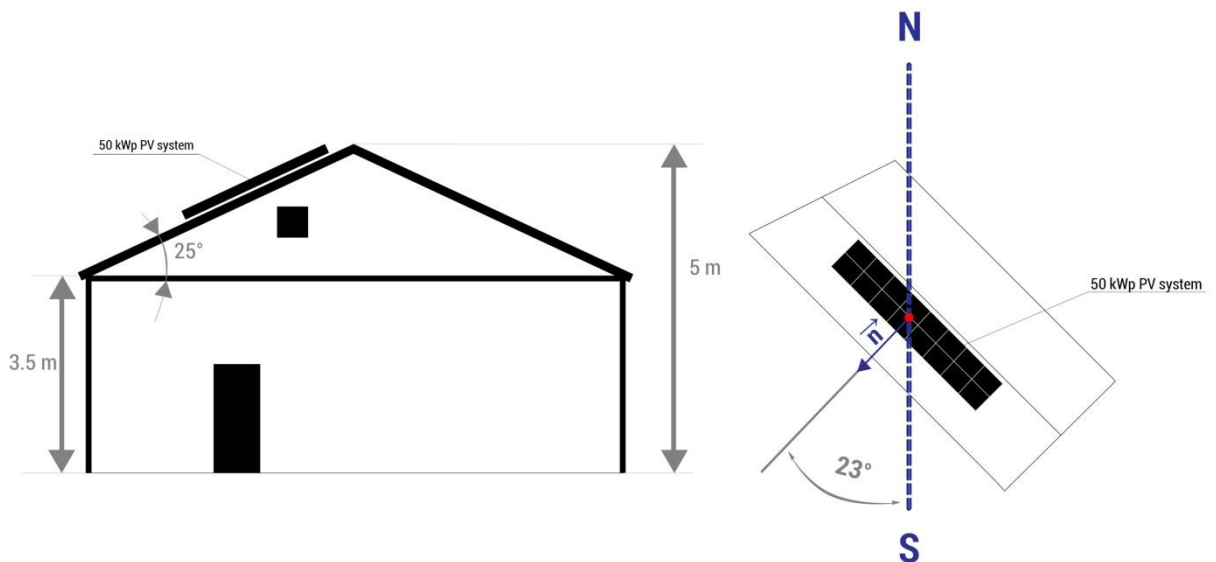


Fig 5.8: Plat and frontal view of the Fintry Sports Club (scheme).

5.1.2 PVUSA model

Many engineering and physical problems involve the exploration of the relationships between two or more variables and modeling the possible link between them. Indeed there are some phenomena that are closely linked by a complex network of relationships, such that the study of the relationship between only two variables is insufficient. Therefore it is necessary to identify all the parameters on which the phenomenon under examination depends and to study its average variation based on them (Corain 2012).

When the exact relationship between two variables is not known it could be useful to identify an empirical model based on the direct observation of the phenomenon.

Regression analysis is a very useful statistical technique for this type of problem. In general, it is assumed that there is only one dependent variable (or response) Y and a certain number k of independent variables X_1, X_2, \dots, X_k (Corain, 2012).

In order to determine such a function it is first necessary to establish its type which is usually assumed linear for simplicity. If the independent variable is unique the function is defined *simple linear regression*, while if the independent variables are more than one the function is defined *multiple linear regression*.

A general simple linear regression model for an generic i -th observation is described by the (5.1):

$$Y_i = B_0 + B_1 X_{1i} + e_i \quad (5.1)$$

Where X_i is the independent variable, Y_i is the dependent variable, B_0 represents the intercept, B_1 represents the partial regression coefficient and e represents the random error (Corain, 2012). By means of some methods such as the *least squares method*, it is possible to estimate the intercept and the regression coefficients in order to obtain the estimated regression line (5.2) for an i -th observation:

$$\bar{Y}_i = b_0 + b_1 X_{1i} \quad (5.2)$$

Where \bar{Y}_i represents the estimated (or expected) value of Y , b_0 represents the estimate of the intercept, b_1 represents the estimate of the partial regression coefficient (Corain, 2012).

Consequently, the residue of the generic observation represents the *error* relative to the value predicted by the model with respect to the observation Y_i , and is defined by the (5.3) (Corain, 2012):

$$e_i = Y_i - \bar{Y}_i \quad (5.3)$$

In the multiple regression model it is assumed that each observed value of the dependent variable can be expressed as a linear function of the relative values of the explanatory variables, with the addition of a residual term that indicates the inability of the model to exactly reproduce the observed reality. Fig 5.9 shows the regression plan for a generic linear model of three variables.

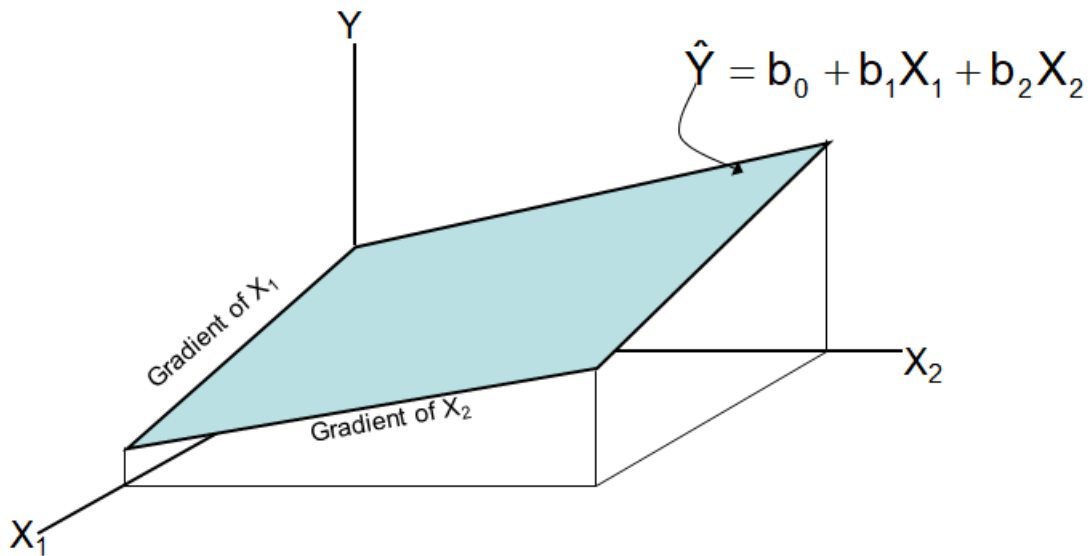


Fig 5.9: Regression plan for a three variables linear model.

Regression analysis is very often used to obtain forecasts. As already mentioned, in the case of this thesis work the PVUSA model was chosen to analyze the phenomenon of photovoltaic generation.

The *PVUSA model* is a linear multiple regression model able to predict the power values generated by any PV system exposed to external conditions by knowing the weather data relative to the place where the PV system should be installed. The PVUSA method “emerged from a cooperative project, a private public partnership that had as its funders the U.S. Department of Energy (DOE) and the California Energy Commission (CEC). This project resulted in the formulation of the PTC-PVUSA Test Conditions, in which values of irradiance (1000 Wm^{-2}), ambient temperature ($20 \text{ }^\circ\text{C}$) and wind speed (1 ms^{-1}) were defined to classify flat-plate PV modules” (Azevedo Dias et al., 2017).

The power data are obtained according to three variables: solar radiation I measured in watts per square meter (Wm^{-2}), wind speed WS measured in meters per second (ms^{-1}) and ambient temperature T measured in degrees Celsius ($^\circ\text{C}$) (5.4).

$$P = \mu_1 I + \mu_2 I^2 + \mu_3 WS + \mu_4 IT \quad (5.4)$$

It is evident that in the equation of the PVUSA model there are four terms of irradiance while for the temperature and the wind speed there is only one each (National Renewable Energy Laboratory, 2009). As a result, irradiance has more weight in evaluating the power generated by a PV system. As stated in a paper of the National Renewable Energy Laboratory (2009), there are a number of evaluations to be noted:

- “Uncertainty in the irradiance carries significantly more weight than uncertainty in the other variables.

- Ambient temperature is highly positively correlated with solar irradiance.
- Rating condition is established for a wind speed of 1 ms^{-1} , a relatively infrequent condition”.

The necessary condition for the PVUSA model to calculate acceptable power values is the use of irradiance data not less than 500 Wm^{-2} (National Renewable Energy Laboratory, 2009).

Subsequently, a new model (Bianchini et al., 2013) obtained from the PVUSA model was proposed. It is reported in (5.5).

$$P = \mu_1 I + \mu_2 I^2 + \mu_3 IT \quad (5.5)$$

In this model the wind speed misses and the only meteorological variables present are the temperature and the solar radiation.

It is important to underline that the three regression coefficients are $\mu_1 > 0$ and $\mu_2, \mu_3 < 0$ respectively. This can be explained by considering the fact that the first term basically provides the almost definitive value of power, while the other two terms relating to square irradiance and temperature represent losses. This also justifies the differences in absolute value between the three coefficients, not by chance μ_1 is far greater in absolute value than μ_2 and μ_3 (Bianchini et al., 2013).

As stated by Bianchini et al. (2013), the PVUSA model shows several interesting features. First of all, “the equation is simple and parsimonious in terms of number of parameters. This implies very little memory occupation and makes it easy to figure out the role of each parameter”. Moreover, the model is linear-in-the-parameters and this allows to estimate the parameters in a simple and efficient way using the classic method of least squares.

Secondly, the equation expresses the power generated by any PV system depending on the meteorological variables for which the forecasts provided by any meteorological service are also available and therefore easy to obtain. On the other hand, in the case where the equation method is applied to a real dataset, there are many studies that show how the prediction error with respect to real data is very small (Bianchini et al., 2013).

The aim of this thesis work is to apply the model (5.5) to the actual data provided for a 50 kWp system installed on the building of the Fintry Sport Club located in Fintry. Reminding the equation (5.5) and knowing that the power quantities P , solar radiation I and temperature T are already known, it is easy to calculate the regression coefficient μ_1, μ_2, μ_3 for a 50 kWp PV system located on the roof of the Fintry Sports Club considering this model as a *multiple linear regression model*.

The *Matlab software* was used to derive the regression coefficients μ_1, μ_2, μ_3 . The equation provided by (5.5) can be considered as a polynomial where the coefficients μ_1, μ_2, μ_3 can be calculated with a least squares fit which minimizes the sum of the squares of the deviations of the model data. From a matrix point of view the system is described by the (5.6):

$$\mathbf{p} = \mu \mathbf{A} \quad (5.6)$$

Where \mathbf{p} represents the power vector containing all n data power values, μ represents the vector of the regression coefficients and \mathbf{A} represents the $n \times 3$ matrix of the solar radiation and temperature values:

$$\mathbf{p}^T = [p_1, p_2, \dots, p_n] \quad (5.7)$$

$$\mu^T = [\mu_1, \mu_2, \mu_3] \quad (5.8)$$

$$\mathbf{A} = [\mathbf{I}, \mathbf{I}^2, \mathbf{IT}] \quad (5.9)$$

With:

$$\mathbf{I}^T = [I_1, I_1, \dots, I_n] \quad (5.10)$$

$$(\mathbf{I}^2)^T = [I_1^2, I_2^2, \dots, I_n^2] \quad (5.11)$$

$$(\mathbf{IT})^T = [I_1 T_1, I_2 T_2, \dots, I_n T_n] \quad (5.12)$$

Where \mathbf{I} is the vector containing the n values of solar radiation, \mathbf{I}^2 the vector containing the n squared values of the solar radiation and \mathbf{IT} the vector containing the n values obtained by the multiplication between the solar radiation and the respective temperature at the same instant of time. The solution is immediately calculated using Matlab through (5.13) applying the *backslash operator*:

$$\mu = \mathbf{A} \backslash \mathbf{p} \quad (5.13)$$

The values of the three regression coefficients for a 50 kWp system using the real data are shown in Tab 5.1:

μ_1	μ_2	μ_3
54,6588	-0,0032	-0,3742

Tab 5.1: Regression coefficients for the 50 kWp system of the Fintry Sports Club calculated using the real data.

5.1.3 Critical issues

However, the real database presents some critical issues that should be commented.

The database provides the power values produced by the 50 kWp system only for the six spring and summer months of the year 2017 (from 26th April to 31st October). This could be a limitation because the model (5.5) would be applied to an incomplete database and consequently the three regression coefficients μ_1 , μ_2 and μ_3 would not take into account the autumn and winter months.

In order to understand if it is actually limiting to consider such a database, it was decided to use the *PVGIS* software (Fig 5.10). *PVGIS* is a simulator created in collaboration between the *Joint Research Center*, the *Institute for Energy and Transport*, the *European Commission*, in particular the *ESTI (European Solar Test)*. This software combines monitoring and geographical knowledge in order to analyze technical, environmental and economic factors of the production of electricity from photovoltaic systems. In short, *PVGIS* photovoltaic provides an inventory of solar energy and its geographical evaluation based on maps, allowing a quick calculation of the average production of the system also related to future years, based on reliable data and tables.

In particular, there is a new version of *PVGIS* that allows you to extrapolate the hourly energy production data by providing some input data.

The goal is to download the hourly energy production data of a 50 kWp PV system located in the same area where the Fintry Sports Club is located and check whether by applying (5.5) to the power data of the whole year before and to the power data of the six months later (from April 24 to October 31) the regression coefficients μ_1 , μ_2 and μ_3 are very different from each other.

It is important to clarify how up to now the new version of *PVGIS* is able to provide hourly data up to 31st December 2016, so it is not possible to download data for the year 2017 analyzed in this thesis work. However, it is evident that in this case it is not important that the year in *PVGIS* coincides with the one analyzed.

Tab 5.2 shows the input data supplied to *PVGIS*, while Fig 5.11 shows the theoretical produced power trend by a 50 kWp PV system installed in the same area where the Fintry Sports Club places using *PVGIS* data.

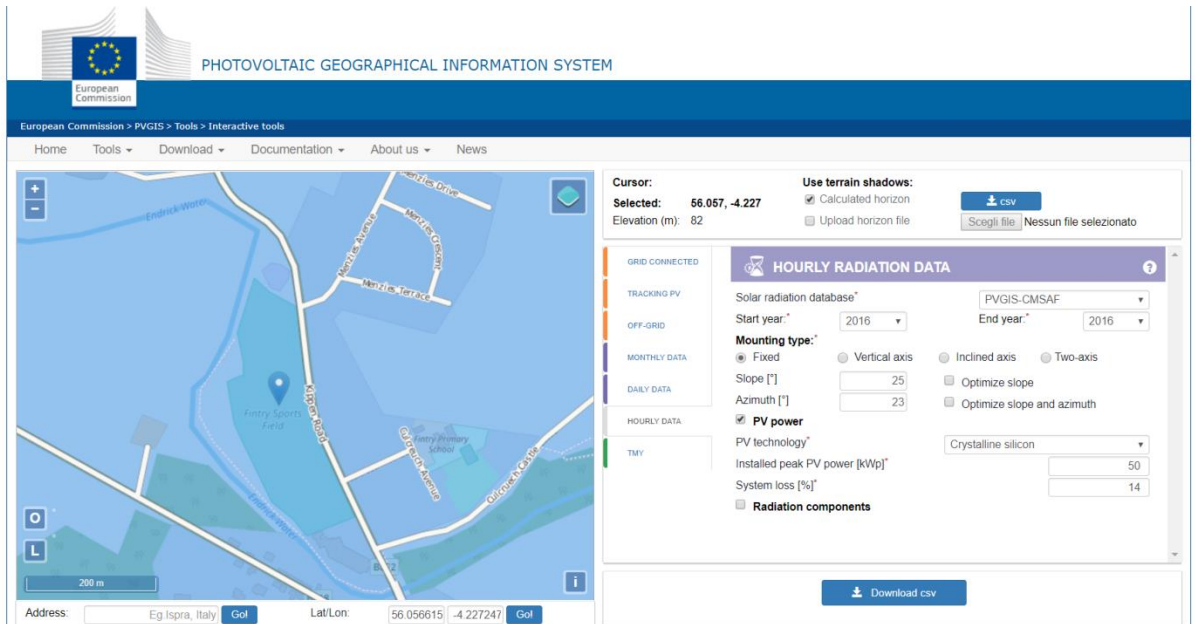


Fig 5.10: PVGIS interface.

Solar radiation database	PVGIS-CMSAF
Start year	2016
End year	2016
Mounting type	Fixed
Slope [°]	25
Azimuth [°]	23
PV technology	Crystalline silicon
Installed peak PV power [kWp]	50
System loss [%]	14

Tab 5.2: Input data for PVGIS to obtain the power data of a 50 kWp system in the same area of the Fintry Sports Club.

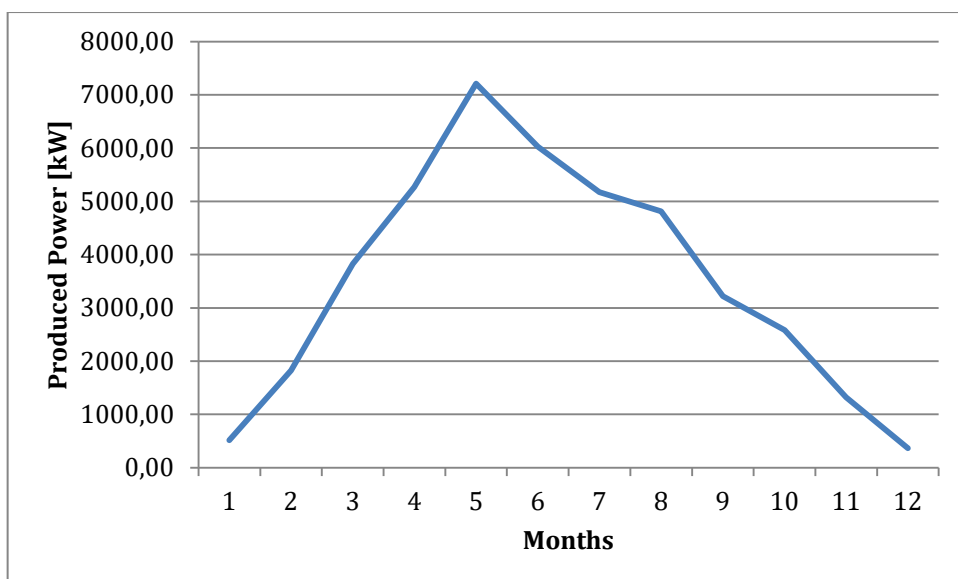


Fig 5.11: Produced power trend in 2016 of the Fintry Sports Club system using PVGIS data.

The results obtained by applying the model (5.5) to the hourly data provided by PVGIS are shown in Tab 5.3.

Database	μ_1	μ_2	μ_3
1 year	47,6801	-0,0020	-0,2230
6 months	47,7965	-0,0020	-0,2313
Percentage difference	0,24%	0,00%	3,59%

Tab 5.3: Results of the model (5.5) applied to the PVGIS data considering the all the year 2016 and only 6 months in 2016.

It is evident that the three regression coefficients calculated considering in one case the data for the whole year 2016 and in the other case the data for only six months of the year 2016 have very similar values. The percentage difference between the values of the two cases is very low so it can be concluded that, for a 50 kWp photovoltaic system located in Fintry, applying the model (5.5) to the whole year generates regression coefficients practically almost equal to those generated when the model is applied to the six months considered.

From the previous first considerations it is clear how it is possible to use the real power data of the 50 kWp PV system supplied from the end of April to the end of October to obtain acceptable values of the three regression coefficients of the model (5.5).

However, an analysis of these data shows that the maximum peak of instantaneous power produced by the 50 kW PV system does not exceed the value of 34,20 kWp, while the values of a system of equal power downloaded from PVGIS have a peak value at 44,55 kWp (Tab 5.4).

Database	$P_{MAX 50kWp}$ [kW]
Real	44,55
PVGIS	34,20

Tab 5.4: Power peaks produced by the 50 kWp PV system using real data and PVGIS data considering the area of the Fintry Sports Club.

This may be due to several factors, such as the fact that the PVGIS data do not take into account any areas of shade due to the presence of trees or elements that represent an obstacle to solar radiation.

However, the main cause of this inconsistency between the peak production values obtained from real data and those obtained from PVGIS can be traced back to temperature. As reported by Kaldellis et al. (2014), "as the cell temperature increases the cell voltage decreases and the corresponding current is slightly increased, all together reducing the power output of a given PV generator". In this regard, Fig 5.12 shows the graph that describes the impact caused on the efficiency of photovoltaic panels

due to the increase in cell temperature and studied by the research team of Soft Energy Applications and Environmental Protection Lab (Kaldellis et al., 2014).

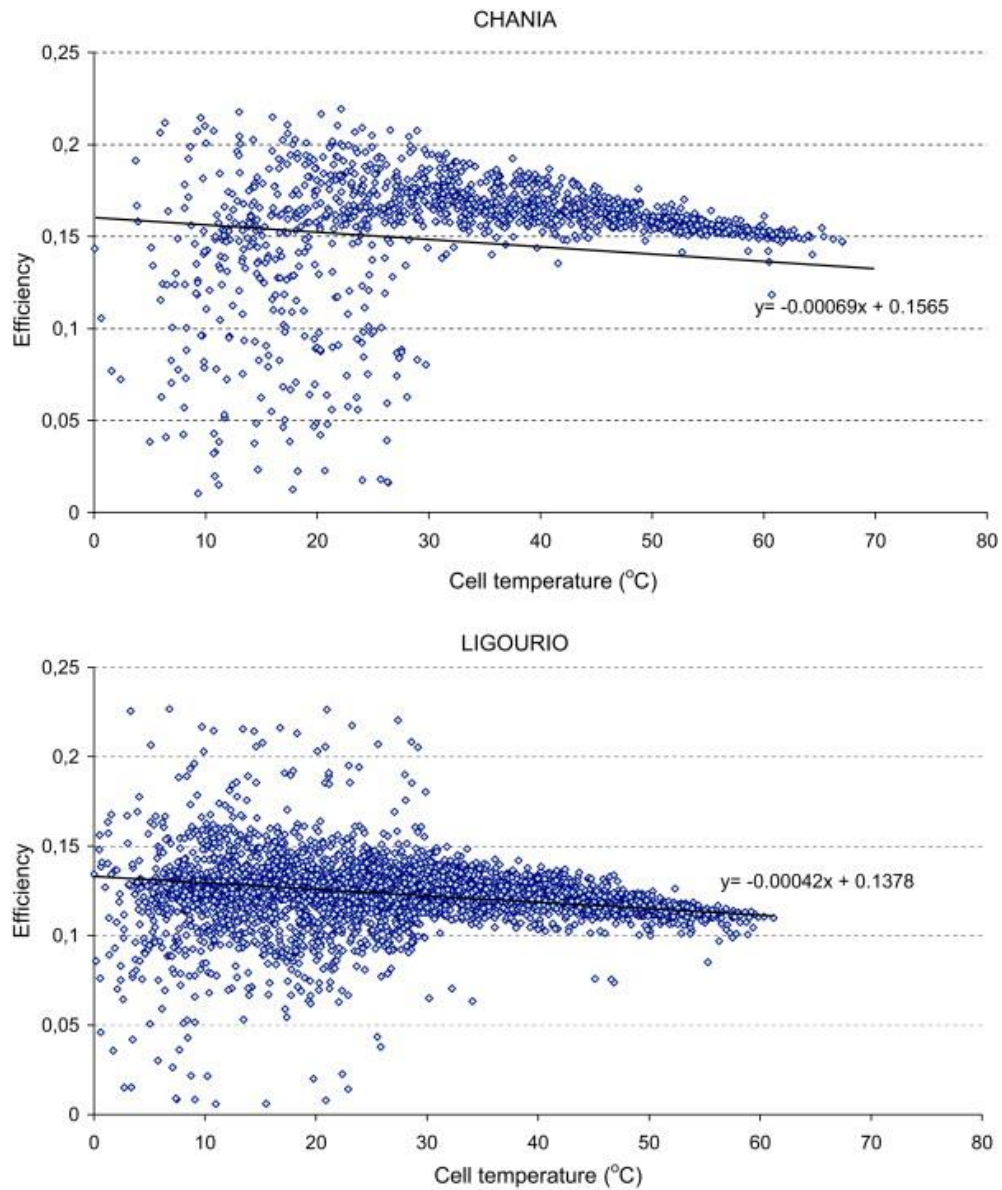


Fig 5.12: Impact of temperature variation on the efficiency of PV modules as recorded by the research team of the lab in field measurements carried out at the Greek regions of Chania and Ligourio (Kaldellis et al., 2014).

It is well known that the negative effect of temperature on the photovoltaic cell depends a lot on the material of the cell itself. From the technical data relating to the type of cell installed on Fintry Sports Club (Fig 5.5), it results that the power of a photovoltaic module decreases by 0,43% per Kelvin degree (K) of increase in the cell temperature.

In the case analyzed, it is necessary to consider the fact that the photovoltaic modules are mounted on corrugated sheets, which heat up a lot if subjected to the effect of solar radiation. Since the roof is isolated, it is evident that solar panels make it very difficult to ventilate. Tab 5.4 shows the power peaks respectively of the real da-

tabase (year 2017) and the downloaded database from PVGIS (year 2016) produced by the 50 kWp PV system while Fig 5.13 and Fig 5.14 show the power trend during a sunny day extrapolated respectively from the real database (year 2017) and the PVGIS database (2016) when the PV system considered reaches the power peak.

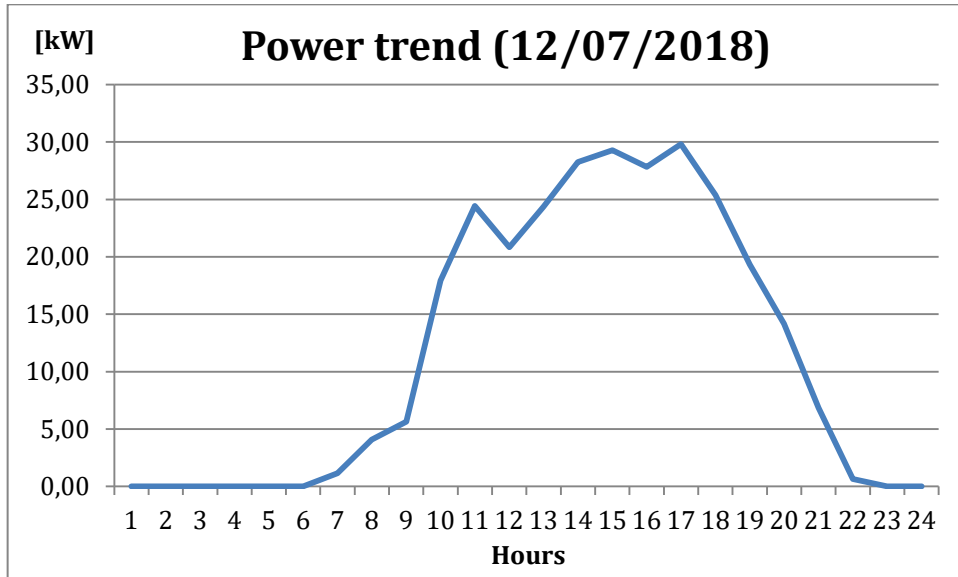


Fig 5.13: Power trend of the 50 kWp PVsystem on 03/05/2016 extrapolated from real data.

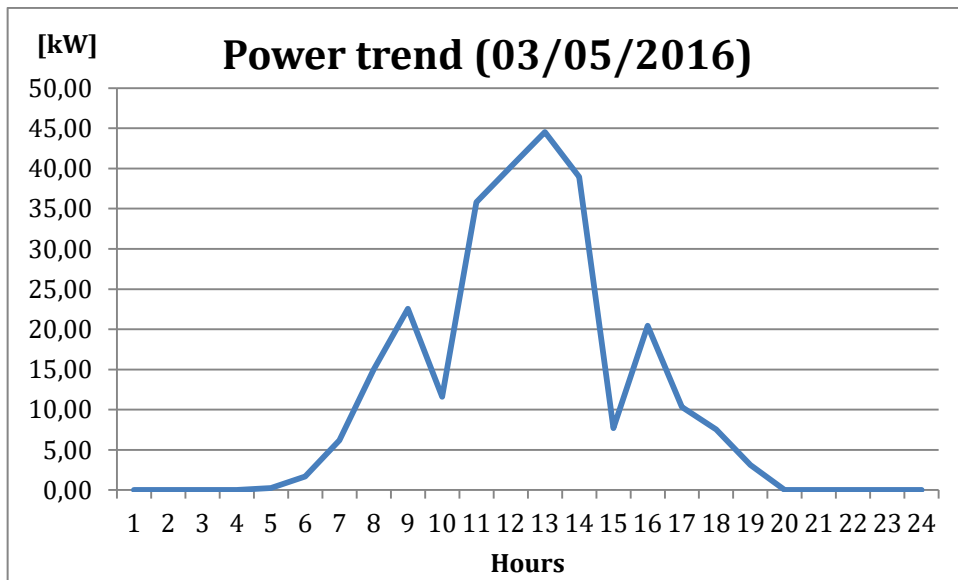


Fig 5.14: Power trend of the 50 kWp PVsystem on 03/05/2016 extrapolated from PVGIS data.

A very similar example is provided by the PV system installed on the roof of the *Polytechnic University of Turin*. This system has a nominal power of 600 kWp and is installed on corrugated metal sheets as well. It consists of *SunForte PM096B00* panels rated at 320 W (Fig 5.15).

SunForte PM096B00 (320 ~ 333 Wp)

Dati elettrici

	320W	325W	327W	330W	333W
Potenza nominale P_N	320W	325W	327W	330W	333W
Efficienza modulo	19.6%	19.9%	20.1%	20.3%	20.4%
Tensione nominale V_{mp} (V)	54.7	54.7	54.7	54.7	54.7
Corrente nominale I_{mp} (A)	5.86	5.94	5.98	6.04	6.09
Tensione a circuito aperto V_{oc} (V)	64.8	64.9	64.9	64.9	64.9
Corrente di corto circuito I_{sc} (A)	6.27	6.39	6.46	6.52	6.58
Tolleranza massima di P_N	0 / +3%				

*I dati riportati rappresentano i valori misurati a STC (Standard Test Conditions)
 * STC: irradiazione 1000W/m², distribuzione spettro AM 1.5, temperatura 25 ± 2° C, in conformità con EN 60904-3
 * I dati elettrici forniti sono valori nominali in base a misurazioni di base e tolleranze di produzione del ±10%, a eccezione della P_N .
 Le classificazioni sono eseguite in base alla P_N .

Coefficiente di temperatura

NOCT	45 ± 2 °C
Coefficiente di temperatura di P_N	-0.33 % / K
Coefficiente di temperatura di V_{oc}	-0.26 % / K
Coefficiente di temperatura di I_{sc}	0.05 % / K

* NOCT: Normal Operation Cell Temperature, temperatura operativa normale cella, condizioni di misurazione: irradiazione 800W/m², AM1.5, temperatura dell'aria 20° C, velocità del vento 1m/s

Caratteristiche meccaniche

Dimensioni (lunghezza x larghezza x spessore)	1559 x 1046 x 46 mm (61.38 x 41.18 x 1.81 pollici)
Peso	18.6 kg (41.0 lbs)
Vetro anteriore	Vetro temperato ad alta trasmissione con AR-Tech, 3.2 mm (0.13 pollici)
Cella	96 celle back-contact ad alta efficienza
Foglio posteriore	Pellicola composita
Telaio	Telaio in alluminio anodizzato
Scatola di derivazione	Classificazione IP-67 con 3 diodi di bypass
Tipo di connettore & Cavi	TE Connectivity PV4: 1x4mm ² (0.04x0.16 pollici ²), Lunghezza: ognuno 1.0 m (39.37 pollici)

Dimensione mm [pollici]

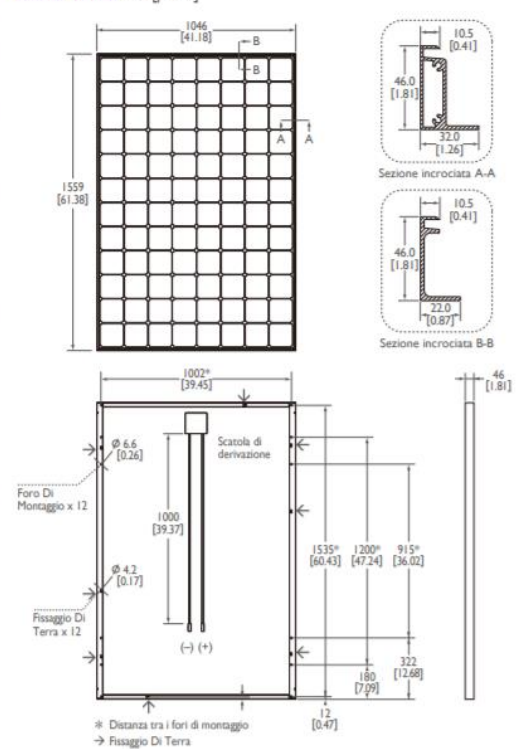


Fig 5.15: Technical specifications of SunForte PM096B00 panels.

Fig 5.16 shows the energy produced by this system during one of the hottest days of 2018 in August, that is on 2nd August 2018.

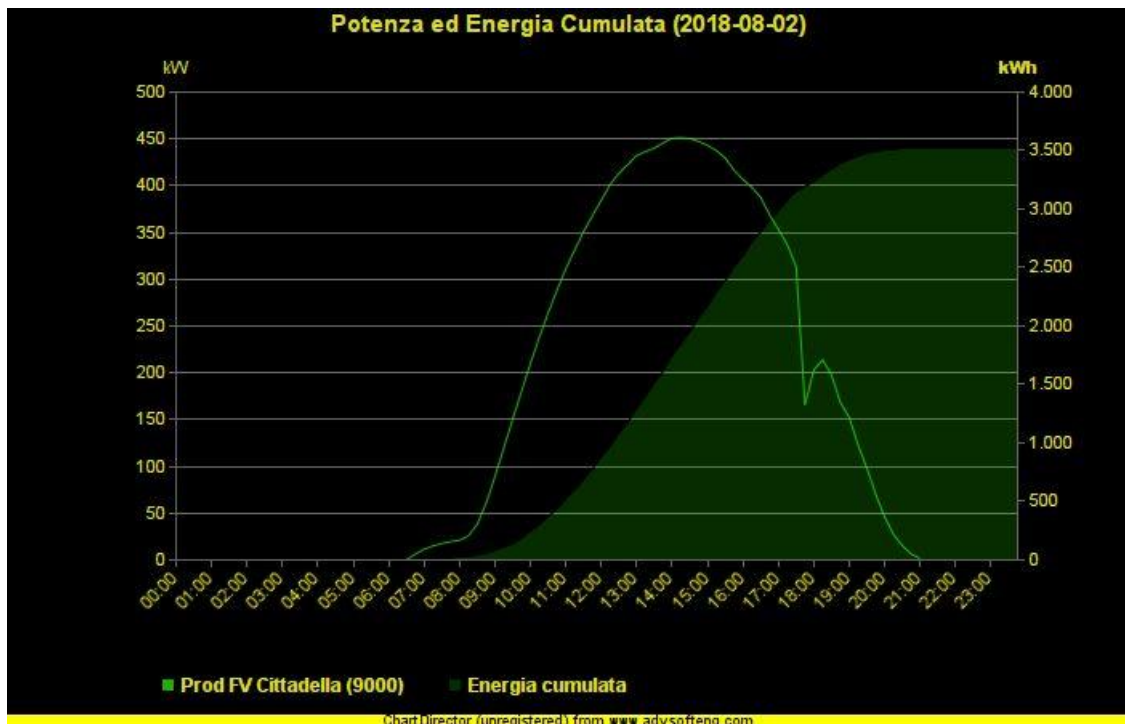


Fig 5.16: Trend of produced energy by the 600 kWp PV system of the Polytechnic University of Turin (www.polito.it).

From the trend shown in Fig 5.16 it is evident that the instantaneous power peak does not exceed 450 kW compared to a nominal instantaneous power equal to 600 kWp. The panels, despite having a lower loss value for each temperature increase of a Kelvin degree ($C_t = -0,33\%/K$, Fig 5.15) than that of the panels used by the Fintry Sports Club ($C_t = -0,43\%/K$, Fig 5.5), do not exploit all the theoretically producible energy and this is due to the too high temperatures that the corrugated sheets on the roof reaches, as it also happens for the PV system of the Fintry Sports Club.

Considering what has been said in points 1 and 2 and considering that it is not conceivable to install photovoltaic modules on corrugated sheets in a residential context, with regard to the calculation of the regression coefficients from (5.5) in this thesis work it was chosen to use the values obtained from the PVGIS data because they represent more truthful and acceptable data for the purposes of an analysis in a residential context compared to the values obtained from the Fintry Sport Club data.

5.1.4 Assignment of the PV system size

A PV system of a certain size is assigned to each of the 42 houses examined. For the choice of the system it is necessary to underline the difference that exists between the concepts of "kilowatt" (kW) and "kilowatt hour" (kWh). Although aesthetically similar, these two units of measurement are completely different.

The kilowatt is a unit of power, and it is the unit that appears for example when a contract is signed with an energy provider. Having a 3 kWp contract with a supplier

indicates that an instantaneous power up to a maximum of 3 kW can be taken from the grid. In case that several household appliances are used simultaneously in a house to exceed the instantaneous limit threshold, the current meter will interrupt the flow of electricity and the house will be in the dark.

Consequently, installing a 3 kW photovoltaic system indicates that the maximum instantaneous power delivered by the panels cannot exceed this threshold. However, since solar energy is intermittent, the performance of the power produced is not constant and the peak will only be reached in optimal conditions that rarely occur.

The kilowatt hour is a unit of energy and therefore expresses all the power delivered during a certain period of time. Ultimately, the kilowatt hour indicates the amount of energy consumed in a day, a month or a year and represent another important parameter to consider when choosing a photovoltaic system.

The sizing of a photovoltaic system is very complex to carry out as it depends on a series of factors not only *climatic* but also *technical, economic, architectural* that must be analyzed in their interaction.

An essential factor to consider is that as an intermittent energy generation technology, the PV technology is characterized by low energy density. In other words a system able to reach a capacity of 3 kWp will be characterized by approximately 24 m² of solar panels (http://www.nextville.it/Solare_fotovoltaico/454/Il_dimensionamento_ottimale). This clearly indicates how the architectural aspect is as important as the energy function.

From an energy point of view one of the main parameters to take into account in order to choose the right size of the PV system is the energy consumption of the house in question. As a first approximation it can be estimated that the PV system could have a nominal power of about the average annual consumption divided by a factor of one thousand in value (<http://www.rinnovabili.biz/calcolo-potenza-fotovoltaico.htm>). For example, if a house produces about 3000 kWh per year of energy it can be considered acceptable to install a 3 kWp PV system.

Tab 5.5 shows the annual consumption values E_{DEMAND} of each node without a PV system during the year 2017, the relative coefficients C obtained by dividing by a factor equal to one thousand and the nominal power P_n of the chosen PV system size.

	Node	E_{DEMAND} [kWh]	C	P_n [kWp]
Group 1	110	3819,41	3,82	3
	80	2674,48	2,67	3
	78	3094,01	3,09	3
	77	3680,33	3,68	3
	76	3596,63	3,60	3
	67	3596,55	3,60	3
	41	3778,93	3,78	3
	31	2081,85	2,08	3
	27	3930,85	3,93	3
	25	3067,73	3,07	3
	12	3287,13	3,29	3

	10	1865,11	1,87	3
	2	3923,61	3,92	3
Group 2	79	5265,94	5,27	6
	73	5156,02	5,16	6
	68	6658,32	6,66	6
	64	5727,30	5,73	6
	62	6893,11	6,89	6
	59	5995,73	6,00	6
	49	6468,35	6,47	6
	47	4046,33	4,05	6
	42	6021,82	6,02	6
	39	4793,64	4,79	6
	36	5133,12	5,13	6
	32	5859,64	5,86	6
	13	4775,44	4,78	6
	9	6124,39	6,12	6
	4	5918,56	5,92	6
Group 3	96	19166,32	19,17	9
	82	14393,67	14,39	9
	75	15612,94	15,61	9
	63	9941,68	9,94	9
	57	12264,56	12,26	9
	53	12384,11	12,38	9
	44	9245,28	9,25	9
	37	15079,49	15,08	9
	23	9752,61	9,75	9
	11	8318,10	8,32	9
	7	7014,41	7,01	9
	6	25501,19	25,50	9
	5	7602,62	7,60	9
	3	20936,06	20,94	9

Tab 5.5: Annual demand of each node in 2017 and relative coefficients calculated to sizing the PV systems.

It is necessary to underline how the PV systems have been assigned to each of the considered houses taking into account only the quantity of energy produced annually. For the choice of the best PV system the variables to be taken into consideration are more: the climatic conditions of the area where the house is located on which to install the PV system, its exposure to sunlight, the size of the roof of the house (area up which in most cases the panels are mounted), the needs of the customer who may wish to focus on the sale of the energy produced or simply to the self-consumption of it.

Without all the data necessary to carry out a detailed, the hypothesis of assigning as a first approximation a PV system of power equal to the value of the annual energy used divided a coefficient equal to one thousand can be considered definitely valid

(<https://www.fotovoltaiconorditalia.it/idee/impianto-fotovoltaico-3-kw-dimensioni-rendimenti>).

Consequently, three different PV system sizes were chosen with nominal power of 3 kWp, 6 kWp and 9 kWp to be assigned to each house according to the different energy needs. The criterion chosen for the PV system assignment is shown in (5.12):

$$P_n = \begin{cases} 3, & C < 4 \\ 6, & 4 \leq C < 7 \\ 9, & C \geq 7 \end{cases} \quad (5.12)$$

The PVUSA multiple linear regression model was used again to calculate the energy produced by a PV system of those sizes. The number of unknowns is now greater because in addition to the values of the new regression coefficients μ_1', μ_2', μ_3' the values of the power delivered by the system and contained in the vector \mathbf{p}' are not known.

However, it is immediate to calculate the values of the regression coefficients of a 1 kWp system knowing the values of the regression coefficients related to the 50 kWp PV system and applying a simple proportion:

$$\mu_{50 \text{ kWp}: 50} = \mu_{1 \text{ kWp}: 1} \quad (5.13)$$

Tab 5.6 shows the values of the regression coefficients for a 1 kWp system. Applying the (5.5) and knowing the regression coefficients it is possible to calculate the energy produced in a year by a 1 kWp PV system installed at Fintry (Tab 5.7).

<i>P_n = 1 kWp</i>		
μ_1	μ_2	μ_3
1,430405	-0,00005	-0,0067

Tab 5.6: Regression coefficients for a 1 kWp system.

Month	<i>P_n = 1 kWp</i>
1	9,90
2	19,41
3	45,90
4	79,08
5	130,52
6	98,24
7	95,82
8	90,63
9	52,10
10	25,59

11	11,60
12	6,99
Tot	665,80

Tab 5.7: Energy produced by a 1 kWp PV system in the same area where the Fintry Sports Club is placed calculated using PVUSA model.

In order to understand if the energy values produced by a 1 kWp PV system are acceptable, it is possible to compare the data supplied by PVGIS for an equal system. As shown in Fig 5.17 the data provided by PVGIS are not too different from the calculated values (the percentage difference between the total values of the annual produced energy is about 8%).

Fixed system: inclination=25°, orientation=23°				
Month	E_d	E_m	H_d	H_m
Jan	0.41	12.7	0.56	17.4
Feb	1.06	29.7	1.39	38.9
Mar	2.11	65.5	2.76	85.5
Apr	3.05	91.6	4.11	123
May	3.59	111	4.93	153
Jun	3.37	101	4.74	142
Jul	3.20	99.1	4.49	139
Aug	2.69	83.4	3.70	115
Sep	2.10	63.0	2.83	85.0
Oct	1.25	38.6	1.64	50.9
Nov	0.64	19.2	0.85	25.5
Dec	0.27	8.44	0.39	12.2
Yearly average	1.98	60.3	2.71	82.3
Total for year		724		988

Fig 5.17: Energy produced by a 1 kWp PV system in the same area where the Fintry Sports Club is placed provided by PVGIS.

As a result, a new set of values for the three regression coefficient is obtained for each of the three different sizes of the selected PV systems (Tab 5.8, Tab 5.9, Tab 5.10).

$P_n = 3 \text{ kWp}$		
μ_1	μ_2	μ_3
2,86081	-0,0001	-0,0134

Tab 5.8: Regression coefficients for a 3 kWp system.

<i>P_n = 6 kWp</i>		
μ_1	μ_2	μ_3
5,72161	-0,0002	-0,0268

Tab 5.9: Regression coefficients for a 6 kW system.

<i>P_n = 9 kWp</i>		
μ_1	μ_2	μ_3
8,58242	-0,0004	-0,0401

Tab 5.10: Regression coefficients for a 9 kW system.

Once the new regression coefficients were obtained, the regression model was applied to each node to obtain the power theoretically produced by a PV system of 3 kWp, 6 kWp and 9 kWp depending on the weather conditions for the year 2017 considered.

The input data related to the nodes are provided in different Microsoft Excel files and discretized by month, ie they contain each data of all the nodes related to a single month. Therefore it was necessary to create a new file in which the data were combined according to the node so as to associate all the weather data for 2017 with each node.

Moreover, the data relating to each node are provided every 30 minutes for which it was necessary to reorder and synchronize such data by suitably modifying the discretization time interval and making it equal to the time interval of discretization of the weather conditions. Consequently, a macro in VBA was performed to synchronize the weather data and power data related to the previously analyzed sports center.

It may be useful to calculate the normal distribution of annual energy data demanded to better visualize the results obtained. Tab 5.11 shows the mean and standard deviation values related to the energy values consumed annually.

Mean μ	Standard Deviation σ^2
18,44	11,56

Tab 5.11: Standard deviation and mean values referring to the annual energy demand in 2017 of each node.

Tab 5.12 shows the values of the normal distribution related to the annual energy consumed E_{DEMAND} .

Node	E_{DEMAND} [kWh]	Normal Distribution
110	3819,41	6,02E-05
80	2674,48	5,04E-05
78	3094,01	5,41E-05
77	3680,33	5,91E-05
76	3596,63	5,84E-05
67	3596,55	5,84E-05

41	3778,93	5,99E-05
31	2081,85	4,51E-05
27	3930,85	6,11E-05
25	3067,73	5,39E-05
12	3287,13	5,58E-05
10	1865,11	4,32E-05
2	3923,61	6,10E-05
79	5265,94	7,03E-05
73	5156,02	6,96E-05
68	6658,32	7,58E-05
64	5727,30	7,26E-05
62	6893,11	7,62E-05
59	5995,73	7,38E-05
49	6468,35	7,53E-05
47	4046,33	6,20E-05
42	6021,82	7,39E-05
39	4793,64	6,74E-05
36	5133,12	6,95E-05
32	5859,64	7,32E-05
13	4775,44	6,72E-05
9	6124,39	7,42E-05
4	5918,56	7,34E-05
96	19166,32	6,05E-06
82	14393,67	3,14E-05
75	15612,94	2,23E-05
63	9941,68	6,83E-05
57	12264,56	4,99E-05
53	12384,11	4,88E-05
44	9245,28	7,22E-05
37	15079,49	2,61E-05
23	9752,61	6,94E-05
11	8318,10	7,56E-05
7	7014,41	7,64E-05
6	25501,19	1,86E-07
5	7602,62	7,66E-05
3	20936,06	2,66E-06

Tab 5.12: Normal distribution values referring to the annual energy used of each node.

Fig 5.18 shows the trend of the normal distribution of the annual energy used values for the analyzed nodes.

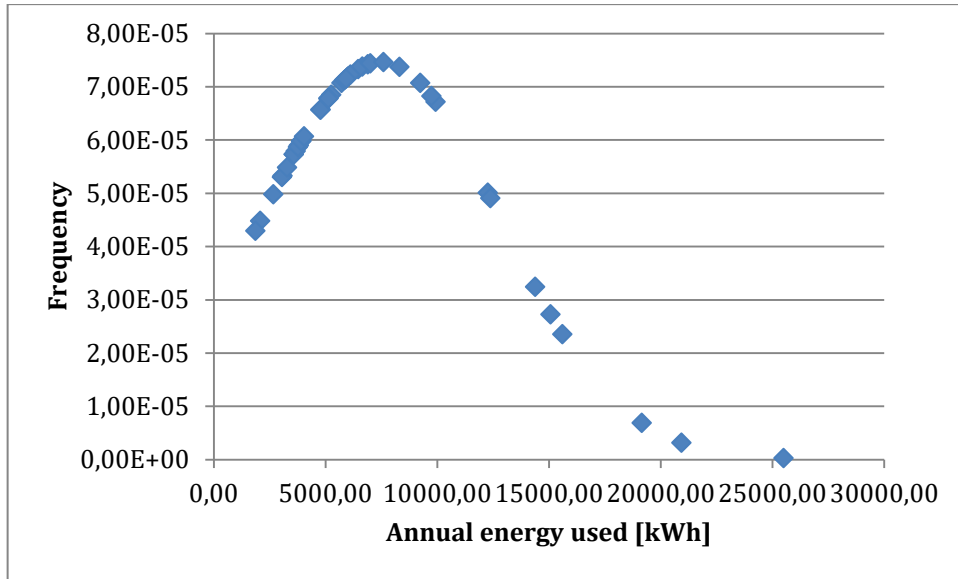


Fig 5.18: Frequency of nodes depending on the total yearly energy used in 2017 of each node.

5.1.5 Results

Depending on the size of the PV system required, the energy produced by the PV system was calculated every 30 minutes. Reminding the (5.5) and knowing that the photovoltaic energy is calculated every 30 minutes, the energy produces is described by (5.16):

$$E_{PV} = 0,5 \cdot (\mu'_1 I + \mu'_2 I^2 + \mu'_3 IT) \quad (5.16)$$

Obtained in kilowatt hour (kWh), with μ'_1 , μ'_2 , μ'_3 the regression coefficients for a PV system of size 3, 6 or 9 kWp according to the considered node.

Therefore the *net energy* E_{NET} is defined as the difference between the demand and the photovoltaic energy, whose value represents the amount of energy required to the network or fed into the grid net of the energy created thanks to the photovoltaic panels depending on the demand is greater than that produced or vice-versa. Consequently the net energy will have positive values if the house requires more energy than the PV system generates while it will have negative values if the energy created thanks to the solar rays, in addition to covering the energy needs of the house, is enough to be given to the network and therefore sold. The energy required to the network in absolute value in case the PV system produces less energy than necessary is indicated with E_{OUT} while the energy fed into the network expressed in absolute value is indicated with E_{IN} . The E_{NET} is described by (5.17):

$$E_{NET} = \begin{cases} -E_{OUT}, & E_{DEMAND} - E_{PV} < 0 \\ 0, & E_{DEMAND} - E_{PV} = 0 \\ E_{IN}, & E_{DEMAND} - E_{PV} > 0 \end{cases} \quad (5.17)$$

For the sake of simplicity, the results relating to the representative node of each of the three groups of houses obtained by considering three different nominal power values of the assigned PV system (nodes 78, 59, 7) are shown below.

The node representative of the first group of houses characterized by PV systems assigned by 3 kWp is *node 78* (Fig 5.19, Fig 5.20 and Fig 5.21).

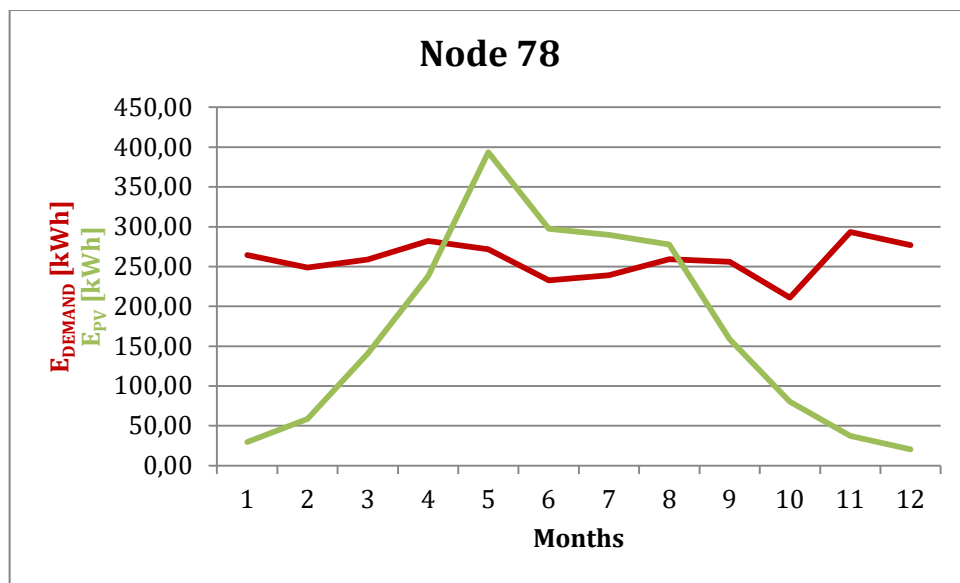


Fig 5.19: Energy trend of the house demand and PV energy produced for the node 78 (group 1).

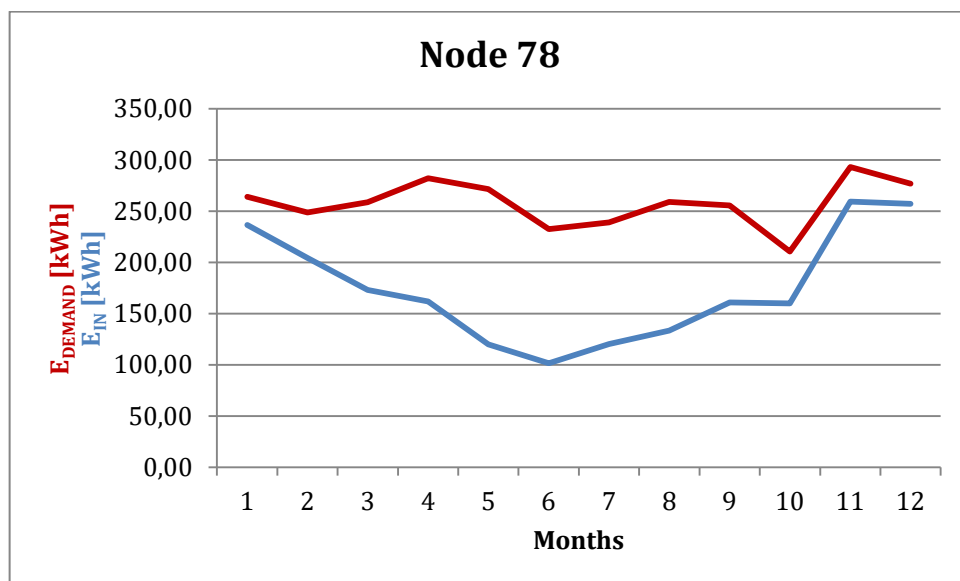


Fig 5.20: Energy trend of the house demand and the net house demand after the installation of a 3 kWp PV system for the node 78 (group 1).

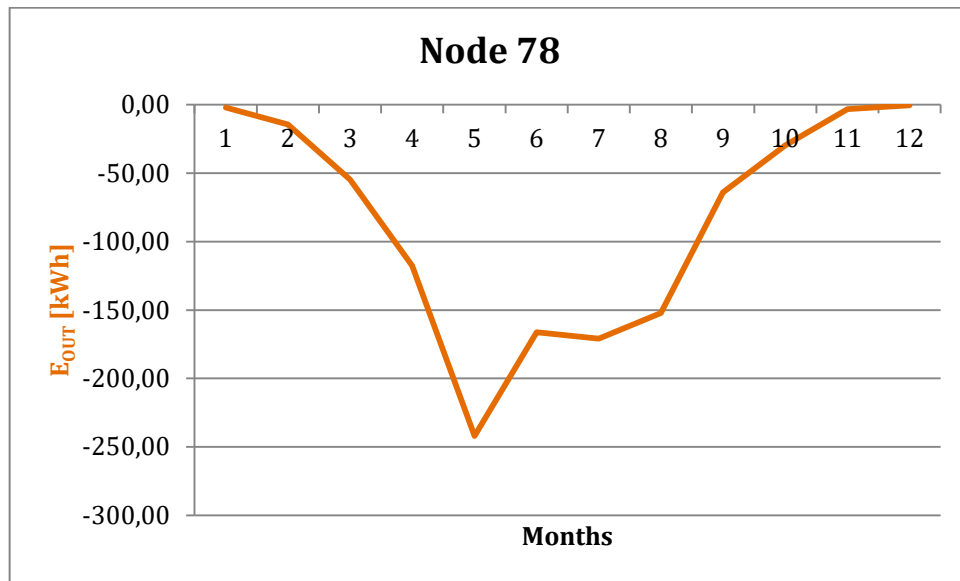


Fig 5.21: Energy trend of the excess energy which is fed into the grid from the node 78 (group 1).

The representative node of the second group of houses characterized by PV systems assigned by 6 kWp is *node 59* (Fig 5.22, Fig 5.23 and Fig 5.24).

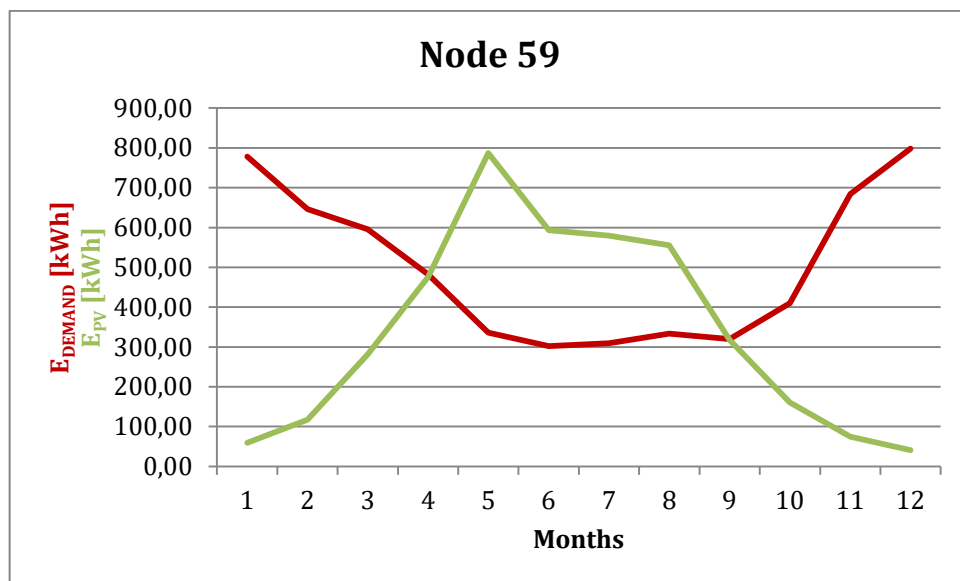


Fig 5.22: Energy trend of the house demand and PV energy produced for the node 59 (group 2).

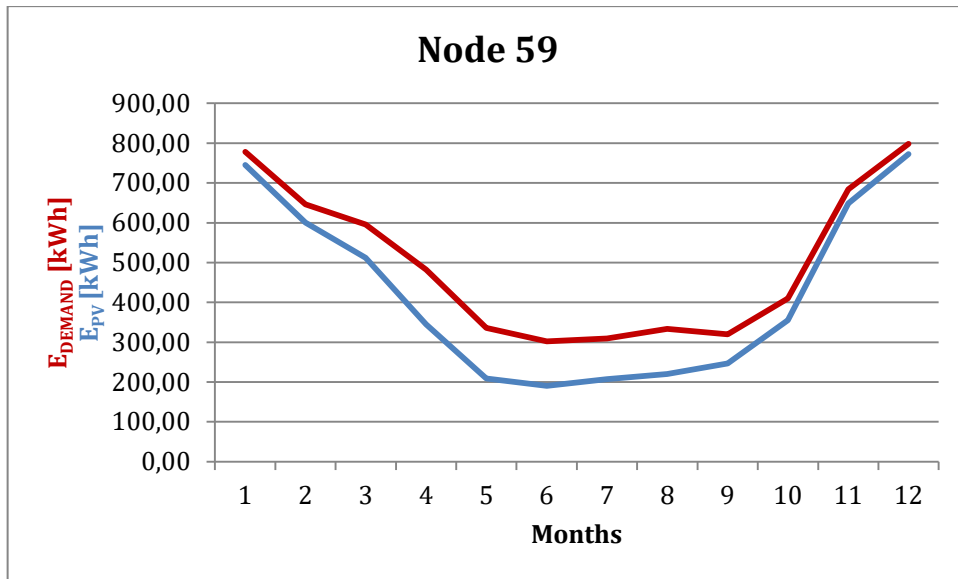


Fig 5.23: Energy trend of the house demand and the net house demand after the installation of a 6 kWp PV system for the node 59 (group 2).

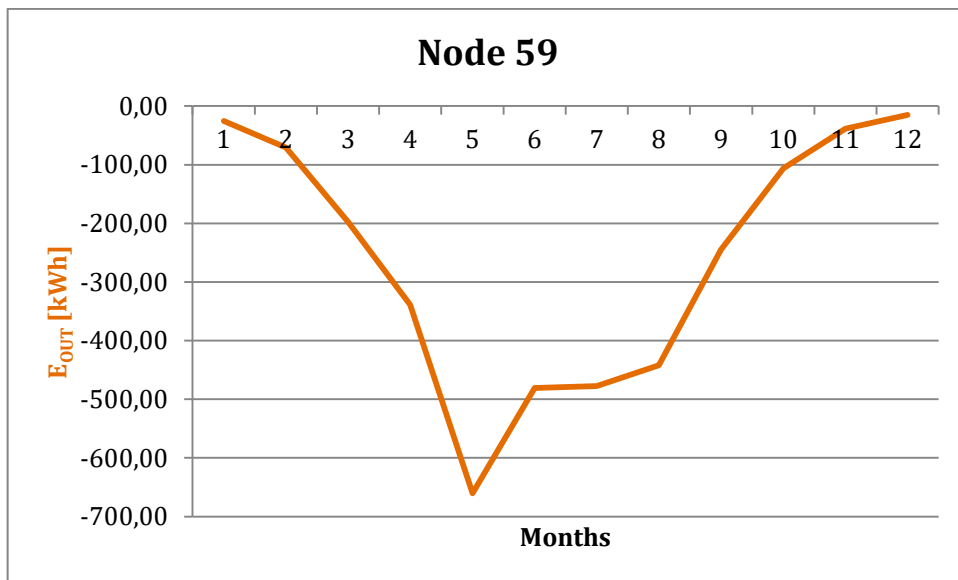


Fig 5.24: Energy trend of the excess energy which is fed into the grid from the node 59 (group 2).

The node representing the third group of houses characterized by PV systems assigned by 9 kWp is *node 7* (Fig 5.25, Fig 5.26 and Fig 5.27).

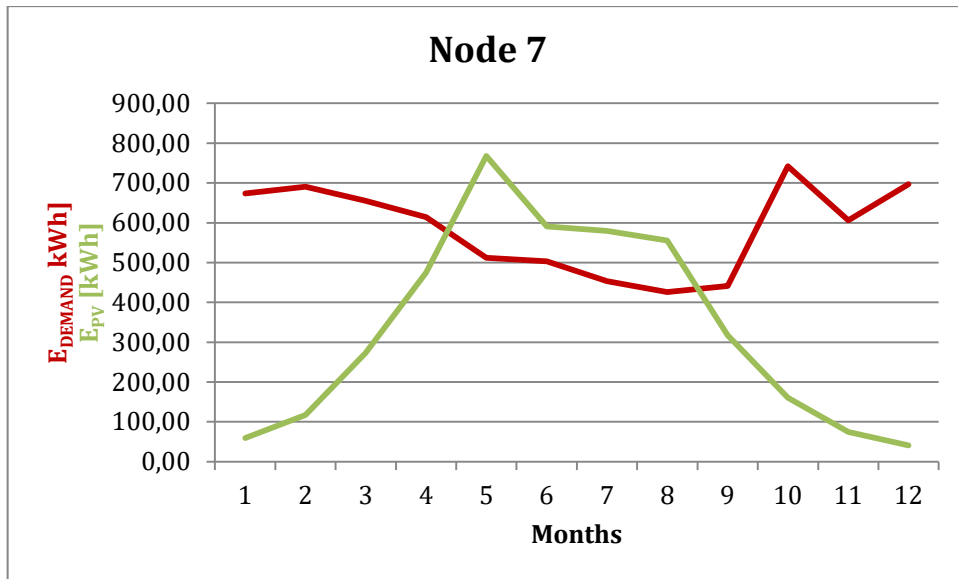


Fig 5.25: Energy trend of the house demand and PV energy produced for the node 7 (group 3).

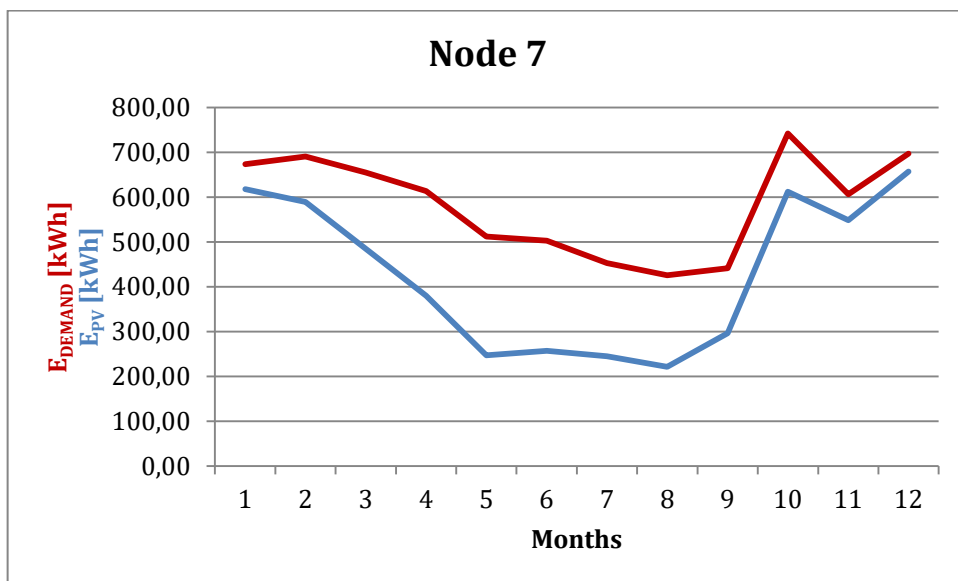


Fig 5.26: Energy trend of the house demand and the net house demand after the installation of a 9 kWp PV system for the node 7 (group 3).

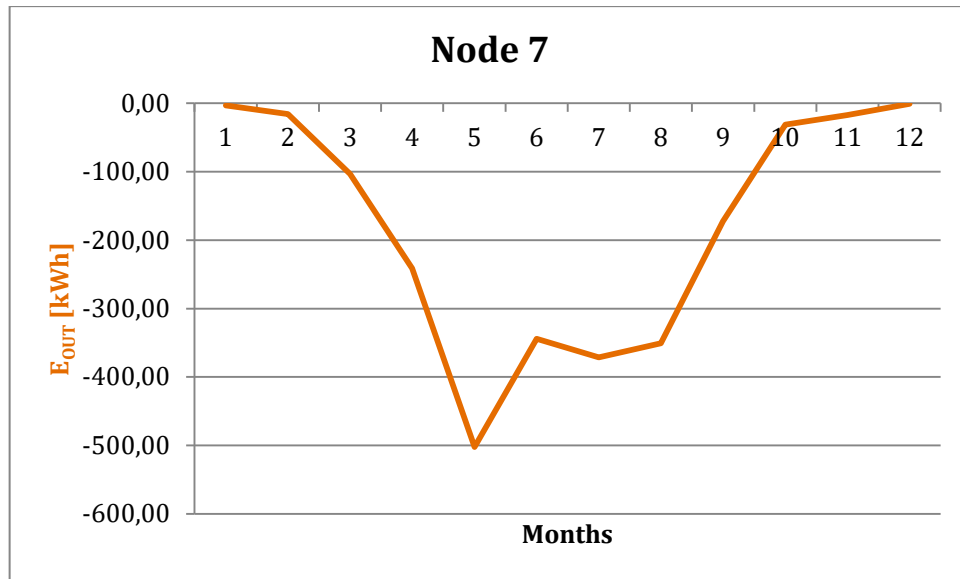


Fig 5.27: Energy trend of the excess energy which is fed into the grid from the node 7 (group 3).

Fig 5.19, Fig 5.22 and Fig 5.25 show the trend of the energy required by the house in the absence of the installed PV system and the trend of the energy produced by the PV system assigned and calculated by applying the PVUSA regression model. The trend of the latter has zero values during the autumn and winter months while it shows positive values during the spring and summer months reaching a maximum value. The area between the demand curve and the solar energy curve represents self-consumption along with the eventual part of excess energy that will be fed into the network.

Fig 5.20, Fig 5.23 and Fig 5.26 show the trends of the new demand that is taken from the grid after the introduction of the PV system compared with the demand before to assign the PV system for nodes 78, 59 and 7 respectively. The new demand is evidently having values lower than those of the demand in the case in which there is no energy produced by the PV system.

On the other hand, the portion of excess energy produced during the diurnal peaks when the demand is much lower is fed into the network and shown in Fig 5.21, Fig 5.24 and Fig 5.27 through a specular trend to the energy produced by the PV system and negative, which represents the sale of this energy.

The sources of income that derive from the installation of a PV system are represented by a reduction in the energy requested from the network and paid to the institution, and by the excess energy fed into the network and sold, albeit at a lower price than that of energy sold by the body.

5.2 Solar-PV-battery system

The solar-PV-battery system is a good alternative to the simple solar-PV system connected to the grid. The combination of the PV system and the BESS (Battery Energy Storage System) makes it possible to store a part of the excess electricity produced by PV inside the battery which will then be used later during the nighttime when the panels do not produce energy or when the PV system cannot completely satisfy the energy demand by itself. Fig 5.28 shows the simplified functional scheme of a combined PV-battery system.

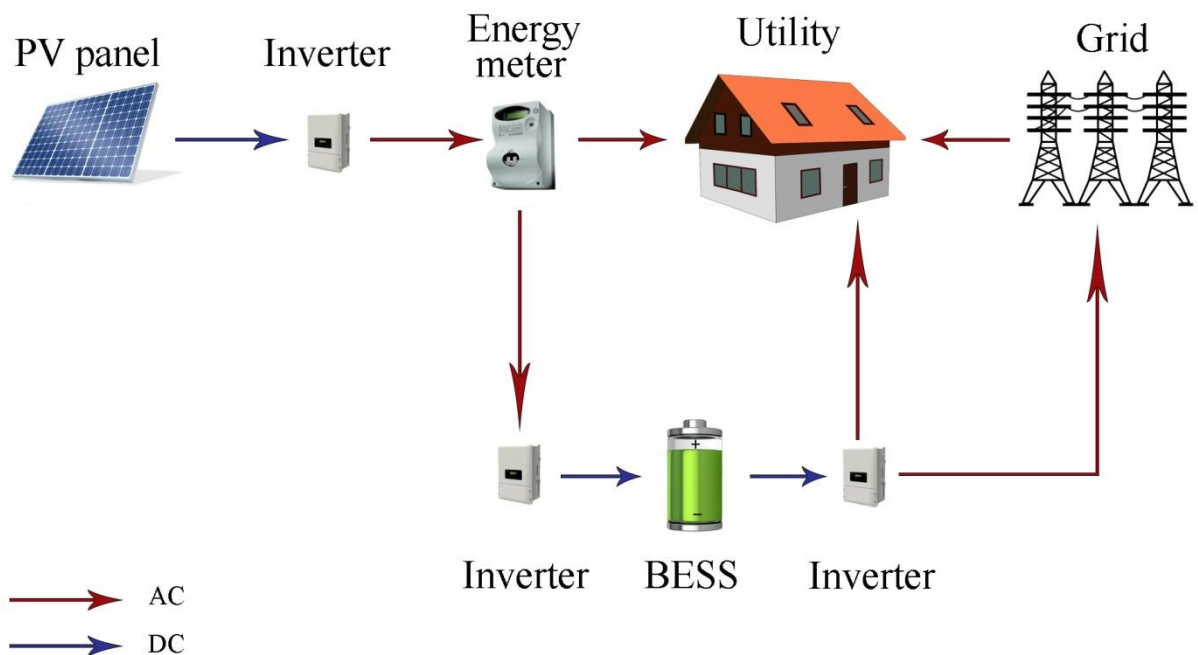


Fig 5.28: Grid-connected PV-battery system scheme.

Energy storage technologies can be grouped according to the similarities of the storage medium. Fig 5.29 shows a classification scheme of the main energy storage systems (AECOM, 2015).

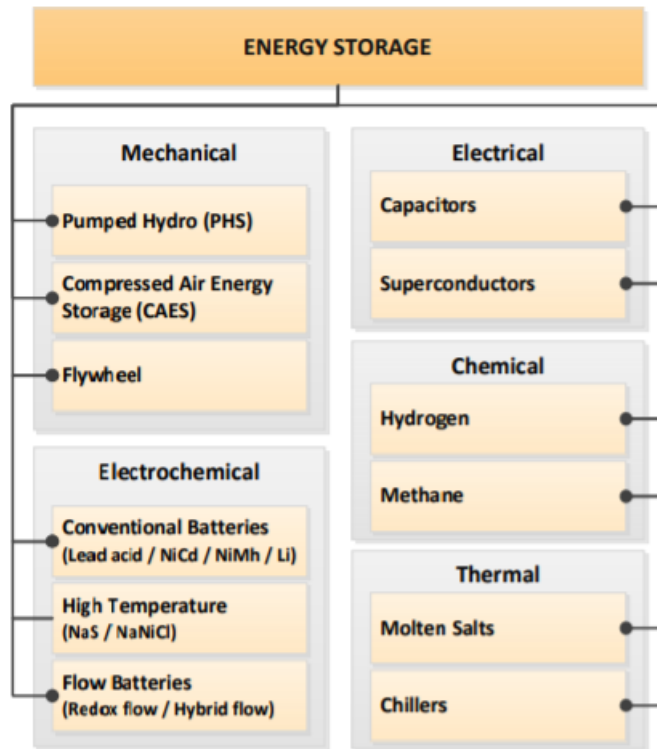


Fig 5.29: Classification of the main energy storage technologies (AECOM, 2015).

As widely reported in the introductory part of this thesis work, the BESS represent the group of energy storage that uses chemical reactions with a certain number of electrochemical cells to allow the flow of electrons. The most common types of batteries are lead-acid batteries, nickel-cadmium (NiCd) batteries, sodium-sulfur (NaS) batteries, lithium-ion batteries, zinc-bromine batteries (ZBr), batteries redox to vanadium (VRB) (Beaudin et al., 2010).

As mentioned, there are different energy storage technologies depending on the storage support used and each of them is in a different phase of development and implementation. Fig 5.30 (AECOM, 2015) shows a comparison between the various energy storage technologies in terms of duration, capital cost and risk. The trend of the maturity curve shows that the most used and fully functional technology is PHS (pumped hydro storage) together with CAES (compressed air energy storage). The BESSs follow immediately, in particular the flow batteries, the lithium-ion batteries and the NaS batteries which are in a phase of distribution with a progressive increase in sales.

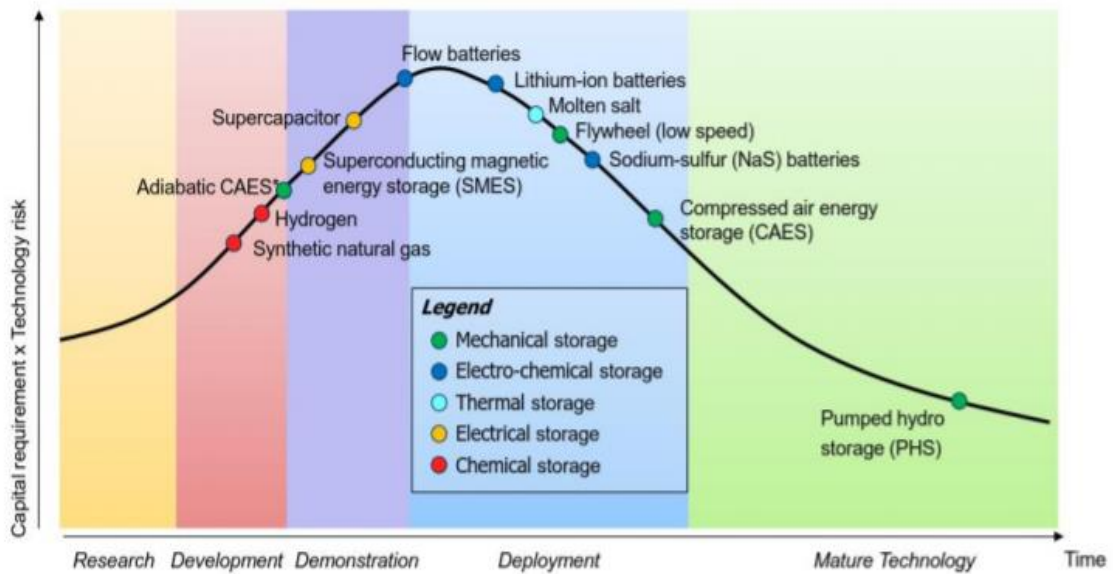


Fig 5.30: Technology maturity curve (AECOM, 2015).

As reported in a paper of AECOM (2015), there is a set of different types of lithium-ion batteries under development, including lithium oxide and cobalt, lithium cobalt manganese, lithium manganese oxide, polymer of lithium and many others. In addition, the same types of lithium-ion batteries may have slightly different characteristics depending on the different manufacturer chosen. Therefore, the lithium-ion battery market is constantly growing and the goal is to reduce capital costs by increasing their energy density.

Even the traditional and older lead-acid batteries are subject to technological improvements thanks to the possible combination with super-capacitors. The idea is to balance the defaults of the two storage devices because the super-capacitors have a high specific power can be loaded and unloaded almost instantly and a high life, but can store much less energy than batteries. The biggest problem with this new technology is the excessively high cost (<http://www.rinnovabili.it/innovazione/storage-ibrido-batterie-supercondensatori-666/>). A paper of AECOM (2015) reports the data collection of the database of the *Department of Energy of the United States* (DoE) in which is reported the historical trend in the project installations (Fig 5.31).

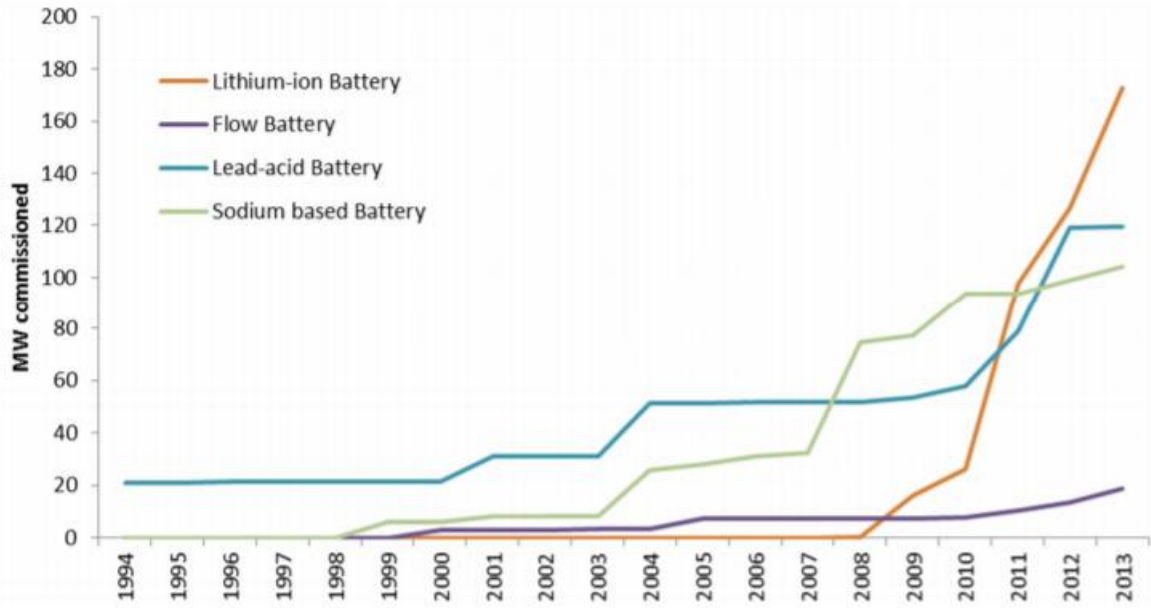


Fig 5.31: Cumulative global capacity of battery storage by technology as listed on the US Department of Energy database (AECOM, 2015).

It is evident that until 2000 the most common technology was lead acid battery, while since 2007 sodium batteries have started to be used more. Subsequently, lithium ion batteries began to spread rapidly to become the best-selling batteries (AECOM, 2015).

5.2.1 Battery model

The battery model was built using Microsoft Excel by setting up a simple logical scheme. However, it does not represent a technical analysis of how the individual components work or how long they work.

In order to understand the built BESS model it is necessary to consider two distinct cases: the first case indicates the situation in which the photovoltaic system is able to produce more energy than the user demand considered, while the second case indicates the situation in which the photovoltaic system produces less energy than the user energy needs. In this regard, some symbols already introduced to indicate certain quantities of energy are recalled and new symbols to indicate other parameters are introduced:

$$E_{PV} = \text{energy produced by the PV system [kWh]}$$

$$E_{DEMAND} = \text{energy required by the user [kWh]}$$

$$E_{SURPLUS} = E_{PV} - E_{DEMAND} = \text{surplus of energy [kWh]}$$

$$E'_{DEMAND} = E_{DEMAND} - E_{PV} = \text{energy required by the user net of } E_{PV} \text{ [kWh]}$$

E_{BESS}^{IN} = energy AC entering the battery [kWh]

$E_{BESS}^{IN'}$ = energy DC entering the battery [kWh]

E_{BESS}^{OUT} = energy DC coming out of the battery [kWh]

$E_{BESS}^{OUT'}$ = energy AC coming out of the battery [kWh]

$E_{STORAGE}$ = energy in the battery [kWh]

$E_{STORAGE}^{MAX}$ = maximum battery capacity [kWh]

$E_{STORAGE}^{MIN}$ = minimum battery capacity [kWh]

E_{IN} = energy taken from the network [kWh]

E_{OUT} = energy fed into the network [kWh]

In the case of a PV-battery system, the net energy E_{NET} defined by (5.17) in the PV system case is defined differently according to the different situations that occur. In case the solar panels produce more energy than required by the user ($E_{PV} > E_{DEMAND}$) then in this case the net energy will be called $E_{SURPLUS}$, that is the excess energy produced by the PV system that can be used to charge the battery or to be fed into the network. In case the energy produced is not sufficient to provide all the energy needed by the user ($E_{PV} < E_{DEMAND}$), the net energy will be called E'_{DEMAND} , that is the amount of energy that the house still needs and which can be taken from the battery or from the network.

Regarding the various components present in a PV-battery system, remember that the batteries are able to accumulate electrical energy in DC, they are characterized upstream and downstream by two inverters capable of transforming DC in AC. The same applies to photovoltaic panels which produce electricity continuously and consequently require a downstream inverter that transforms electricity and makes it usable by users.

In the case studied it is assumed that the value of energy produced by the photovoltaic system indicated with E_{PV} is the energy output from the inverter, therefore already transformed into AC and reduced in value because of the losses inside the photovoltaic inverter. Regarding the two inverters of the battery, the internal losses of these components must be considered through their efficiency whose value is provided by the chosen manufacturer. The same reasoning applies to the internal losses of the battery which is taken into account considering the efficiency of the batteries supplied by the manufacturer.

5.2.1.1 PV energy greater than demand

Considering a typical hot and sunny working day during which the house is almost uninhabited while the PV system produces a lot of energy, then the photovoltaic energy is likely to be far greater than the demand of the user. In the event that the PV system produces an amount of E_{PV} energy greater than that required E_{DEMAND} , there

will be an excess amount of energy $E_{SURPLUS}$ that will be supplied to the battery or fed into the network depending on the various situations that may occur. In the first case it may happen that the sum between the amount of excess energy $E_{SURPLUS}$ and the amount of energy $E_{STORAGE}$ already present in the battery is greater than the maximum capacity of the battery itself $E_{STORAGE}^{MAX}$. This situation can lead to two different conclusions depending on the amount of energy already present in the battery. If the battery is fully charged then the energy surplus is totally fed into the network and then resold to the institution. In other words, considering the boundary conditions (5.18):

$$\begin{cases} E_{PV} > E_{DEMAND} \\ E_{STORAGE} + E_{BESS}^{IN'} \geq E_{STORAGE}^{MAX} \\ E_{STORAGE} = E_{STORAGE}^{MAX} \end{cases} \quad (5.18)$$

The excess energy produced by the photovoltaic system is fed into the grid entirely:

$$E_{OUT} = E_{SURPLUS} \quad (5.19)$$

$$E_{BESS}^{IN} = E_{BESS}^{IN'} = 0 \quad (5.20)$$

Fig 5.32 shows the logical scheme of the situation just described.

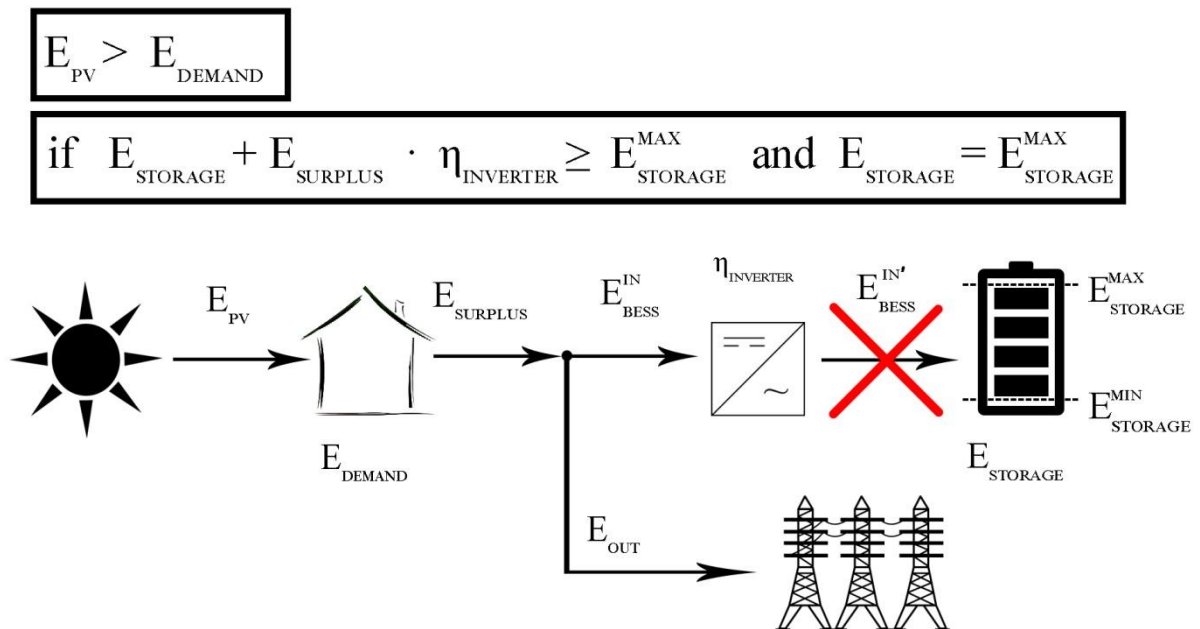


Fig 5.32: Logic functional scheme of the PV-BESS system when the PV system produces an excess of energy and the battery is completely charged.

On the contrary, if the battery is not fully charged then the excess energy must first recharge the battery by going through the upstream inverter and then, once the maximum capacity is reached, be fed into the grid. In terms of energy, given the boundary conditions (5.21):

$$\begin{cases} E_{PV} > E_{DEMAND} \\ E_{STORAGE} + E_{BESS}^{IN'} \geq E_{STORAGE}^{MAX} \\ E_{STORAGE} < E_{STORAGE}^{MAX} \end{cases} \quad (5.21)$$

A certain amount of excess energy will fill the battery while the remainder will be fed into the network:

$$E_{OUT} = E_{BESS}^{IN'} - (E_{STORAGE}^{MAX} - E_{STORAGE}) \quad (5.22)$$

Where the energy given by the difference between the maximum capacity of the batteries and the energy already present inside the battery represents the amount of energy to be supplied to the battery in order to recharge it. Fig 5.33 shows the logical scheme of the situation just described.

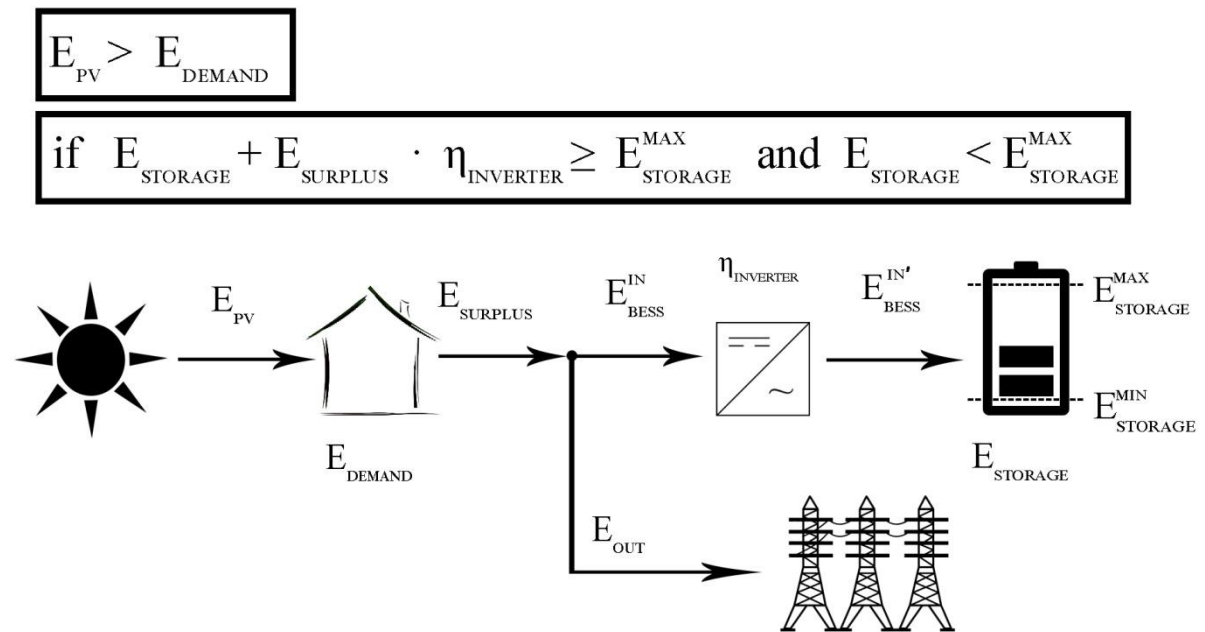


Fig 5.33: Logic functional scheme of the PV-BESS system when the PV system produces an excess of energy and the battery is not completely charged.

On the other hand, when the sum between the amount of energy already present in the battery and the excess of energy produced by the PV system is less than the maximum capacity of the battery, then the excess energy will be totally directed towards

the battery in order to reload. In terms of energy, given the boundary conditions (5.23):

$$\begin{cases} E_{PV} > E_{DEMAND} \\ E_{STORAGE} + E_{BESS}^{IN'} \geq E_{STORAGE}^{MAX} \end{cases} \quad (5.23)$$

The excess energy is completely supplied to the battery:

$$E_{BESS}^{IN} = E_{SURPLUS} \quad (5.24)$$

$$E_{BESS}^{IN'} = E_{BESS}^{IN} \cdot \eta_{INVERTER} = E_{SURPLUS} \cdot \eta_{INVERTER} \quad (5.25)$$

$$E_{OUT} = 0 \quad (5.26)$$

Fig 5.34 shows the logical scheme of the situation just described.

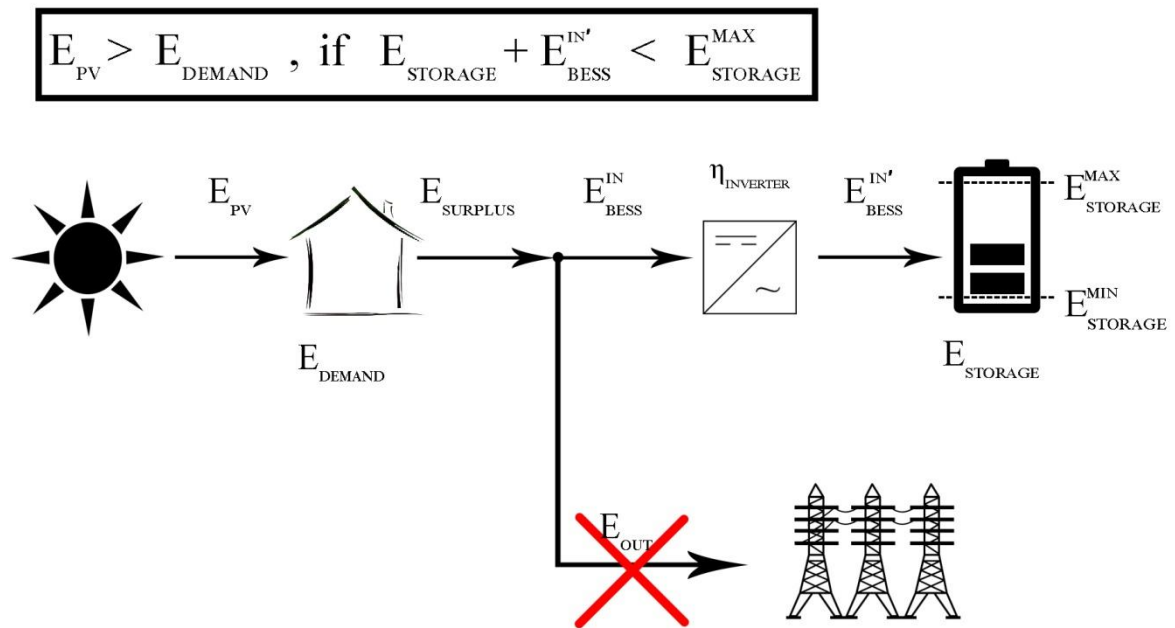


Fig 5.34: Logic functional scheme of the PV-BESS system when the PV system produces an excess of energy which is not able to completely fill the battery.

5.2.1.2 PV energy less than demand

Despite of what previously stated, there may be cases in which the energy produced by the photovoltaic system is not able to ensure the complete energy needs of the users. It could happen that during a not very sunny day and several people at home

at the same time, the demand is substantial. In this case the logical distribution of the energy flows changes.

It is necessary to distinguish three different cases. If the user requires a certain amount of E_{DEMAND} energy and if the amount of E_{PV} energy produced by the PV system is not able to cover the entire required quota, then there will be a certain amount of energy required E'_{DEMAND} net of energy produced by the PV system that the user must take from the battery or from the grid.

In the event that the energy present in the battery is greater than that required by the user (net of the energy produced by the photovoltaic panels), then the user can take the necessary from the battery. In terms of energy, given the boundary condition (5.27):

$$E_{BESS}^{OUT'} \geq E'_{DEMAND} \quad (5.27)$$

The energy required by the user will be taken exclusively from the battery:

$$E_{IN} = 0 \quad (5.28)$$

$$E'_{DEMAND} = E_{BESS}^{OUT'} \quad (5.29)$$

Fig 5.35 shows the logical scheme of the situation just described.

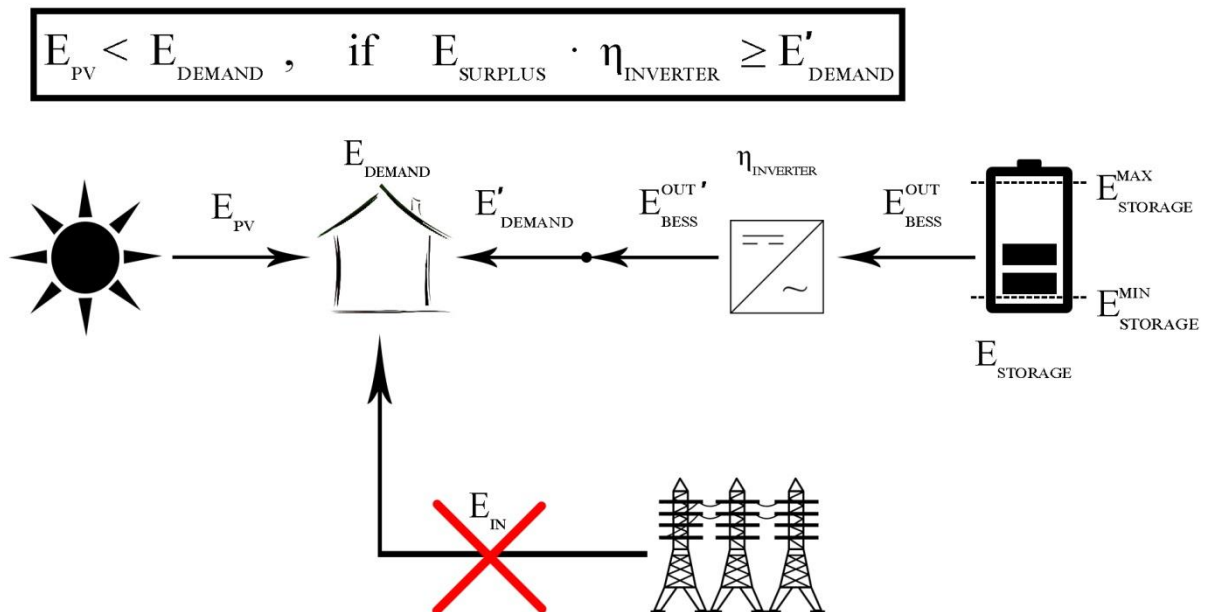


Fig 5.35: Logic functional scheme of the PV-BESS system when the PV system produces less energy than required by the user and the battery is able to provide all the energy it needs.

In the specific case in which the energy present in the battery is equal to the required energy, the functional-logic diagram does not change and the battery will be completely discharged to provide the energy needs of the users.

However, when the energy contained in the battery is not sufficient to power the user, the latter is forced to request the remaining amount of demand directly from the network. In terms of energy, given the boundary condition:

$$E_{BESS}^{OUT'} < E'_{DEMAND} \quad (5.30)$$

The energy required by the user will be supplied in part by the battery and partly by the network:

$$E'_{DEMAND} = E_{BESS}^{OUT'} + E_{IN} \quad (5.31)$$

Where E_{IN} represents the share of energy taken from the network. Fig 5.36 shows the logical scheme of the situation just described.

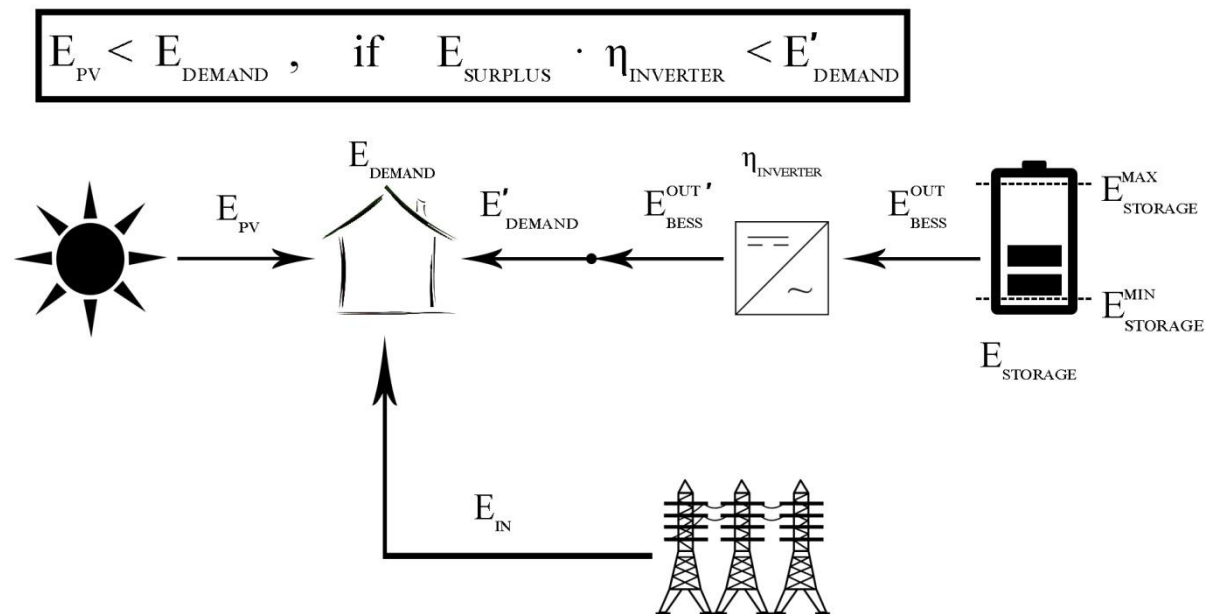


Fig 5.36: Logic functional scheme of the PV-BESS system when the PV system produces less energy than required by the user and the battery is not able to provide all the energy it needs.

In the extreme case it may happen that the battery is unloaded, then the user will be forced to take the entire demand from the network:

$$E_{STORAGE} = 0 \quad (5.32)$$

$$E'_{DEMAND} = E_{IN} \quad (5.33)$$

It is important to underline how the division in various cases shown by the functional-logical schemes is not exactly correct. The charging and discharging of the battery, the supply of energy to the user, the withdrawal of energy from the combined network to the removal of energy from the battery, the introduction of excess energy into the network are all phenomena which occur instantly and which could not be divided into various "cases". However, they are able to give an idea of the behavior of the energy flows that come into play in a PV-BESS system depending on the various situations that may occur moment by moment.

5.2.2 Assignment of battery size

As already stated in the case of PV systems previously analyzed, the allocation of a battery does not follow all the criteria that should theoretically be considered to make the most appropriate choice. The starting data are only energy consumption data for the year 2017, it is not known what are the needs of the tenants of the houses, the layout of the houses, the availability in investing in a solar-PV-battery system or simply in a solar-PV system.

Having only energy information, it was decided to consider the average energy consumption during the nighttime \bar{E}_{NIGHT} as the only parameter for the allocation of the batteries, that is the average daily value of energy consumed when the value of the solar radiation is zero.

Fig 5.16 shows the average daily energy consumption during the nighttime of each node in 2017.

Node	\bar{E}_{NIGHT} [kWh]
110	2,59
80	2,99
78	1,74
77	1,95
76	2,37
41	2,90
31	1,12
27	3,18
25	1,93
12	1,65
10	1,32
2	2,50
79	3,13
73	3,40
64	3,43
47	2,54

42	2,96
39	2,85
36	3,68
32	3,85
13	2,87
4	2,88
67	6,64
68	4,33
62	5,15
59	6,53
49	5,73
9	5,26
96	8,65
82	7,47
63	6,38
53	7,91
44	5,86
37	8,95
23	5,54
11	6,33
7	4,75
5	5,57
75	13,34
57	13,25
6	18,99
3	14,07

Tab 5.13: Average energy used during the nighttime in 2017 for each node.

As can be seen from the last table, the values of energy consumed during nighttime vary between about 2 kWh and 20 kWh. In order to better visualize the values in the table it may be useful to consider the normal distribution of energy data. Tab 5.14 shows the mean and standard deviation values for the average daily energy values consumed during nighttime.

Mean μ	Standard Deviation σ^2
5,20	3,84

Tab 5.14: Standard deviation and mean values referring to the average energy consumption during the nighttime in 2017 of each node.

Calculating the values of the normal distribution relative to the average energy consumed during the nighttime, it is possible to obtain the Gaussian curve of these values (Fig 5.37).

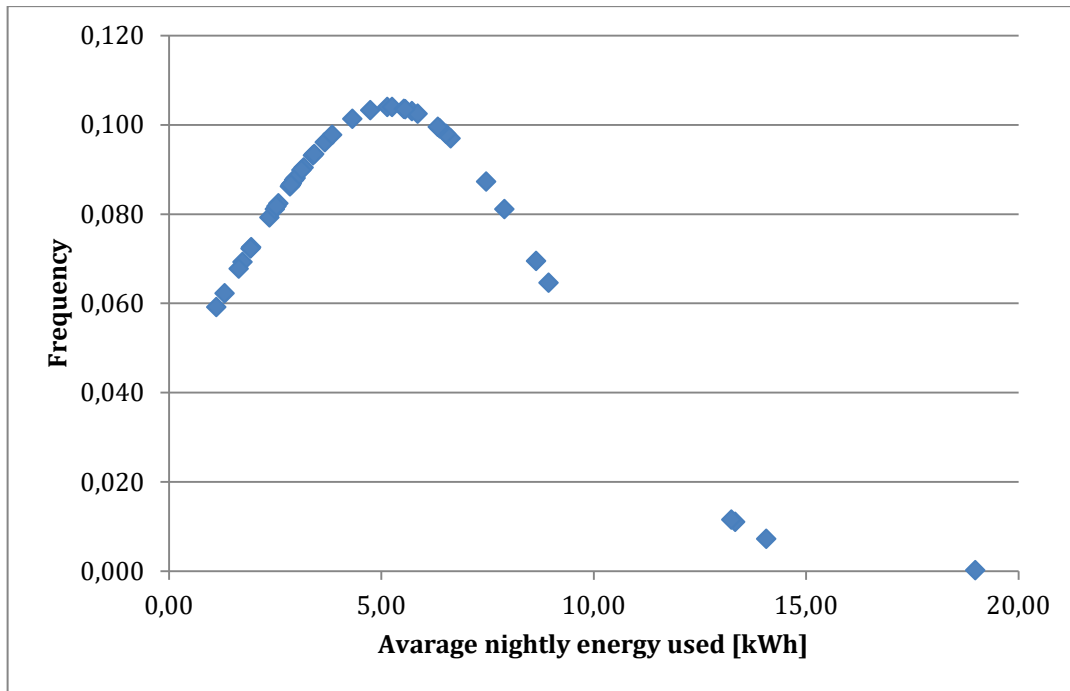


Fig 5.37: Frequency of nodes depending on the average energy used during the nighttime in 2017 of each node.

The size of the batteries for domestic use currently on the market produced by the major world manufacturers such as *Sonnen*, *Panasonic*, *Tesla*, etc. is usually between a minimum of 4 kWh and a maximum of 16 kWh. Consequently, it was decided to adopt three different sizes: a 4 kWh, a 10 kWh and a 16 kWh battery, adopting a very simple logic based exclusively on consumption for the year 2017 whose values are known. Indicating with \bar{E}_{NIGHT} the amount of average energy consumed during the nighttime ($I=0$) and with $E_{STORAGE_n}$ the value of the nominal capacity of the battery chosen, it was established the (5.34):

$$E_{STORAGE_n} = \begin{cases} 4, & \bar{E}_{NIGHT} < 4 \\ 10, & 4 \leq \bar{E}_{NIGHT} < 10 \\ 16, & \bar{E}_{NIGHT} \geq 10 \end{cases} \quad (5.34)$$

As happened for the assignment of the PV system, even in the case of the assignment of the BESSs, three different groups are obtained and indicated with group 1, group 2, group 3 to which the batteries with nominal energy capacity of 4, 10 and 16 kWh respectively belong (Tab 5.15).

	Node	\bar{E}_{NIGHT} [kWh]	$E_{STORAGE_n}$ [kWh]
Group 1	110	2,59	4
	80	2,99	4
	78	1,74	4
	77	1,95	4

	76	2,37	4
	41	2,90	4
	31	1,12	4
	27	3,18	4
	25	1,93	4
	12	1,65	4
	10	1,32	4
	2	2,50	4
	79	3,13	4
	73	3,40	4
	64	3,43	4
	47	2,54	4
	42	2,96	4
	39	2,85	4
	36	3,68	4
	32	3,85	4
	13	2,87	4
	4	2,88	4
Group 2	67	6,64	10
	68	4,33	10
	62	5,15	10
	59	6,53	10
	49	5,73	10
	9	5,26	10
	96	8,65	10
	82	7,47	10
	63	6,38	10
	53	7,91	10
	44	5,86	10
	37	8,95	10
	23	5,54	10
	11	6,33	10
	7	4,75	10
5	5,57	10	
Group 3	75	13,34	16
	57	13,25	16
	6	18,99	16
	3	14,07	16

Tab 5.15: Average energy consumption during the nighttime in 2017 of each node and relative belonging group based on the size of the battery.

5.2.3 Choice of the battery

In order to simplify the thesis work, it was decided to use the batteries of the German manufacturer named *Sonnen GmbH*. Sonnen is an energy company based in Wildpoldsried, in the Oberallgäu district of Germany. An article published in 2017

(<http://www.qualenergia.it/articoli/20170612-nuovi-studi-di-mercato-sonnen-il-leader-energy-storage-europa-germania->) states that some market studies conducted from EuPD Research and Frost & Sullivan indicate that Sonnen is growing at such a high rate that it is a candidate for leadership in the energy storage industry in Germany and Europe. In addition to doubling its turnover in 2016, according to these studies the German manufacturer occupies the first position for energy storage systems in Germany and Europe. The article states that in its recent study reported in 2016, the market research company based in Bonn EuPD Research placed the Sonnen in first place, with a 22% share in Germany and Europe. Fig 5.38 (<http://www.qualenergia.it/articoli/20170612-nuovi-studi-di-mercato-sonnen-il-leader-energy-storage-Europe-Germany->) shows the graph of the market shares of the major energy storage companies in Europe.

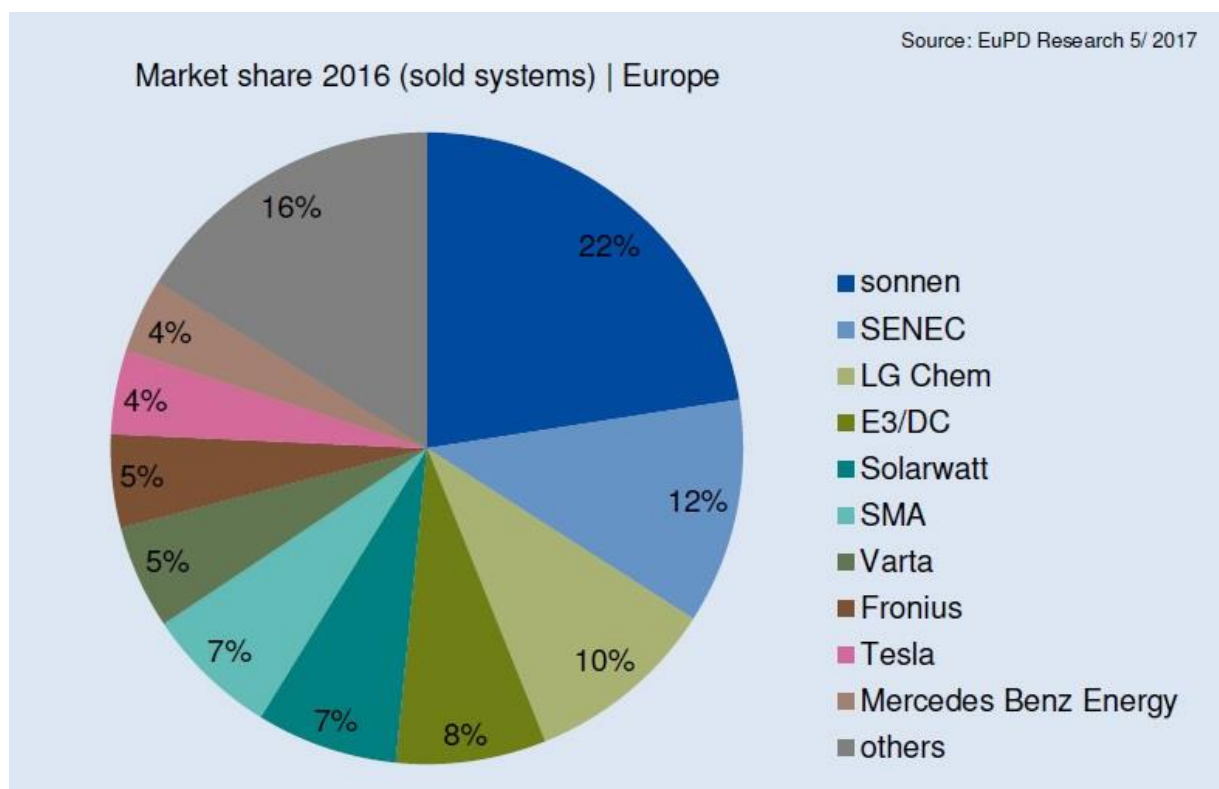


Fig 5.38: Market share 2016, Europe (<http://www.qualenergia.it/articoli/20170612-nuovi-studi-di-mercato-sonnen-il-leader-energy-storage-europa-germania->).

Moreover, the article states that during the same period a market study was conducted by Frost & Sullivan which demonstrates how Sonnen owns the largest market share in Germany as well.

Ultimately, it was immediate to choose to use the batteries produced by the Sonnen in the analysis carried out in this thesis. In particular, it was decided to use the *three-phase eco 8.0* batteries in the versions of 4, 10 and 16 kWh. Fig 5.39 and Fig 5.40 show the technical data of the selected batteries.

Technical Data sonnenBatterie

	eco 8.0/2	eco 8.0/4	eco 8.0/6	eco 8.0/8	eco 8.0/10	eco 8.0/12	eco 8.0/14	eco 8.0/16
Grid Version (three phase)								
Rated inverter power (W) (charging/discharging)	1,500	2,500	3,000	3,300	3,300	3,300	3,300	3,300
Maximum inverter efficiency	96 %							
Variety ¹ (2-10 kWh)								
Weight kg	55	96	121	146	171	-	-	-
Dimensions H/W/D cm	70/64/22	137/64/22	137/64/22	137/64/22	137/64/22	-	-	-
Variety ¹ (2-16 kWh)								
Weight kg	55	107	132	157	182	207	232	257
Dimensions H/W/D cm	70/64/22	184/64/22	184/64/22	184/64/22	184/64/22	184/64/22	184/64/22	184/64/22
	eco 8.2/2	eco 8.2/4	eco 8.2/6	eco 8.2/8	eco 8.2/10	eco 8.2/12	eco 8.2/14	eco 8.2/16
Grid Version (single phase)								
Rated inverter power (W) (charging/discharging)	1,500	2,000	2,500	2,500	2,500	2,500	2,500	2,500
Maximum inverter efficiency	93 %							
Variety ¹ (2-10 kWh)								
Weight kg	71	112	137	162	187	-	-	-
Dimensions H/W/D cm	70/64/22	137/64/22	137/64/22	137/64/22	137/64/22	-	-	-
Variety ¹ (2-16 kWh)								
Weight kg	71	123	148	173	198	223	248	273
Dimensions H/W/D cm	70/64/22	184/64/22	184/64/22	184/64/22	184/64/22	184/64/22	184/64/22	184/64/22

Fig 5.39: Technical data of the chosen Sonnen batteries (www.sonnenbatterie.de).

Technical Data sonnenBatterie

	eco 8/2	eco 8/4	eco 8/6	eco 8/8	eco 8/10	eco 8/12	eco 8/14	eco 8/16
Maximum battery efficiency	98 %							
Usable battery capacity (kWh)	2.0	4.0	6.0	8.0	10.0	12.0	14.0	16.0
Cell chemistry	LFP (Lithium Iron Phosphate)							
Ambient temperature range	5° - 40 °C							
Dust & water protection	IP 21							
Tests and directives	VDE-AR-N_4105, Low Voltage Directive 2006/95/EG, UL1642, IEC62133							
Battery service life	designed for 20 years							
Warranty	10 years ²							
Cycles	10,000 ³							
Charging time to 90 %, approx.	1.5 h	1.5 h	2 h	2.5 h	3 h	3.5 h	4 h	4.5 h
Recommended for use with annual household consumption up to [kWh] (based on experience)	2,500	3,300	4,400	5,500	6,600	7,700	8,800	9,900
Available options								
Colour of cabinet ³	black or silvergrey							
Multi-Touch-Display	18 cm width							

Fig 5.40: Other technical data of the chosen Sonnen batteries (www.sonnenbatterie.de).

5.2.4 Results

The installation of a BESS changes the energy flows compared with the case of a PV system without the support of a battery. The accumulation of energy causes the energy produced by the PV system to be exploited even when the photovoltaic panels are not working. In other words, the energy previously produced by photovoltaic panels can be used at a later stage, as it usually happens during the evening and the nighttime. Consequently, if the battery is chosen appropriately, the amount of energy requested to the network will be still lower and the gain relatively high.

It is important to underline that the values of the yields used to calculate the losses respectively in the two inverters upstream and downstream of the battery and the losses inside the battery were extrapolated from the technical data of the chosen batteries shown in Fig 5.39 and Fig 5.40 and the values are respectively reported in (5.35) and (5.36):

$$\eta_{INVERTER} = 0,96 \quad (5.35)$$

$$\eta_{BATTERY} = 0,98 \quad (5.36)$$

For the sake of simplicity, the results of the representative node of each of the three groups of houses considering three different sizes for the choice of batteries (nodes 4, 44, 75) are shown.

The node representing the first group of houses characterized by an assigned battery with nominal capacity equal to 4 kWh is *node 4* (Fig 5.41, Fig 5.42, Fig 5.43).

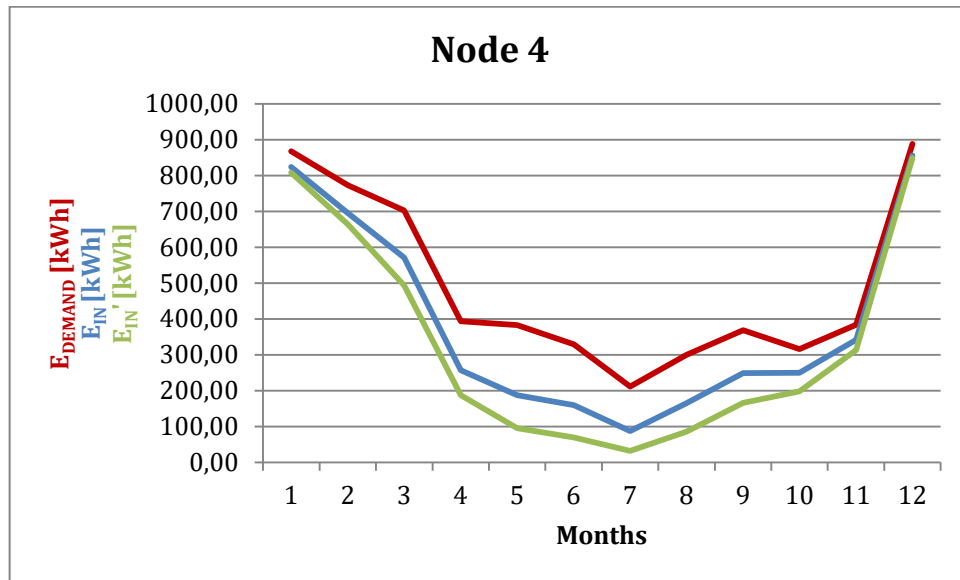


Fig 5.41: Demand trend without PV system, demand trend with assigned PV system and demand trend with the assigned PV-BESS system for the node 4.

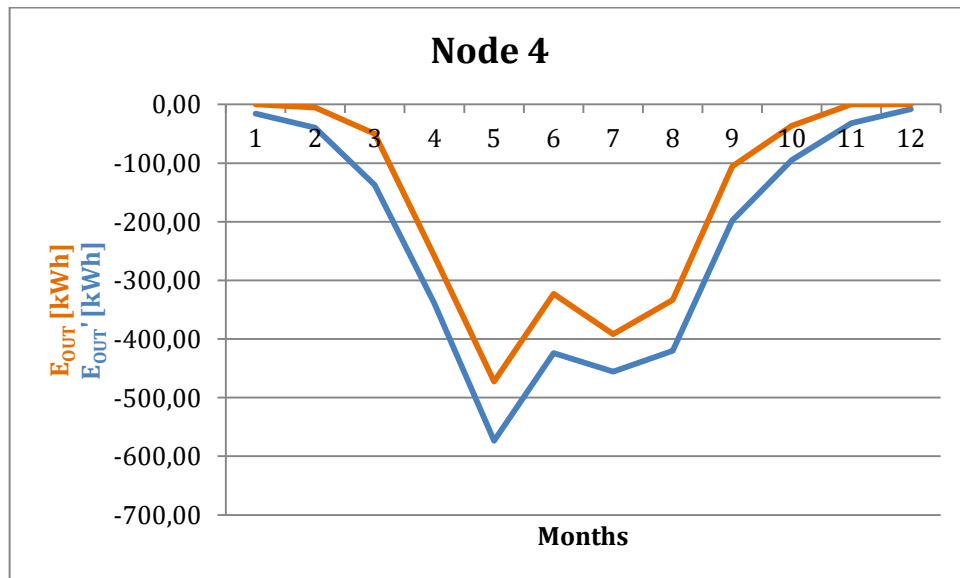


Fig 5.42: Trend of the energy fed into the grid in the case of the assigned PV system and in the case of the assigned PV-BESS combined system for the node 4.

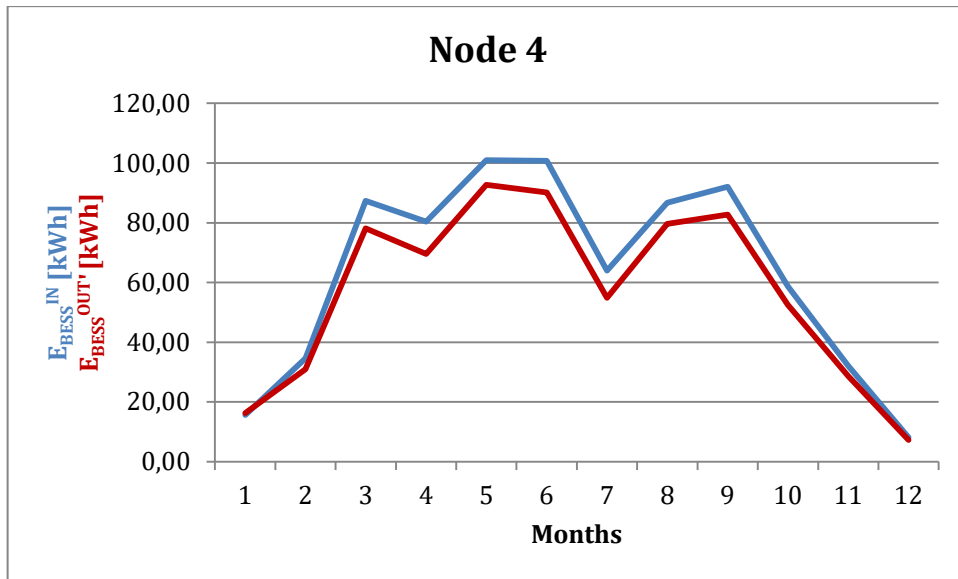


Fig 5.43: Trend of the energy absorbed and the energy given by the BESS measured upstream of the inverter at the input and downstream of the inverter at the output for the node 44.

The node representing the second group of houses characterized by an assigned battery with nominal capacity equal to 10 kWh is *node 44* (Fig 5.44, Fig 5.45, Fig 5.46).

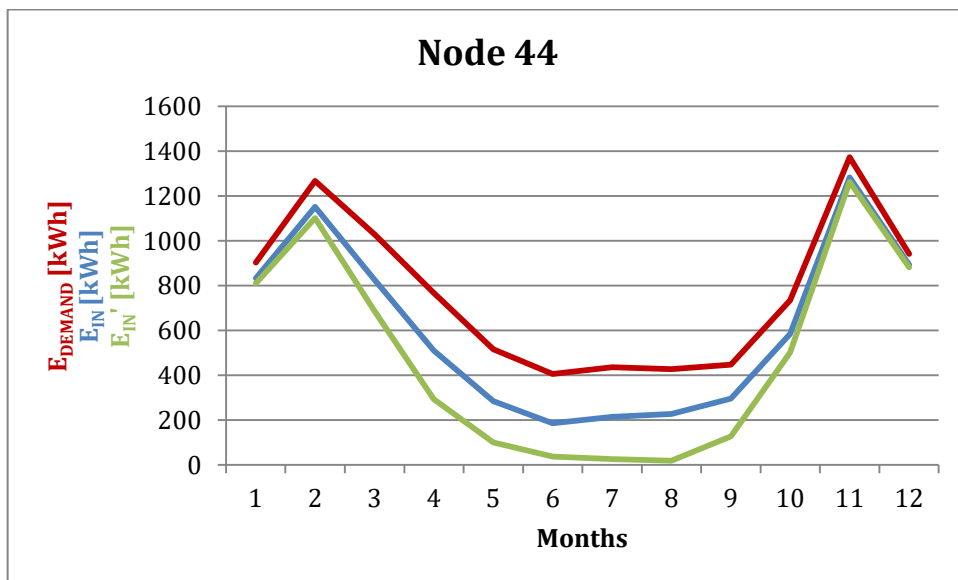


Fig 5.44: Demand trend without PV system, demand trend with assigned PV system and demand trend with assigned PV-BESS system for the node 44.

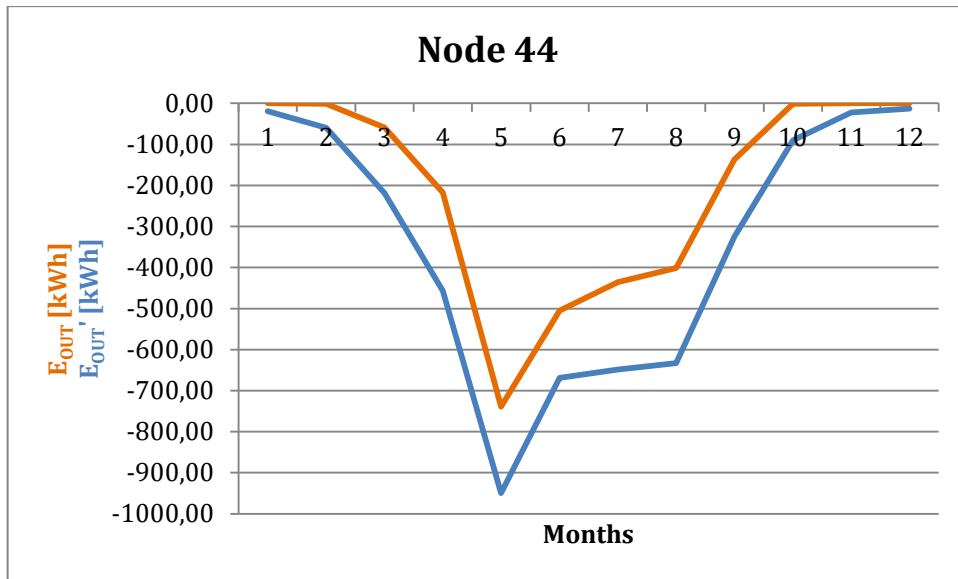


Fig 5.45: Trend of the energy fed into the grid in the case of the assigned PV system and in the case of the assigned PV-BESS combined system for the node 44.

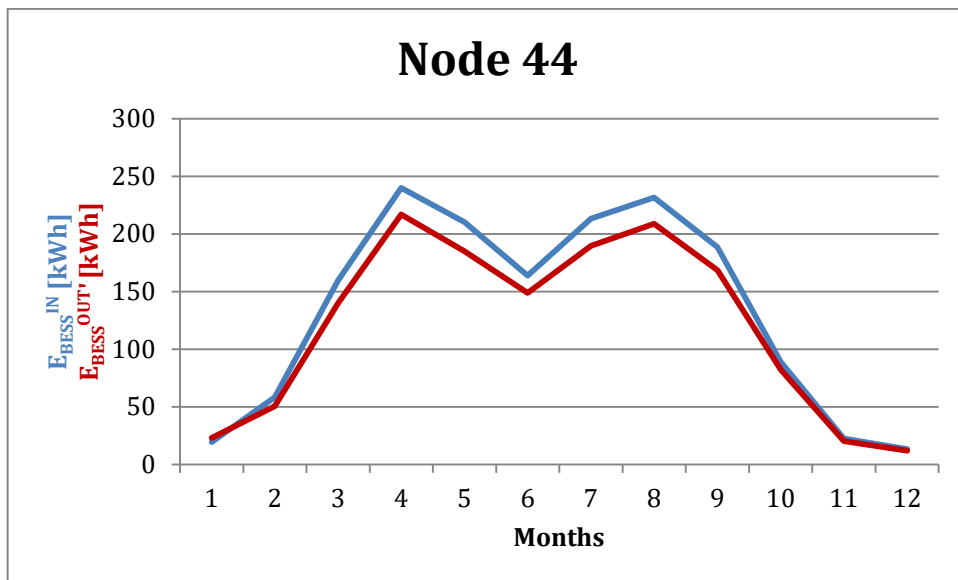


Fig 5.46: Trend of the energy absorbed and the energy given by the BESS measured upstream of the inverter at the input and downstream of the inverter at the output for the node 44.

The node representing the third group of houses characterized by an assigned battery with nominal capacity equal to 16 kWh is *node 75* (Fig 5.47, Fig 5.48 and Fig 5.49):

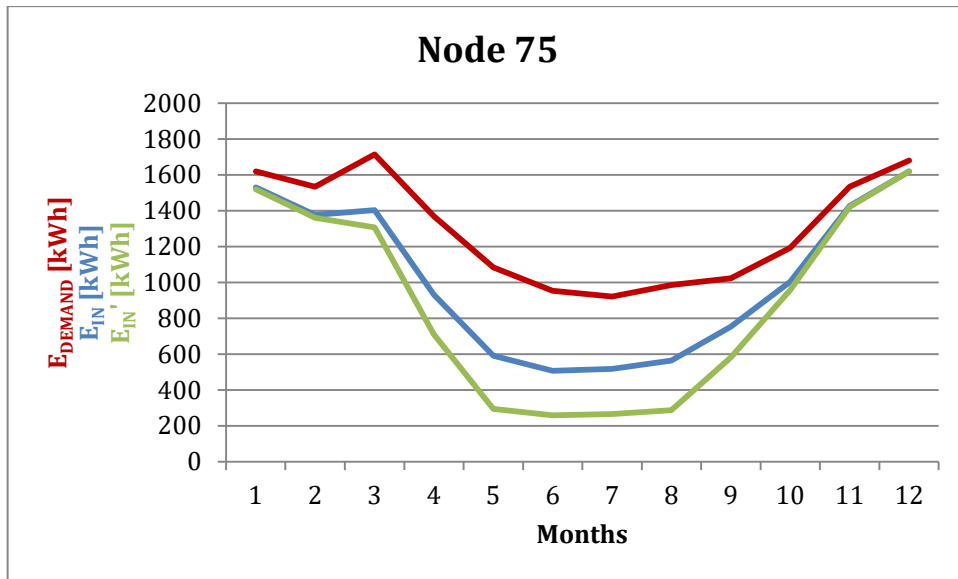


Fig 5.47: Demand trend without PV system, demand trend with assigned PV system and demand trend with assigned PV-BESS system for the node 75.

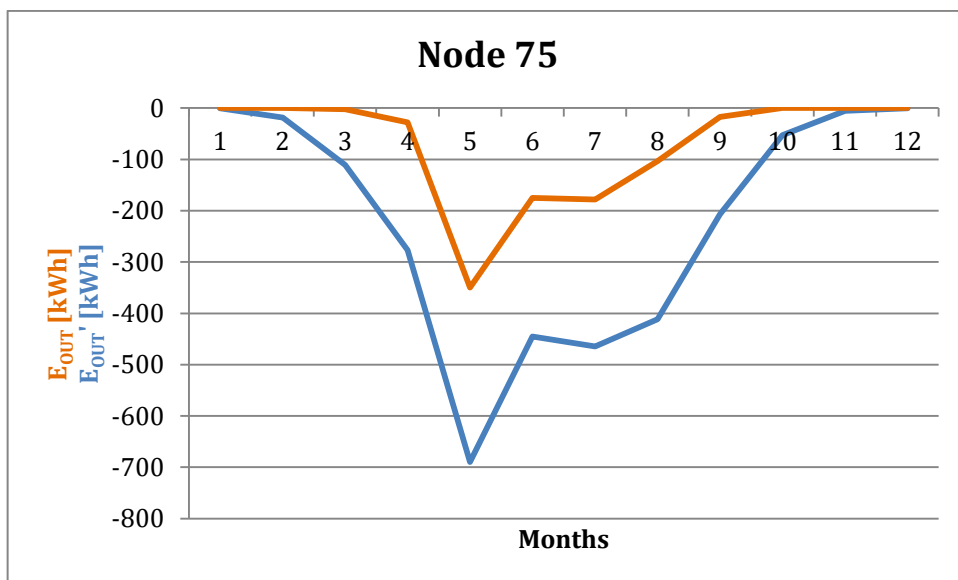


Fig 5.48: Trend of the energy fed into the grid in the case of the assigned PV system and in the case of the assigned PV-BESS combined system for the node 75.

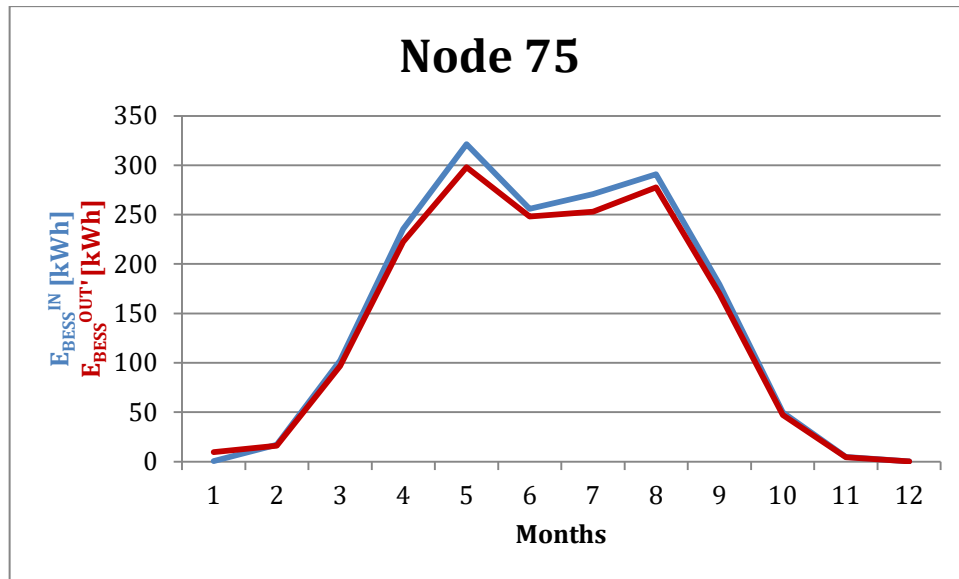


Fig 5.49: Trend of the energy absorbed and the energy given by the BESS measured upstream of the inverter at the input and downstream of the inverter at the output for the node 75.

Comparing the energy required to the network in the case in which no PV system is installed with the energy required in the case where a PV system is assigned and in the case where a PV-BESS combined system is assigned (Fig 5.41, Fig 5.44 and Fig 5.47) it is evident that the first energy (E_{DEMAND}) is represented by a curve positioned above the other two. In fact, the second energy curve (E_{IN}) required by the grid in the case of a grid-connected PV system is characterized by lower values than the first curve thanks to the energy input of the photovoltaic panels. Finally, the third energy curve (E'_{IN}) required by the network in the case of a combined PV-BESS system is characterized by even lower values than the first two curves as the user can exploit either the energy produced instantly by the solar panels and a share of excess energy produced during the daytime hours from the panels and stored in the battery. This represents the first source of savings, which is the maximum when a BESS accumulation system is associated with a PV system.

In parallel, the excess energy that is transferred to the network (Fig 5.42, Fig 5.45 and Fig 5.48) is clearly lower in absolute value in the case of a combined PV-BESS system compared to the case in which the battery is absent ($E_{OUT} > E'_{OUT}$). This happens because the excess energy produced by the photovoltaic panels is not completely fed into the grid but is used in part to charge the battery. This indicates a lower gain for the sale of energy, which should however be offset by a lower amount of energy required to the network knowing that the price of energy sold and fed into the network is much lower than the price of energy required to network. Finally, the trends of the energy absorbed and the energy given by the battery shown in Fig 5.43, Fig 5.46 and Fig 5.49 respectively for nodes 4, 44 and 75 presents a "bell" shape similar to that of the energy produced E_{PV} by the PV system. This happens because the recharging of the battery is directly proportional to the energy produced by the panels. It is evident how the curve will have very low values during the autumn and winter months while it will have high values during the spring and summer months. Moreover, the values shown represent the energy values measured upstream of the

inverter at the input of the battery and downstream of the inverter at the output of the battery, so it is clear how the two curves have a difference in level due to the losses inside the inverter and inside the battery, respectively considered in our case equal to 4% and 2%.

Ultimately from a power point of view a grid-connected PV-BESS combined system is much more convenient than a simple grid-connected PV system. The energy demand of the users to the network is much lower due to the combined energy supply of the panels and the battery, and the expenses in the bill decrease drastically. However, a more detailed economic analysis is needed to understand whether these benefits from the point of view of energy savings are cheap enough to justify investing in a PV system and a battery.

6. ECONOMIC ANALYSIS

6.1 Market Review

One of the reasons why renewable energy for electricity production has received the most attention in the world is the increase in fossil fuel prices and the risks that the environment is facing due to the alarming increase in greenhouse gases. This last problem was already dealt with in December 1997 by about 160 countries meeting in *Kyoto* in Japan to fix the general guidelines for the reduction of polluting emissions responsible for irreversible climate change and global warming that could lead to the melting of glaciers in poles of the Earth and other catastrophic consequences. The treaty required the industrialized countries to adopt a serious policy to reduce polluting emissions with the aim of achieving a minimum reduction of around 5% in 2012 compared to the emissions recorded in 1990 (<https://eur-lex.europa.eu/legal-content/IT/TXT/?uri=LEGISSUM%3A128060>).

A few years later, in 2016, the first universal climate change binding agreement on climate change was signed in Paris. It was signed in April and ratified by the European Union in October. Article 2 of the Paris Agreement summarizes the objectives that the signatory countries aim to achieve, namely to maintain the increase in the average world temperature below 2 °C compared to pre-industrial levels and to continue the action aimed at limiting this increase to 1,5 °C compared to pre-industrial levels, promote low-emission development of greenhouse gases without threatening food production and making financial flows consistent with a path leading to low-carbon development and climate resilient ([https://eur-lex.europa.eu/legal-content/IT/TXT/?uri=CELEX:22016A1019\(01\)](https://eur-lex.europa.eu/legal-content/IT/TXT/?uri=CELEX:22016A1019(01))).

As reported in a not very recent article by Bhandari et al. (2009), photovoltaics have been growing rapidly since the beginning of this century. However, the most serious problem that hinders the full integration of the photovoltaic system is represented by the very high cost and not accessible without subsidies and supports. Nevertheless, the article Bhandari et al. (2009) state that "costs are decreasing rapidly since its commercial application began in the 1980s". As reported in the article (Bhandari et al., 2009) "it is believed that, due to the rapid increase in prices of electricity produced from fossil fuels on the one hand and improvements in PV technology on the other, it will come a day in a future in which the price of electricity generated by conventional fuels will be equal to or even higher than the price of electricity generated by solar photovoltaics".

A possible analysis to understand the relationship between costs and prices in relation to the quantity produced is that linked to the *learning curve* (LC). The experience curve allows to analyse the trend of the total unit cost in relation to the cumulative volume of production.

It has been shown that as the cumulative production volume increases, the average cost of the asset decreases and this decrease is linked to the highest level of production efficiency due to experience. As stated by Elshurafa et al. (2018), the idea of LC derives from empirical evidence the equation for the learning curve is expressed as (Trappey et al., 2016):

$$C_Q = C_1 Q^{-\beta} \quad (6.1)$$

Where C_Q is the marginal cost of production of the unit Q -th, C_1 is the production cost of the first unit, Q is the cumulative production and β is the parameter of learning and it is negative because the cost decreases as the production increases.

As stated by Elshurafa et al. (2018), "typical industries have values β between 0,15 and 0,5 corresponding to a LC of 90% - 70% respectively". If a product has, for example, a 90% LC it means that every time its cumulative production doubles the price will decrease and will be 90% of the initial one. Ultimately the price would decrease by 10% and this is indicated as a progress report (PR). As a consequence PR results to be equal to $PR = 1 - LC$ (Elshurafa et al., 2018).

As stated by Bhandari et al. (2009), "the cost per unit product decreases according to the learning rate $1-PR$ for each doubling of the cumulative production".

There are many articles cited by Bhandari et al. (2009) in which the growth of photovoltaics in the world is studied, with an estimate of the annual growth rate of over 20% worldwide and an estimate of the global electricity demand met by photovoltaic equal to 20% in 2050 which will increase at 50% in 2100.

Fig 6.1 (Bhandari et al., 2009) shows the derived experience curves for different PR values of 75%, 80%, 85% and 90% during the period 2006-2060.

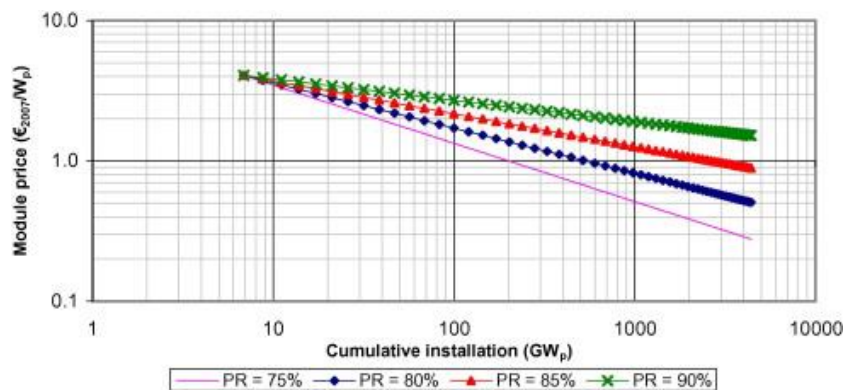


Fig 6.1: PV experience curve based on world module price from 2006 to 2060 (Bhandari et al., 2009).

From an article of IRENA (2016) the global investment costs for solar PV will decrease by 57%, from 1810 USD/kW in 2015 to 790 USD/kW in 2025 (Fig 6.2).

	Global weighted average data								
	Investment costs (2015 USD/kW)		Percent change	Capacity factor		Percent change ²	LCOE (2015 USD/kWh)		Percent change
	2015	2025		2015	2025		2015	2025	
Solar PV	1 810	790	-57%	18%	19%	8%	0.13	0.06	-59%
CSP (PTC: parabolic trough collector)	5 550	3 700	-33%	41%	45%	8.4%	0.15 -0.19	0.09 -0.12	-37%
CSP (ST: solar tower)	5 700	3 600	-37%	46%	49%	7.6%	0.15 -0.19	0.08 -0.11	-43%
Onshore wind	1 560	1 370	-12%	27%	30%	11%	0.07	0.05	-26%
Offshore wind	4 650	3 950	-15%	43%	45%	4%	0.18	0.12	-35%

Fig 6.2: Global weighted average solar and wind power investment costs, capacity factors and LCOEs, 2015 and 2025 (IRENA, 2016).

A study carried out by Agora (2015) analyzes the learning curve of PV systems to estimate how the quantity produced will vary and how prices will vary in the future. Four different scenarios are analyzed in which the first is the most pessimistic one in which an annual growth rate of about 5% is assumed (CAGR) while the fourth is an "extreme" scenario that is not based on a bottom hypothesis -up on the growth of the market, but rather takes as its starting point a photovoltaic-based energy system in 2050, assuming that the photovoltaic provides 40% of the global electricity demand in a scenario of "high electrification". Fig 6.3 shows the trend of the learning curve forecast of the three scenarios assuming an annual growth rate of PV systems equal to 5%, 7.5% and 10% respectively. Fig 6.4 shows instead the range of future costs in the different scenarios.

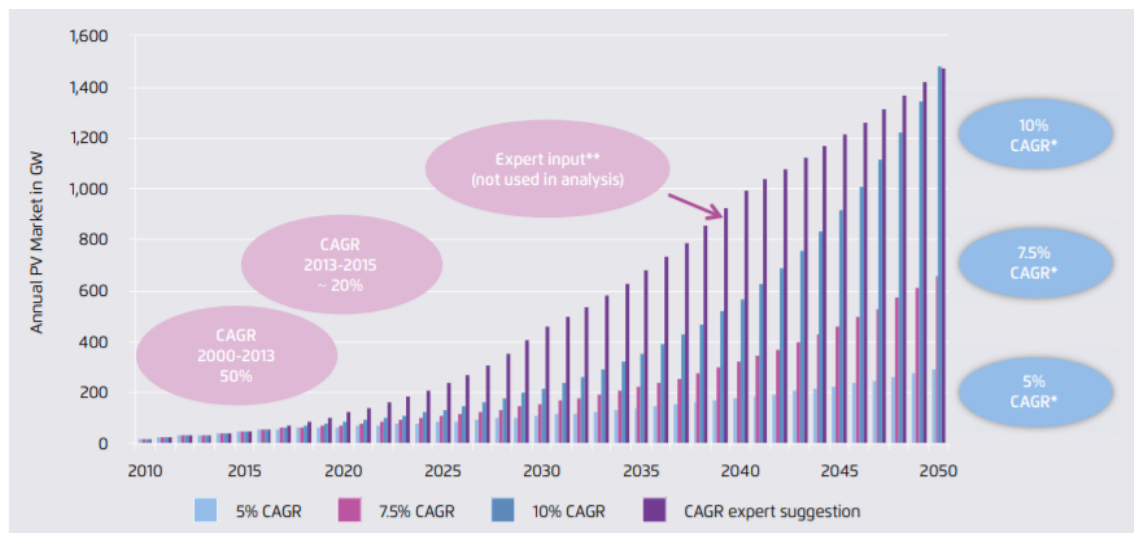


Fig 6.3: Three long-term scenarios are developed using assumptions on yearly market growth rates from 5% to 10% per year after 2015 (AGORA, 2015).

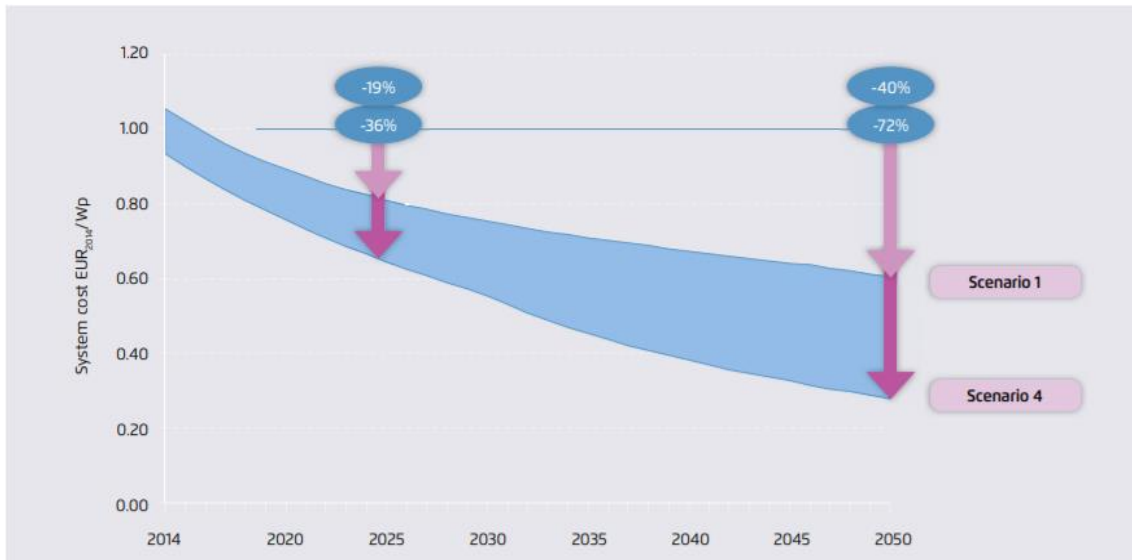


Fig 6.4: Range of future cost developments in the different scenarios (AGORA, 2015).

What has been said for the PV systems market is also valid for the battery market. Many studies have shown that the battery market is growing strongly. As reported by Jessica Lipsky (2015) many industries are showing a growing demand for lithium-ion batteries as many companies aim to diversify battery-related activities. The article cites transport companies and utilities, battery manufacturers, automobile manufacturers and chemical companies as potentially interested industries. The article states that in addition to the automotive field, manufacturers are increasing the use of batteries in homes even if numerous studies have shown that the annual demand for automotive batteries will far exceed that of secondary applications.

Schmidt et al. (2017) report in their article the learning curve of the most common BESS systems including the lithium-ion battery (Fig 6.5).

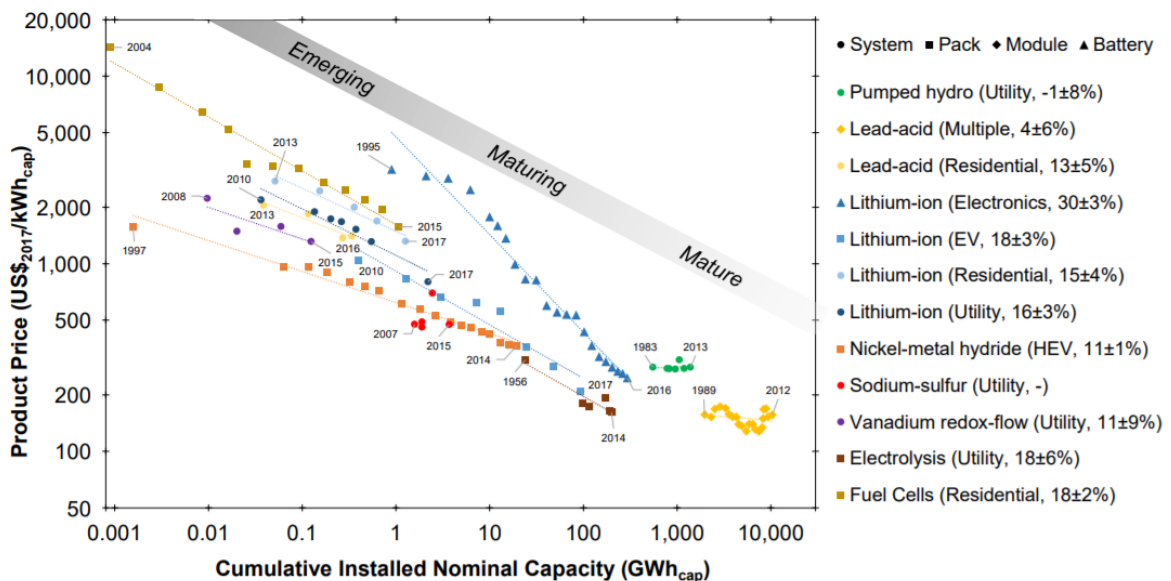


Fig 6.5: Learning curve of the BESS related to the cumulative production.

The forecast of an increasing sale of batteries in the coming years is closely linked to the expected decrease in battery prices. As reported by AMECOM (2015), the battery market could take off similarly to what happened to the PV system in the last five years. Analyzing what happened in the last decade it is clear that there has been great progress in the chemistry and technology of the batteries that have led to an improvement in performance and a significant reduction in costs.

In Fig 6.6 (Schimdt, 2017) the forecast regarding the lowering of the BESS prices up to 2050 is shown.

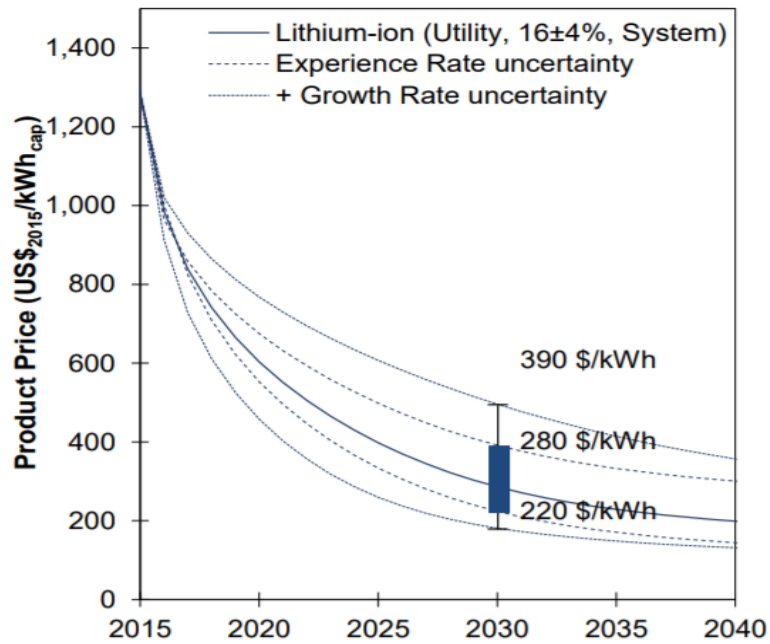


Fig 6.6: Learning curve of the forecast about the future BESS price.

About PV system costs, Martinez-Cesena et al. (2012) state that the capital costs for a PV system can be basically divided into the cost of the initial investment and periodic costs as shown by:

$$C_{tot} = C_i + C_{O\&M} \quad (6.2)$$

Where the initial investment C_i includes all the costs to finance the photovoltaic system infrastructure, while the periodic costs $C_{O\&M}$ include management and maintenance costs and any loan payments.

The cost of the initial investment is characterized by a component related to the materials that make up the modules which represents about 40% of the total value and a component related to the BOS costs (Balance of System), ie all those costs related to the PV system with the exception of the cost of the modules (IRENA, 2012). In (6.3) the calculation of the initial investment is shown:

$$C_i = C_{mod} + C_{BOS} \quad (6.3)$$

Where C_{mod} represents the costs of the modules and C_{BOS} the BOS costs. For a residential and small-scale system, BOS costs represent approximately 55-60% of total costs C_i (IRENA, 2012). The BOS costs include the inverters, the components necessary for mounting and racking the PV system, the combiner box and various electrical components, site preparation and installation, battery storage. Elshurafa et al. (2018) even state that nowadays the BOS costs have a greater weight on the total cost of the photovoltaic system reaching a percentage of 68% (Fig 6.7) due to the sharp decline in module prices in recent years.

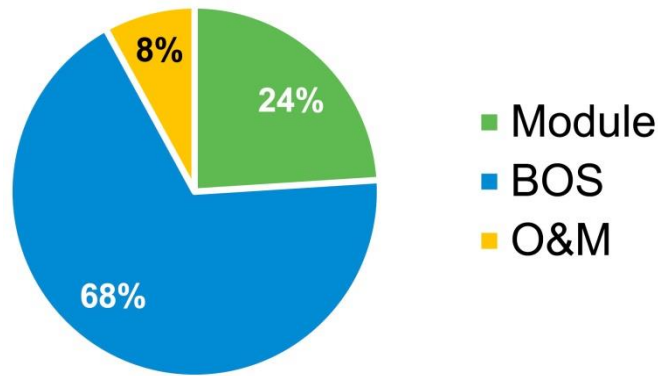


Fig 6.7: Contribution of the module, BOS and O&M costs to the LCOE of a typical solar system (Elshurafa et al., 2018).

6.2 Results

The analysis carried out consists in the calculation of the payback of the considered PV systems and the combined PV-battery systems. Nowadays in Italy the cost of the PV system can be deducted from taxes at 50%, so the final price is halved. In addition, the photovoltaic system generates savings thanks to the so-called net-metering, which is a regulation governed by the Authority for electricity and gas for the mechanism that allows to feed the electricity produced by a PV system into the grid but not immediately self-consumed, which will be taken at a later date to remedy the demand of the user. This service is economically regulated by the so called *Gestore dei servizi energetici* (GSE) in the form of a financial contribution and can be combined with the tax deduction.

The analysis carried out in this thesis work takes into account the incentive on photovoltaic currently present in UK called *feed-in tariff* (FIT). The FIT represents a tariff able to exploit the energy produced by a PV system so that the owner of such system is paid only for producing energy.

The feed-in tariff "is an instrument of energy policy aimed at supporting the development of new projects in renewable energy, based on long-term purchase contracts for electricity produced by them" (Cory et al., 2010 by thesis).

These purchase contracts are stipulated for a long duration between 10-25 years and concern the electricity produced. The payment for the individual kWh of energy commonly varies according to the technology considered, the size and location of the project and the quality of the source to object.

The FIT scheme is the most used incentive system for the renewable sector until today.

The *Net Present Value* (NPV) method was used to calculate the payback. This method consists in calculating the future cash flows to check whether they are sufficient or not to cover the initial investment. The NPV is defined by:

$$NET = -C_i + \sum_{t=1}^n \frac{\Delta CF_t}{(1+i)^t} + \frac{E_n}{(1+i)^n} \quad (6.4)$$

Where C_i indicates the initial investment, ΔCF_t indicates the change in the cash flows generated by the investment, i is the discount rate that takes into account the changing value of money, n represents the duration of the investment and E_n represents any extraordinary transactions that they only concern the last year. The change in cash flows ΔCF_t is calculated as the subtraction between the monetary revenues and the monetary operating costs shown in (6.5).

$$\Delta CF = \Delta MR - \Delta MOC \quad (6.5)$$

In the case of a PV system or a combined PV-BESS system, the monetary revenues are null before the installation of the system, while after the installation of the system they are equal to the cost of the energy introduced into the network and more resold the respective incentive applied (in our case the FIT). The monetary operating costs are represented by the cost of the energy withdrawn from the network and supplied to the user to satisfy the user's demand before installation and represented by the cost of energy taken from the network net of self-consumption after the installation, for which:

$$\Delta MR = MR_f - MR_i = (E_{out} \cdot p_{out} + E_{PV} \cdot p_{FIT}) - 0 \quad (6.6)$$

$$\Delta MOC = MOC_f - MOC_i = (E_{in} \cdot p_{in}) - (E_{DEMAND} \cdot p_{in}) \quad (6.7)$$

Where p_{in} represents the price of energy purchased by the network, p_{out} represents the price of energy sold to the network and p_{FIT} represents the price of the FIT incentive, all expressed in pence/kWh. As is clear from the (6.4) the value of NET results in negative starting because of the initial investment which is considered as negative flow since it is an outflow. When the NET turns out to be negative then the investment is not convenient since it means that the cash flows have failed at least to equal

the initial outflow C_i ; when the NET turns out to be positive then the investment is convenient; in the case of NET equal to zero, then the investment is indifferent, ie it does not represent either a gain or a loss (Tab 6.1).

NET>0	Convenient investment
NET<0	Not convenient investment
NET=0	Indifferent investment

Tab 6.1: Investment productivity based on the value of NET.

In order to calculate the payback of a given investment, it can be done starting from the NET equation. Basically the payback will occur when the NET passes from negative values to positive values, or rather the real payback will occur when the NET will be null:

$$NET = 0 \quad (6.8)$$

$$C_i + \sum_{t=1}^n \frac{\Delta CF_t}{(1+i)^t} + \frac{E_n}{(1+i)^n} = 0 \quad (6.9)$$

The value of n which cancels the NET can be obtained from the equation. This method is called *discounted payback* since the sums are discounted by the discount rate i which takes into account the value of money. However, on an industrial level, sometimes an alternative method is used called *simple payback* where the summations are made without actualizing. It is clear that with the same investment, the simple payback is lower in value than the discounted payback.

In the previous analysis, three different PV system sizes were assigned to the considered nodes and subsequently three different BESS sizes, consequently the economic analysis takes into account nine different criteria that consider the nine possible combinations of the PV and BESS system, which are represented in Tab 6.2:

Criteria	Groups combinations	N° nodes	Representative node
C1	Group 1 PV - Group 1 BESS	12	10
C2	Group 2 PV - Group 1 BESS	10	64
C3	Group 3 PV - Group 1 BESS	0	—
C4	Group 1 PV - Group 2 BESS	1	67
C5	Group 2 PV - Group 2 BESS	5	49
C6	Group 3 PV - Group 2 BESS	10	96
C7	Group 1 PV - Group 3 BESS	0	—
C8	Group 2 PV - Group 3 BESS	0	—
C9	Group 3 PV - Group 3 BESS	4	3
Tot		42	

Tab 6.2: Criteria taken in account for the economic analysis.

Tab 6.2 shows that some criteria have no nodes, so the analysis is reduced to six possible combinations of the PV and BESS systems. In particular, the calculation of the NET and therefore of the payback have been made considering first the case of a PV system and then the case of the combined PV-battery system.

As regards the input data for the calculation of the NET, the cost of electricity was provided by the Anglo-Saxon government website (www.gov.uk), in particular by the *Department for Business, Energy and Industrial Strategy* and are reported in Fig 6.8:

Table 2.2.3 Average annual domestic standard electricity bills in 2017 for UK regions with average unit costs based on consumption of 3,800kWh/year^{(1)(P)}

Payment type Region ⁽²⁾	Pence per kWh and pounds							
	Credit		Direct debit		Prepayment		Overall	
	Unit cost	Bill	Unit cost	Bill	Unit cost	Bill	Unit cost	Bill
East Midlands	17,08	649	15,31	582	16,01	608	15,80	601
Eastern	17,32	658	15,48	588	16,19	615	16,00	608
London	17,69	672	15,91	605	15,91	604	16,49	626
Merseyside & North Wales	18,73	712	16,75	636	17,25	656	17,25	656
North East	17,68	672	15,69	596	16,40	623	16,24	617
North Scotland	18,92	719	17,10	650	17,73	674	17,59	669
North West	17,55	667	15,71	597	16,27	618	16,22	616
Northern Ireland	14,69	558	14,45	549	14,41	548	14,48	550
South East	17,93	681	16,08	611	16,59	630	16,53	628
South Scotland	17,34	659	15,54	591	16,16	614	16,03	609
South Wales	18,34	697	16,56	629	16,98	645	17,02	647
South West	18,84	716	16,95	644	17,39	661	17,41	662
Southern	17,70	673	15,78	599	16,43	624	16,23	617
West Midlands	17,69	672	15,64	594	16,34	621	16,22	616
Yorkshire	17,39	661	15,28	581	16,04	609	15,89	604
UK ⁽²⁾	17,63	670	15,81	601	16,28	619	16,30	619

Fig 6.8: Average annual domestic standard electricity bills in 2017 for UK regions with average unit costs based on consumption of 3800 kWh/year (www.gov.uk).

It is necessary to underline that the prices shown in Fig 6.8 are calculated considering an annual energy consumption equal to 3800 kWh, so in the hypothesis of calculation it is necessary to consider a possible error due to the approximation made using these values to calculate the cost in the cases analyzed in which the annual consumption turns out to be different. The p_{in} price chosen from the table in Fig 6.8 is equal to 17,59 pence/kWh and coincides with the energy price for an annual consumption of 3800 kWh in the North of Scotland (the same area where the village of Fintry is located) and placed in the column called *Overall*.

About the cost of a PV system in Scotland, on the same website of the government (www.gov.uk) an average total cost of a photovoltaic system in the UK is provided for the year 2017 and shown in the figure:

Year	Month	0-4kW					4-10kW					10-50kW					
		Number of installations	£ per kW installed				Number of installations	£ per kW installed				Number of installations	£ per kW installed				
			Median	Mean	Lower CI	Upper CI		Median	Mean	Lower CI	Upper CI		Median	Mean	Lower CI	Upper CI	
2017	April	1.186	1.669	1.864	1.817	1.910	110	1.283	1.368	1.280	1.456	61	1.014	1.101	1.008	1.194	
	May	1.898	1.794	1.920	1.885	1.954	149	1.364	1.495	1.425	1.564	94	1.089	1.196	1.107	1.284	
	June	1.745	1.698	1.824	1.788	1.860	207	1.425	1.531	1.462	1.601	95	1.127	1.137	1.074	1.200	
	July	1.491	1.636	1.768	1.732	1.805	168	1.415	1.534	1.448	1.621	92	1.041	1.105	1.010	1.200	
	August	1.918	1.660	1.821	1.786	1.856	173	1.372	1.500	1.427	1.573	109	1.114	1.199	1.123	1.275	
	September	1.975	1.733	1.878	1.845	1.911	210	1.370	1.482	1.412	1.552	124	1.025	1.099	1.053	1.144	
	October	1.635	1.659	1.815	1.778	1.851	176	1.407	1.519	1.437	1.601	86	1.098	1.172	1.101	1.243	
	November	2.006	1.720	1.812	1.780	1.843	178	1.428	1.513	1.434	1.591	99	1.111	1.122	1.068	1.177	
	December	1.390	1.733	1.829	1.792	1.866	162	1.439	1.521	1.444	1.598	86	1.122	1.218	1.134	1.303	
	2018	January	1.378	1.685	1.811	1.772	1.849	129	1.365	1.522	1.425	1.619	86	1.048	1.101	1.052	1.151
	February	1.293	1.714	1.854	1.817	1.891	129	1.419	1.583	1.476	1.689	82	1.125	1.209	1.104	1.313	
	March	1.793	1.714	1.885	1.848	1.922	194	1.431	1.546	1.471	1.621	134	1.043	1.176	1.090	1.261	
Total 2017/18		19.708	1.701	1.840	1.830	1.850	1.985	1.393	1.509	1.486	1.533	1.148	1.080	1.153	1.131	1.175	

-10,4%

Fig 6.9: Solar PV costs data (www.gov.uk).

The value considered is the average between 2017 and 2018 in the column called *Median* in the system section between 4 and 10 kWp and equal to 1393 £/kWp installed. However, it would not be wrong to consider the last section with calculated prices based on systems between 10 and 50 kWp because the project considered assumes the assignment of a photovoltaic system for each house considered in the village of Fintry, so it can be considered a single system with very high capacity.

About the price of batteries, the official website of *Sonnen* (<https://sonnen.de/stromspeicher/sonnenbatterie-eco/#product-config>) provides the prices for batteries of all the needed sizes for domestic use. Tab 6.3 shows the prices of the types of batteries considered:

$E_{STORAGE}^{MAX}$ [kWh]	C_{tot} [€]
4	6299,00
10	12799,00
16	17699,00

Tab 6.3: Sonnen battery prices (<https://sonnen.de/stromspeicher/sonnenbatterie-eco/#product-config>).

About incentives, the value of the FIT depends on many factors, among which the most important is the energy efficiency of the building. In this case it was assumed that the analyzed houses have the highest energy level, being part of an innovative project such as *Smart Fintry*. For a building with the highest energy level on which a PV system with a size between 0 kWp and 10 kWp is installed, the FIT in force from 1st October 2018 to 31st December 2018 is equal to 3,86 pence/kWh (<https://www.ofgem.gov.uk/environmental-programmes/fit/fit-tariff-rates>). At the same time, the tariff concerning the energy fed into the network and therefore sold is equal to 3,72 pence/kWh (<https://www.ofgem.gov.uk/environmental-programmes/fit/fit-tariff-rates>).

Finally, assuming a maximum life value respectively equal to 25 years for PV systems and to 15 years for BESS and a discounting rate of 1,20%, the simple NET and the discounted NET were calculated for the cases mentioned with and without the presence of the battery considering one representative node for each criteria.

Tab 6.4 shows the input parameters to calculate the NET value, the following figures show the cash flows of the investments in PV systems for the nodes 10, 64 and 96

(respectively Fig 6.10, Fig 6.11, Fig 6.12, Fig 6.13, Fig 6.14, Fig 6.15) while Tab 6.5 shows which year represent the payback.

Node	10	64	96
Parameters			
Pn [kWp]	3	6	9
C_i [€]	4179	8358	12537
n	25	25	25
i	1,20%	1,20%	1,20%
ΔMR_i [€]	0,00	0,00	0,00
ΔMR_f [€]	147,59	270,32	378,93
ΔMOC_i [€]	328,07	1007,43	3371,36
ΔMOC_f [€]	212,09	682,12	2790,81
ΔCF [€]	263,57	595,63	959,48

Tab 6.4: Parameters to calculate the NET value and the payback for the nodes 10, 64 and 96.

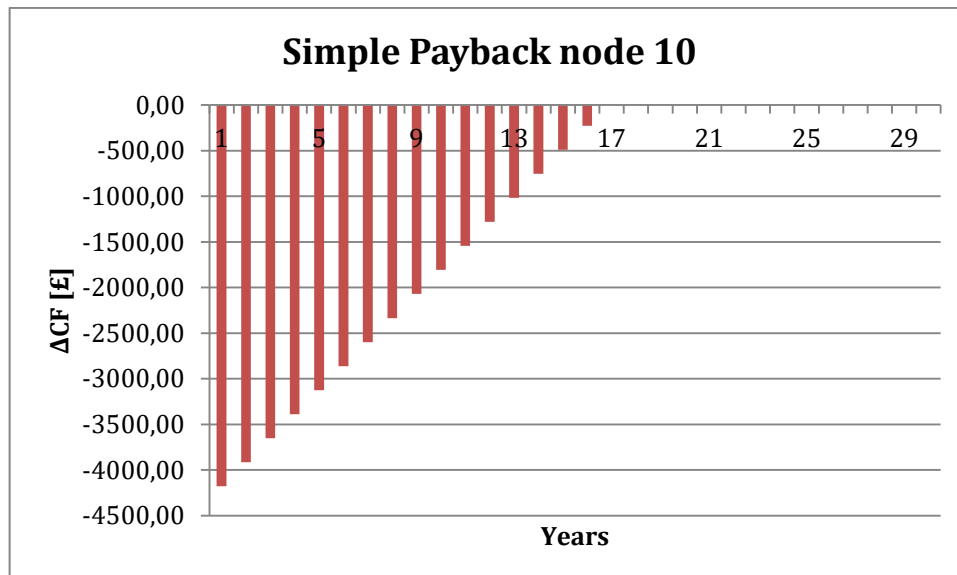


Fig 6.10: NET trend considering the simple payback for the node 10.

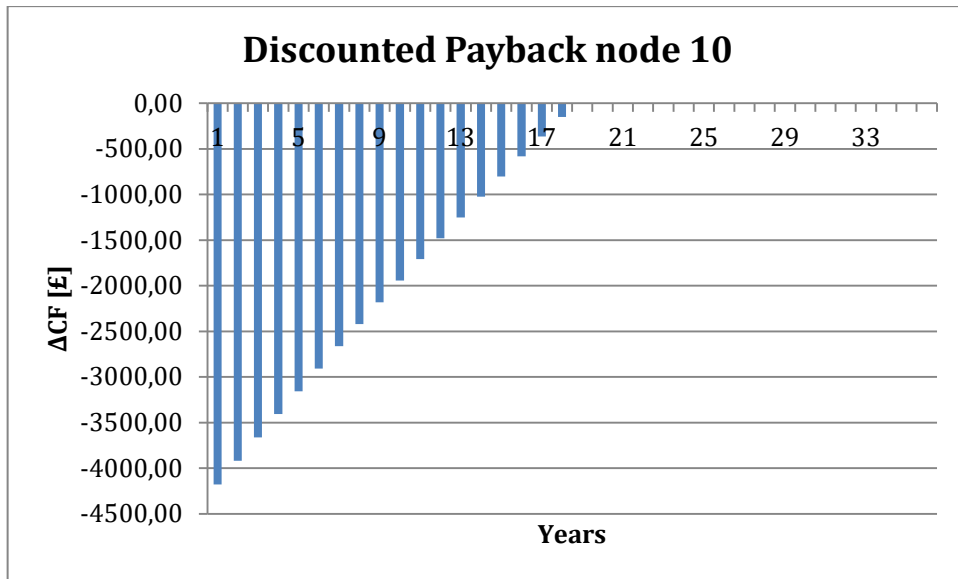


Fig 6.11: NET trend considering the discounted payback for the node 10.

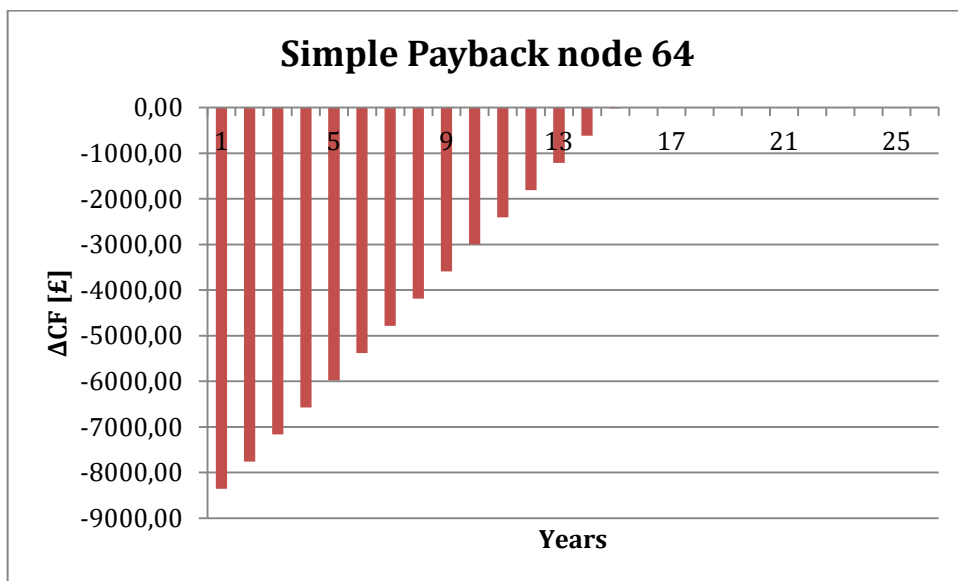


Fig 6.12: NET trend considering the simple payback for the node 64.

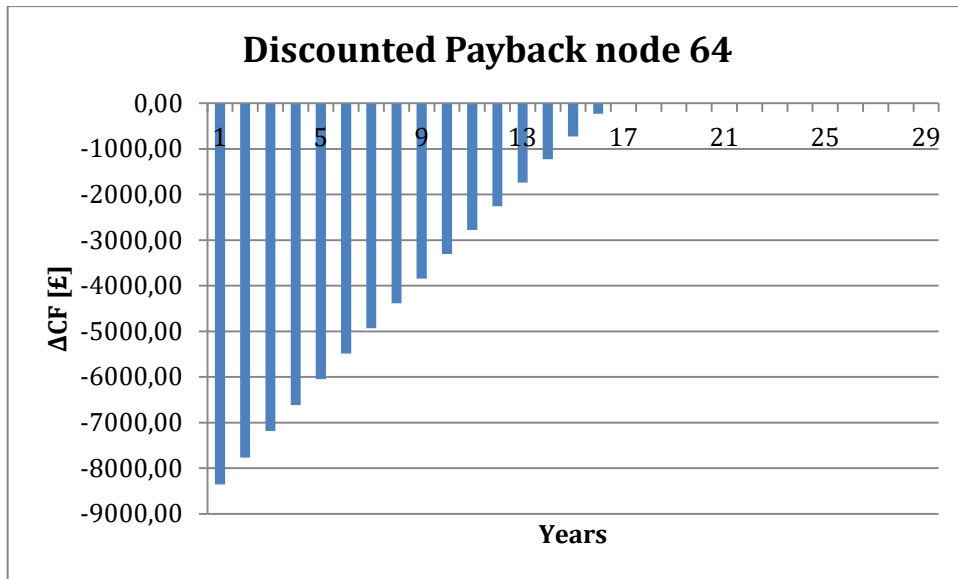


Fig 6.13: NET trend considering the discounted payback for the node 64.

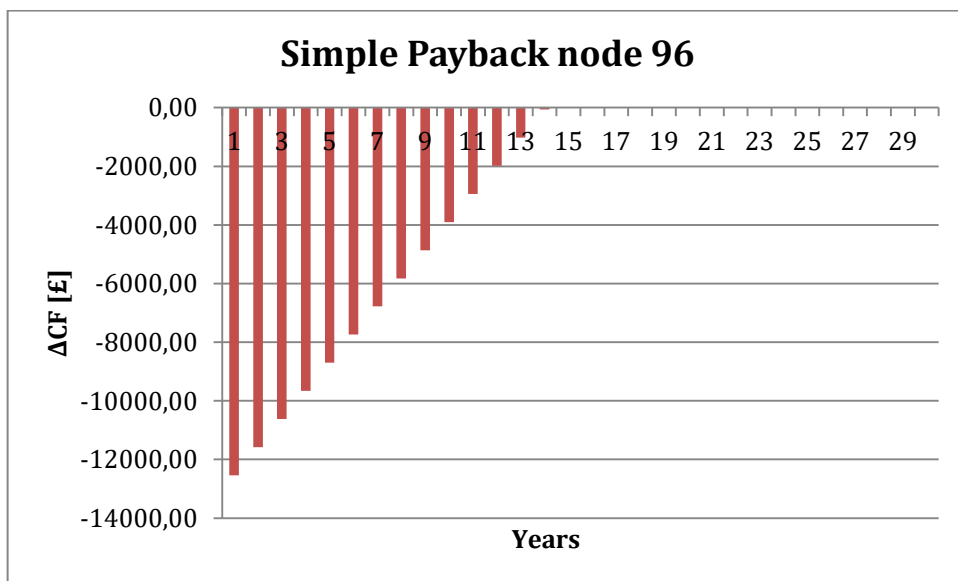


Fig 6.14: NET trend considering the simple payback for the node 96.

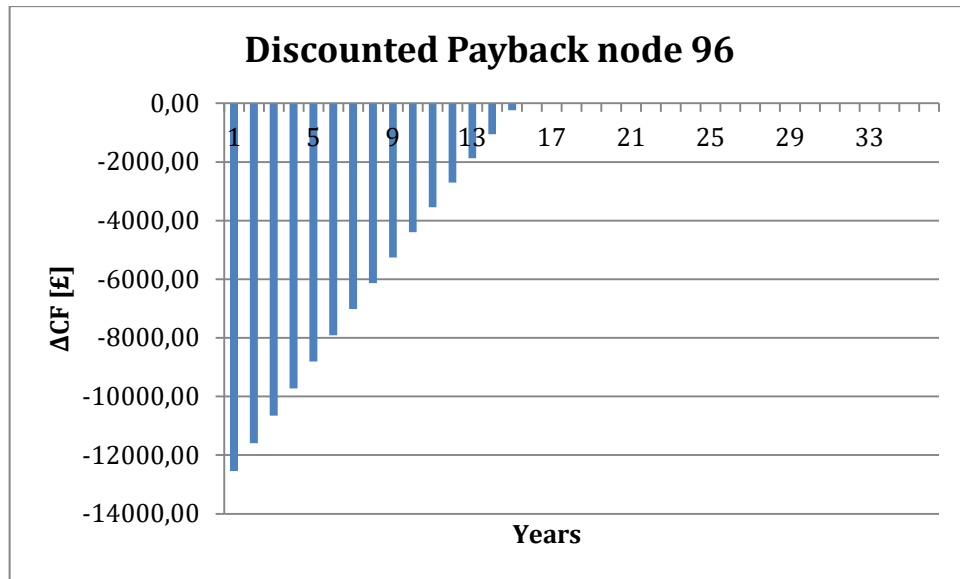


Fig 6.15: NET trend considering the discounted payback for the node 96.

Node	PV size [kWp]	Simple Payback [year]	Dicounted Payback [year]
10	3	16	18
64	6	15	16
96	9	14	15

Tab 6.5: Simple and discounted paybacks for the representative nodes of the three different PV sizes.

Tab 6.6 shows the input parameters to calculate the NET value, the following figures show the cash flows of the investments in PV-BESS systems for the representative nodes of the analyzed criteria described in Tab 6.2 (respectively Fig 6.16, Fig 6.17, Fig 6.18, Fig 6.19, Fig 6.20, Fig 6.21, Fig 6.22, Fig 6.23, Fig 6.24, Fig 6.25, Fig 6.26, Fig 6.27) while Tab 6.7 shows which year represent the payback.

Criteria Node	1 10	2 64	4 67	5 49	6 96	9 3
Parameters						
P_n [kWp]	3	6	3	6	9	9
BESS capacity [kWh]	4	4	10	10	10	16
C_i' [€]	10478	14657	16978	21157	25336	30236
n	25	25	25	25	25	25
i	1,20%	1,20%	1,20%	1,20%	1,20%	1,20%
ΔMR'_i [€]	0,00	0,00	0,00	0,00	0,00	0,00
ΔMR'_f [€]	120,19	233,06	123,28	199,98	310,45	267,05
ΔMCO'_i [€]	328,07	1007,43	632,63	1137,78	3371,36	3682,65
ΔMCO'_f [€]	129,42	569,76	439,45	608,73	2584,21	2752,88
ΔCF' [€]	318,84	670,73	316,47	729,03	1097,60	1196,82

Tab 6.6: Parameters to calculate the NET value and the payback for the analyzed criteria.

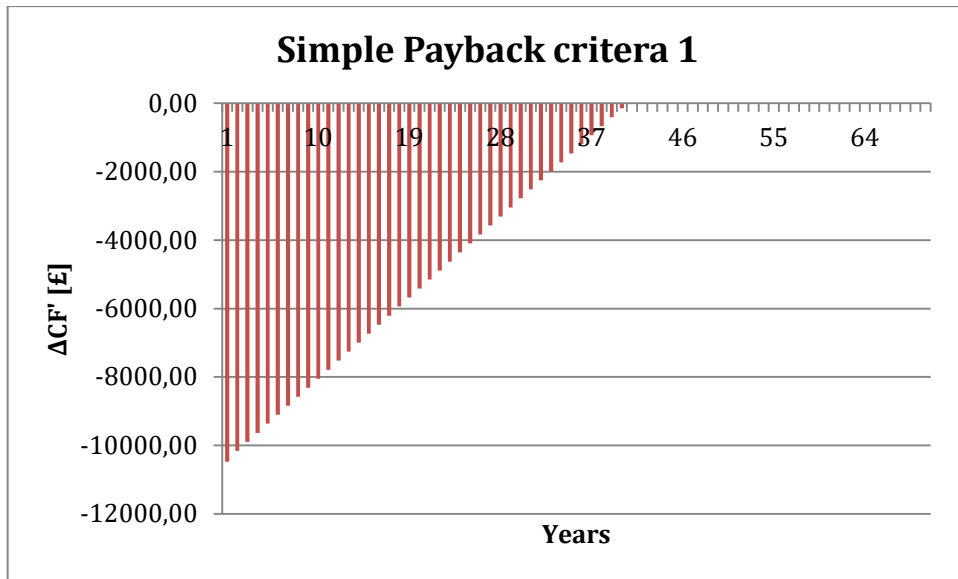


Fig 6.16: NET trend considering the simple payback for the criteria 1.

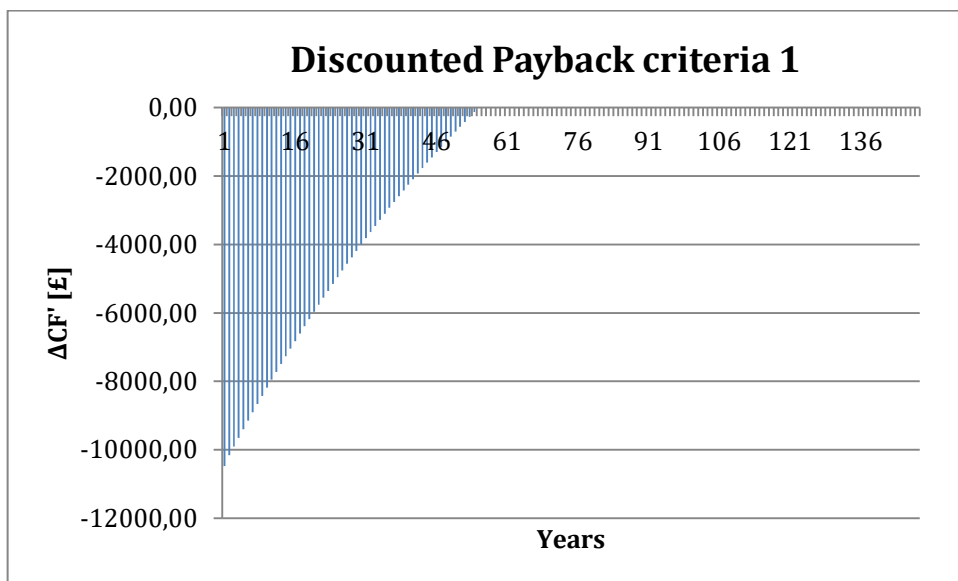


Fig 6.17: NET trend considering the discounted payback for the criteria 1.

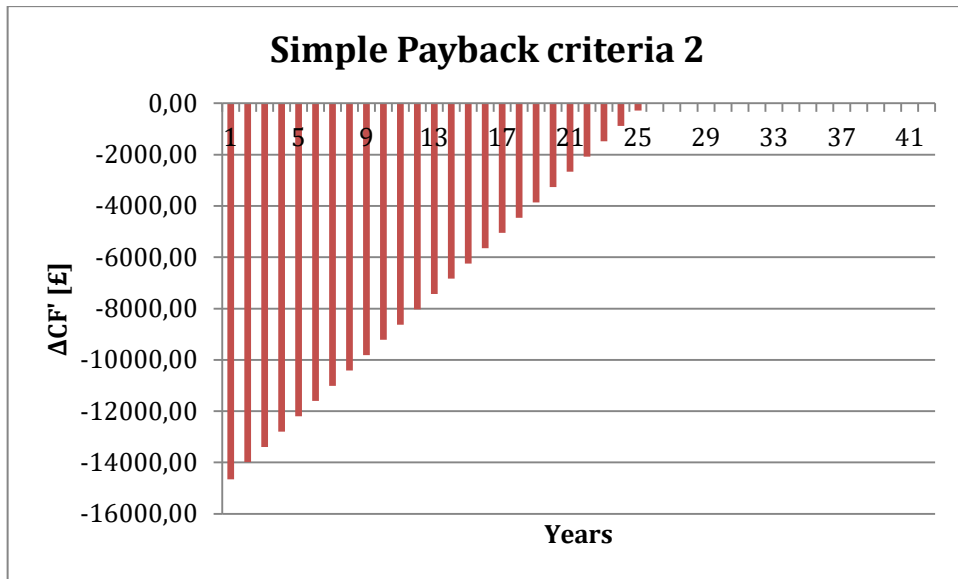


Fig 6.18: NET trend considering the simple payback for the criteria 2.

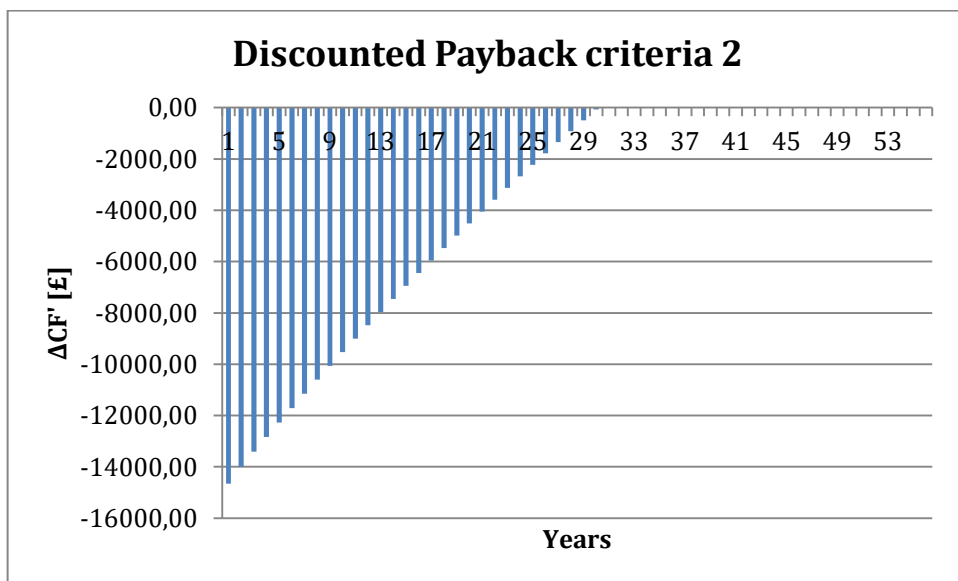


Fig 6.19: NET trend considering the discounted payback for the criteria 2.

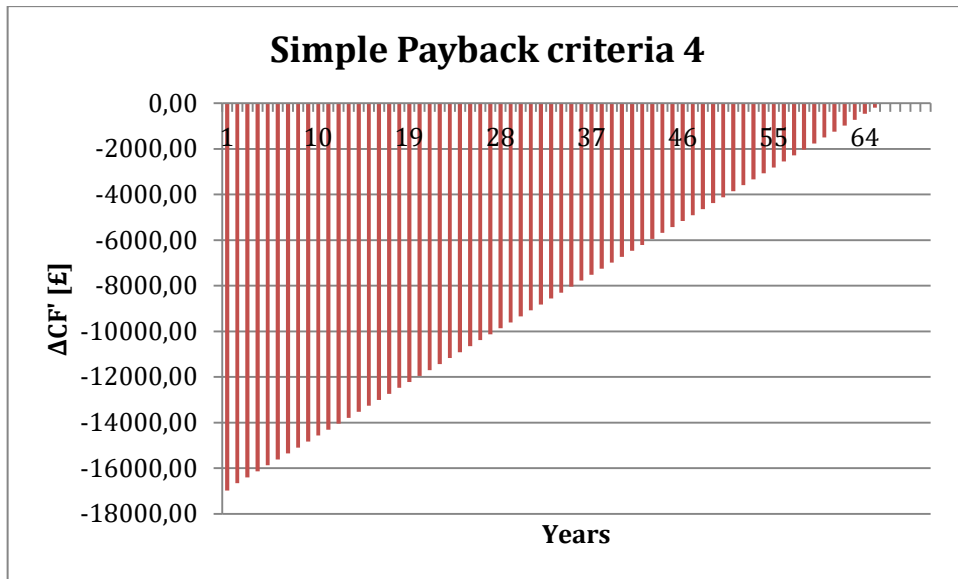


Fig 6.20: NET trend considering the simple payback for the criteria 4.

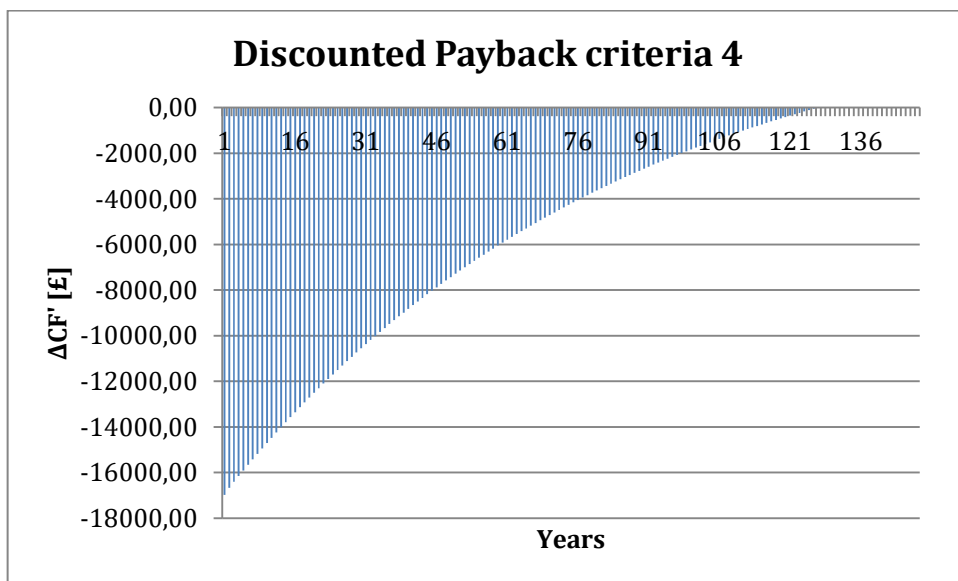


Fig 6.21: NET trend considering the discounted payback for the criteria 4.

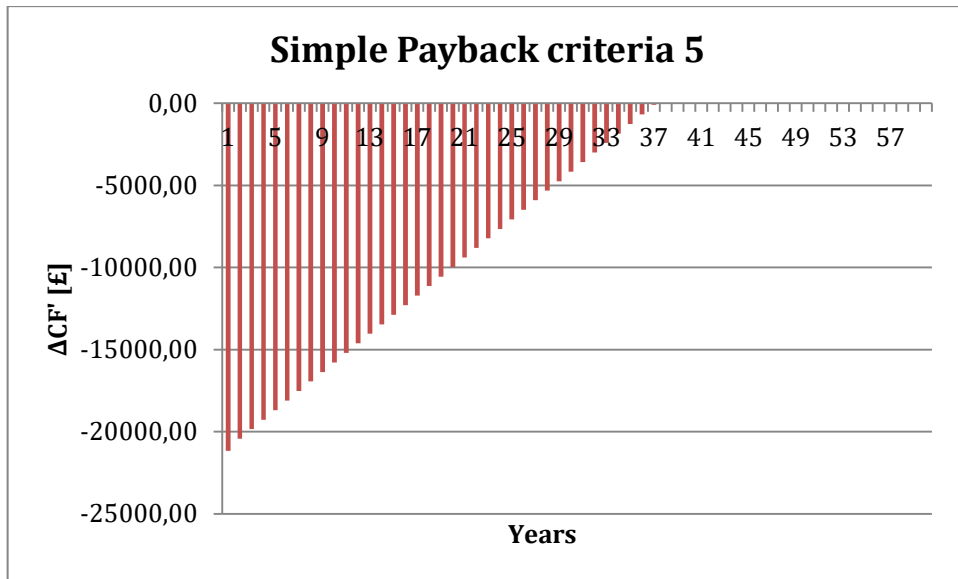


Fig 6.22: NET trend considering the simple payback for the criteria 5.

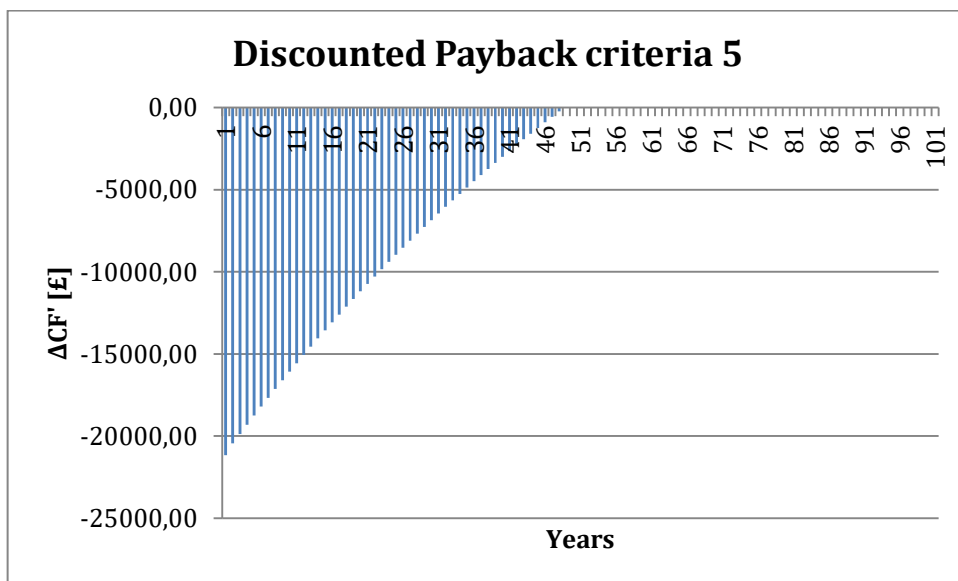


Fig 6.23: NET trend considering the discounted payback for the criteria 5.

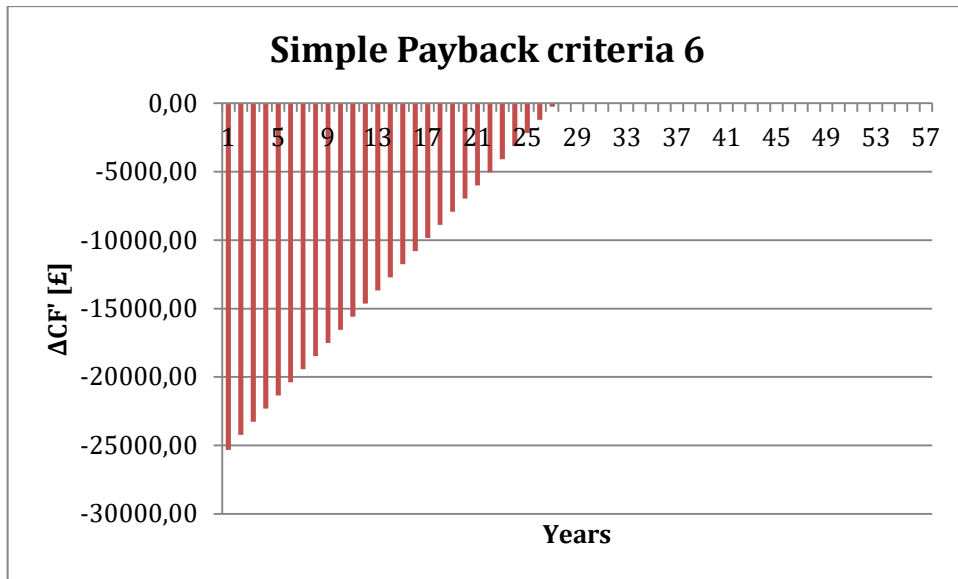


Fig 6.24: NET trend considering the simple payback for the criteria 6.

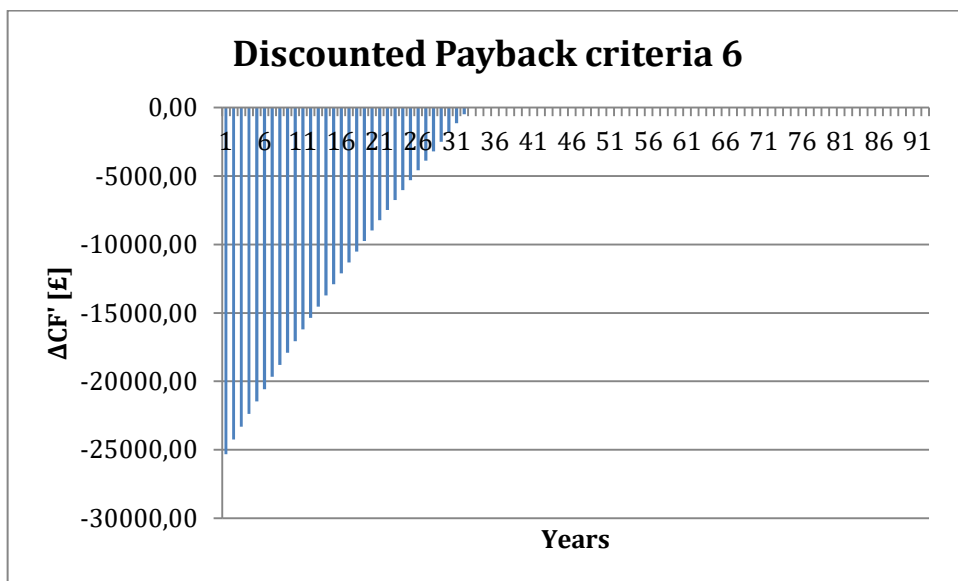


Fig 6.25: NET trend considering the discounted payback for the criteria 6.

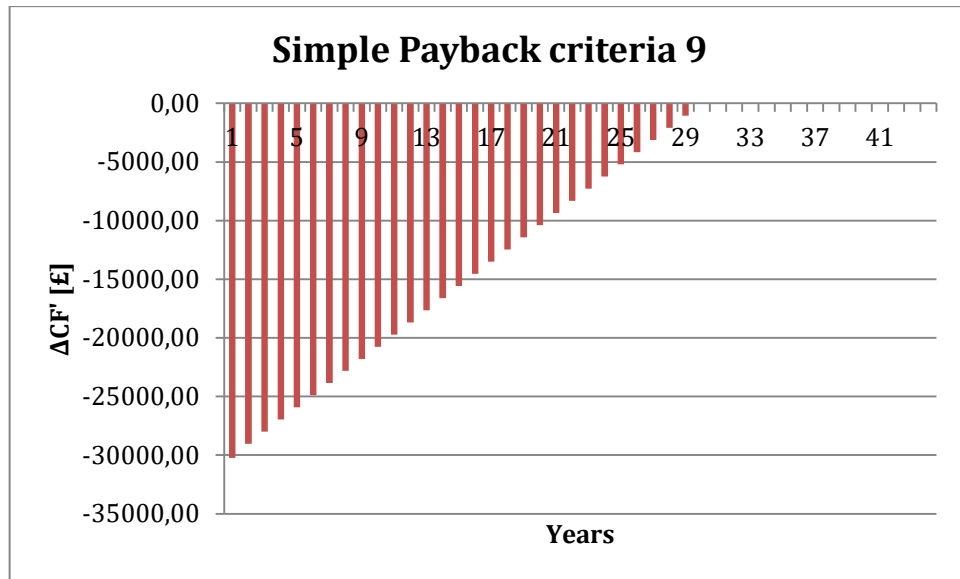


Fig 6.26: NET trend considering the simple payback for the criteria 9.

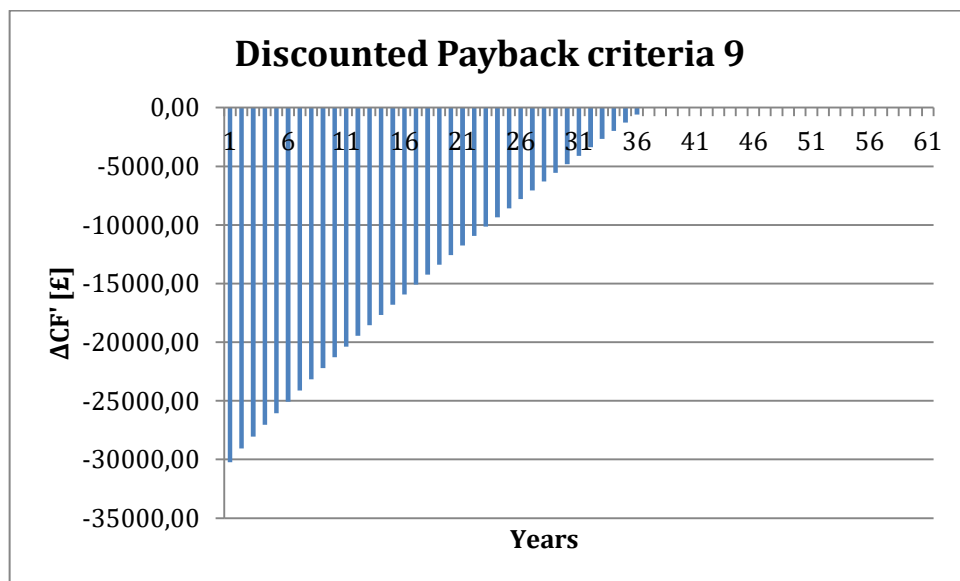


Fig 6.27: NET trend considering the discounted payback for the criteria 9.

Criteria	Node	Simple Payback [year]	Discounted Payback [year]
1	10	40	54
2	64	25	30
4	67	65	126
5	49	37	48
6	96	27	32
9	3	30	36

Tab 6.7: Simple and discounted paybacks for the representative nodes of the analyzed criteria.

It is important to underline that for the calculation of the NET and therefore of the payback the maintenance costs and the costs of disposal of the panels when the system will no longer have an acceptable efficiency were not considered, neither the degradation of the system and a consequent loss in efficiency over time.

7. CONCLUSIONS

Analysing the results of the NET calculation for the representative nodes in case a PV system is installed and in case a combined PV-BESS system is installed, the payback is not acceptable and therefore the investment is not convenient, mostly considering the lifetime of PV systems and BESS.

The reasons why such investments are not convenient can be multiple, so it is necessary to take different aspects into account.

The first aspect is represented by the capital cost of PV systems and batteries. The learning curves shown above describe the phenomenon of lowering the prices of such systems for each doubling of production (Fig 6.2, Fig 6.6). The result of these analyses is the forecast of future prices of such systems that could stimulate the growth of investments in this sector.

For example, it would be interesting to study the possible scenario that would occur in 2025 considering the decrease of the capital cost, with the same tariff of energy and of the incentive (in this case the FIT). Respectively from Fig 6.4 (considering the intermediate scenario) and Fig 6.6 it is possible to derive the approximate percentage reduction of the capital costs of either the PV systems and the batteries in order to calculate the cash flows for the cases examined in the village of Fintry. Tab 7.1 shows the values of the capital costs of today's PV and BESS systems respectively and that expected in 2025.

System	Price [£]		Percentage reduction [%]
	2018	2025	
PV [1 kWp]	1393	599	30%
BESS [4 kWh]	6299	2520	51,58%

Tab 7.1: Capital costs of PV systems and BESS in 2018 and forecast of capital costs of PV system and BESS in 2025.

Assuming a possible scenario of the year 2025, making the same investments made for the houses of the village of Fintry but imposing the new capital cost expected in the new year considered, it is possible to calculate the values of the payback for nodes 10, 64 and 96 in case of a PV system (Tab 7.2, Fig 7.1, Fig 7.2) and for the nodes representing criteria 1, 2, 4, 5, 6 and 9 in case of a combined PV-BESS system (Tab 7.3, Fig 7.3, Fig 7.4).

Node	scenario 2018		scenario 2025	
	Simple Payback [year]	Discounted Payback [year]	Simple Payback [year]	Discounted Payback [year]
10	16	18	12	12
64	15	16	10	11
96	14	15	10	10

Tab 7.2: Possible scenario in 2025 considering a decrease of the capital costs of PV systems considering the same energy tariff and FIT in force nowadays.

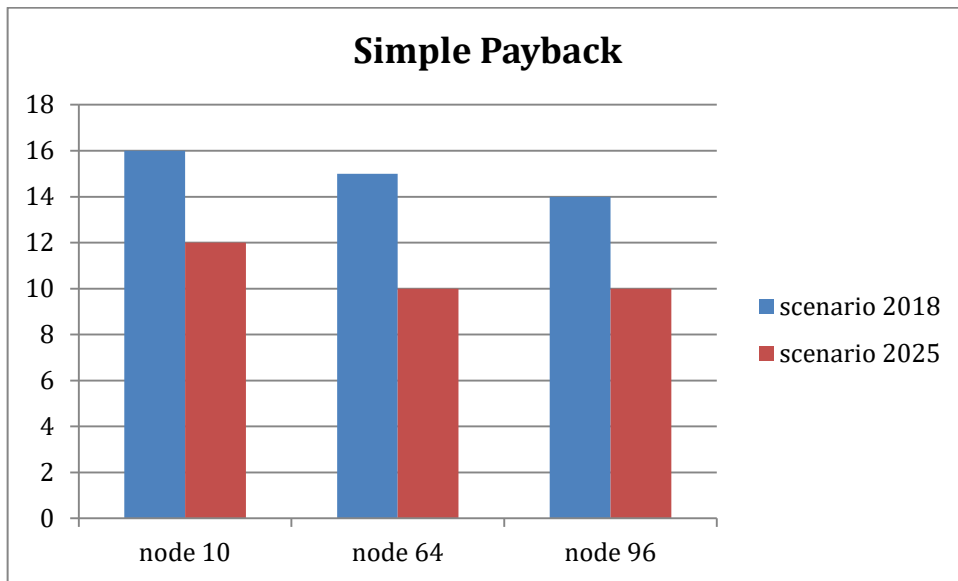


Fig 7.1: Chart of the different simple paybacks considering the two different scenarios (2018 and 2025) in case of the PV systems analyzed.

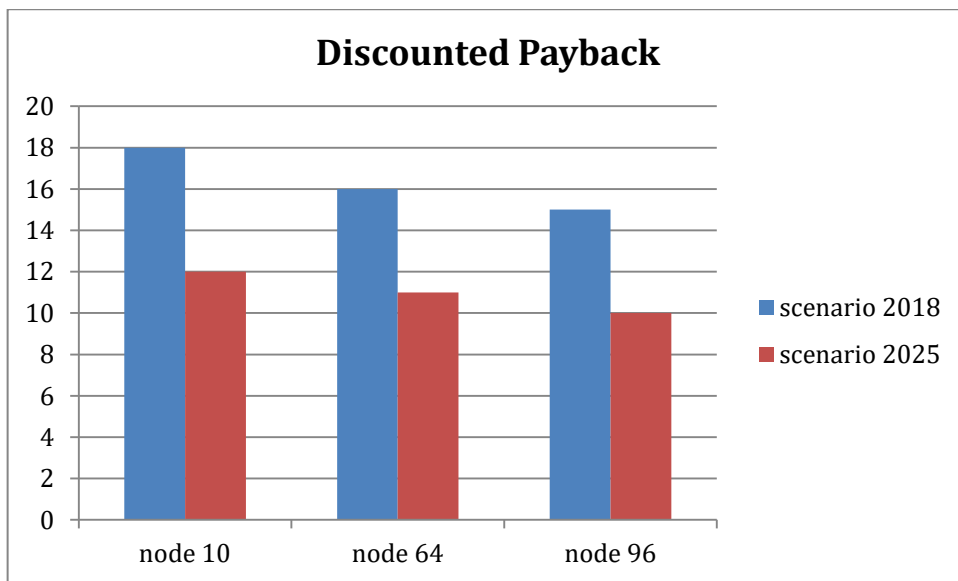


Fig 7.2: Chart of the different discounted paybacks considering the two different scenarios (2018 and 2025) in case of the PV systems analyzed.

Criteria	Node	scenario 2018		scenario 2025	
		Simple Payback [year]	Discounted Payback [year]	Simple Payback [year]	Discounted Payback [year]
C1	10	40	54	23	27
C2	64	25	30	15	17
C4	67	65	126	35	46
C5	49	37	48	21	24
C6	96	27	32	16	18
C9	3	30	36	17	19

Tab 7.3: Possible scenario in 2025 considering a decrease of the capital costs of PV systems and BESS considering the same energy tariff and FIT in force nowadays.

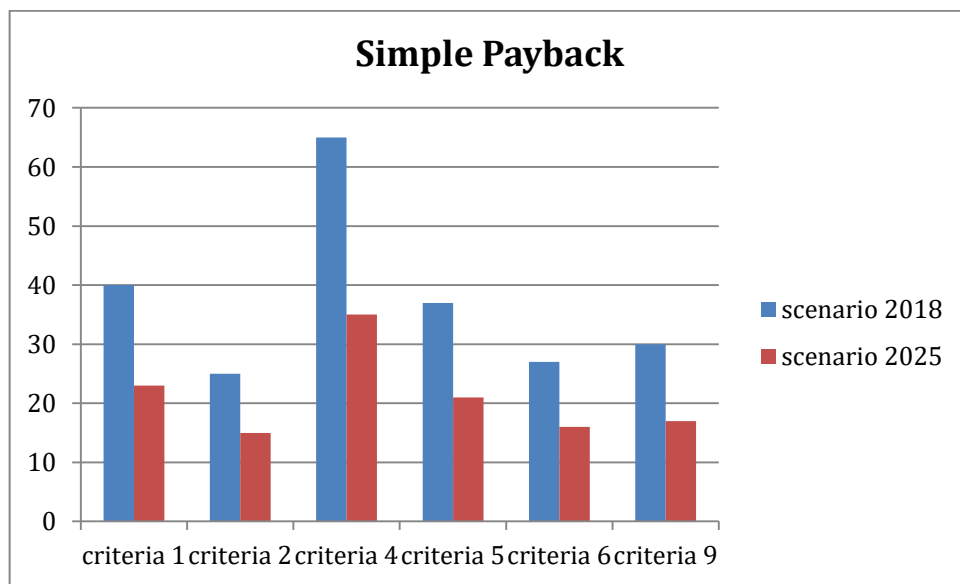


Fig 7.3: Chart of the different simple paybacks considering the two different scenarios (2018 and 2025) in case of the combined PV-battery systems analyzed.

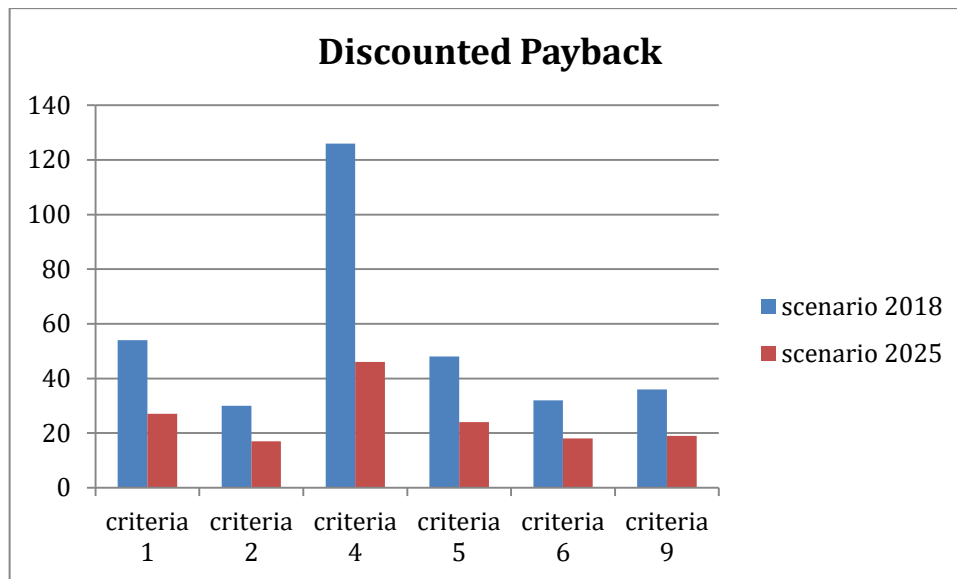


Fig 7.4: Chart of the different discounted paybacks considering the two different scenarios (2018 and 2025) in case of the combined PV-battery systems analyzed.

The obtained payback values considering the capital costs in 2025 are much lower than the values obtained considering the current capital costs. For a PV system it may be acceptable to obtain paybacks lower than 10 years while for combined PV-BESS systems the investment continues to be not much convenient. The costs of the considered batteries (Sonnen) are too high compared to how much actual gain can be obtained by storing the excess energy in them, despite having considered very high capital cost reductions.

A second aspect is represented by the climatic data of temperature and solar radiation of the areas considered. According to PVGIS, the energy produced in Fintry is about 720 kWh/kWp per year (Fig 5.17), while for example in South of Italy and specifically in Acri, a little town placed in Calabria (Fig 7.5), according to PVGIS it is possible to produce 1320 kWh/kWp in the situation of optimization of slope and azimuth angles (Fig 7.6), that is about 50% more energy produced. In Southern Italy there are even better cases. From a study carried out by Squatrito et al. (2014) on the Mediterranean greenhouses in the South of Sicily is a great convenience for photovoltaic investments even in the absence of incentives or tax deductions, while for PV systems with capacities exceeding 50 kWp it is possible to reach the parity of the network.

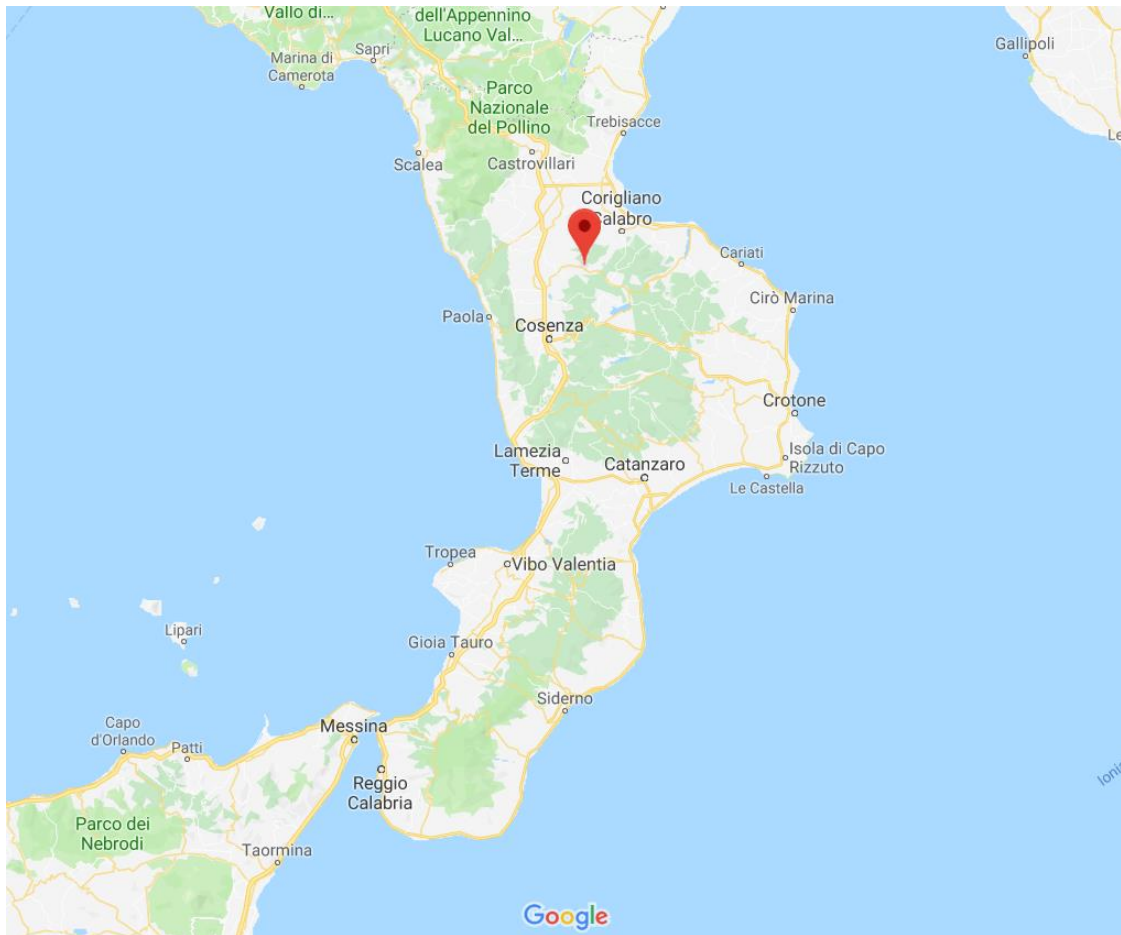


Fig 7.5: Acri (CS), Italy (www.google.com/maps)

Fixed system: inclination=31°, orientation=3° (optimum)				
Month	E_d	E_m	H_d	H_m
Jan	2.30	71.3	2.97	92.1
Feb	2.50	70.0	3.30	92.3
Mar	3.69	114	5.01	155
Apr	4.01	120	5.50	165
May	4.35	135	6.09	189
Jun	4.85	145	6.92	207
Jul	5.07	157	7.31	227
Aug	4.93	153	7.17	222
Sep	3.92	117	5.58	167
Oct	3.35	104	4.64	144
Nov	2.46	73.9	3.29	98.8
Dec	1.97	61.2	2.57	79.5
Yearly average	3.62	110	5.04	153
Total for year		1320		1840

Fig 7.6: Energy produced by a 1 kWp PV system in Acri (CS), Italy, provided by PVGIS.

A third aspect is represented by the *FIT scheme*. The FIT scheme was introduced in UK in April 2010 with the aim of promoting the development of renewable and low-carbon electricity generation technologies (Cherrington et al., 2013). The scheme is applicable for anyone who installs a technology between solar photovoltaic (PV), wind, hydro, micro combined heat and power (CHP), anaerobic digestion (AD) currently up to a capacity of 5 MW or 2 kW for CHP (www.ofgem.gov.uk).

The FIT scheme provides for three financial incentives: a *generation tariff*, ie the energy provider pays a fixed tariff for each unit (kWh) of electricity generated; *export tariff*, ie all technologies receive an additional fixed tariff for each unit of electricity supplied to the network; finally the *electricity bill savings* thanks to self-consumption.

Ultimately the FIT scheme is a government program, payments are made quarterly based on the meter reading provided to the respective energy provider. The rates are different and depend on the type of system installed and the level of energy efficiency of the house.

As already mentioned previously, in this work of thesis it was assumed that all the considered houses guarantee the highest level of energy efficiency so as to be able to access the rates shown in the first row of Tab 7.4.

For example, it would be interesting to compare the current FIT scheme in force in Scotland with the old FIT scheme in force in UK between 2010 and 2011, and with the old Italian incentive scheme called "*Conto Energia*", now no longer in force.

The Italian Conto Energia is the Italian incentive regulation of the solar photovoltaic source regarding the systems connected to the electricity grid. It was introduced through the Legislative Decree number 387 of 2003. However, the concrete start of the measures occurred only in 2005 with the introduction of the so called *Primo Conto Energia*.

The Conto Energia was designed in Italy as a stimulus for the growth of investments in photovoltaics. Before it there was an incentive plan that provided a capital grant that covered up to 75% of the capital invested. The entry in force of the Conto Energia represented the transition from the capital grant to the one on the operating account, and it was clearly more convenient.

Similar to the FIT scheme used in the UK, the Conto Energia foresaw that the electricity produced by the PV systems was purchased by the company managing the electricity grid (GSE) on the basis of long-term contracts and with rates that have changed over the years according to the different Conto Energia.

The Primo Conto Energia in Italy envisaged two options for connection to the network: the *net-metering* and the *transfer into the network*. The net-metering means that the electrical network works as a sort of battery, that is, it allows the accumulation of excess energy and re-use it when the system does not work. The option to sell the network provided that the energy produced in excess does not constitute a credit but is sold to an energy manager at the rates set by the AEEG (Electricity and Gas Authority) and proportional to the annual production of power.

It would be interesting to compare the FIT scheme with the tariffs of the Secondo Conto Energia (GSE, 2009), which started in 2007 and lasted for 3 years. It has been considered the most convenient incentive ever had in Italy. Tab 7.4, Tab 7.5 and Tab 7.6 show the different rates in UK in 2018, in UK in 2010 and in Italy in 2007.

Description	Total Installed Capacity [kW]	FIT [pence/kWh]
Standard Solar photovoltaic receiving the higher rate	0-10	3,86
	10-50	4,11
	50-250	1,75
Standard Solar photovoltaic receiving the middle rate	0-10	3,47
	10-50	3,70
	50-250	1,58
Standard Solar photovoltaic receiving the lower rate	0-10	0,20
	10-50	0,20
	50-250	0,20
Export tariff		5,24

Tab 7.4: FIT in force in UK from 1th October 2018 to 31th December 2018 (www.ofgem.gov.uk).

Description	FIT [pence/kWh]
Solar photovoltaic with total installed capacity of 4 kW or less, where attached to or wired to provide electricity to a new building before first occupation	39,60
Solar photovoltaic with total installed capacity of 4 kW or less, where attached to or wired to provide electricity to a building which is already occupied	45,40
Solar photovoltaic (other than stand-alone) with total installed capacity greater than 4 kW but not exceeding 10 kW	39,60
Export tariff	3,20

Tab 7.5: FIT in force in UK between 2010 and 2011 (www.ofgem.gov.uk).

Potenza nominale dell'impianto (kW)		Tipologia di impianto fotovoltaico		
		1 Non integrato	2 Parzialmente integrato	3 Integrato
A)	$1 \leq P \leq 3$	0,392	0,431	0,480
B)	$3 < P \leq 20$	0,372	0,412	0,451
C)	$P > 20$	0,353	0,392	0,431

Tab 7.6: Tariff [€/kWh] of the Italian Secondo Conto Energia in force between 2007 and 2010 (GSE, 2009).

Regarding the value of export tariff for the Secondo Conto Energia, it should be calculated on the basis of various parameters whose regulation is provided by the GSE. For simplicity, an approximate value of 0,10 €/kWh was considered (Cerino Abdin et al., 2018), which would correspond to 0,088 £/kWh if this tariff was converted nowadays.

In the examined case, the FIT considered is the one related to the highest level of energy efficiency and the tariff value is equal to 3,86 pence/kWh of energy generated while the FIT in UK in 2011 was 39,60 pence/kWh for a system of maximum 4 kWp installed on a new building or for a system of a size between 4 kWp and 10 kWp and 45,40 for a an already occupied building. About the Secondo Conto Energia in Italy the energy generated was paid 0,412 €/kWh (that would be 0,36 £/kWh nowadays) for systems partially integrated with nominal power between 3 kWp and 20 kWp.

It would be interesting to calculate the payback of the analyzed cases using the incentives in force in Scotland in 2010 and in Italy in 2007. Tab 7.7 shows the simple payback and the discounted payback in case of PV systems for representative nodes 10, 64 and 96 considering the tariff of new buildings before the occupation for the FIT of 2010 and a partial integrated PV system tariff for the Italian Secondo Conto Energia, while Fig 7.7 and Fig 7.8 show a chart representing the different values obtained. Tab 7.7 shows the simple payback and the discounted payback for the representative nodes of the criteria (nodes 10, 64, 67, 49, 96, 3) using the same tariffs, while Fig 7.9 and Fig 7.10 show a chart representing the different values obtained.

Node	FIT 2018		FIT 2011		Second Energy Account 2007	
	Simple Payback [year]	Discounted Payback [year]	Simple Payback [year]	Discounted Payback [year]	Simple Payback [year]	Discounted Payback [year]
10	16	18	5	5	5	5
64	15	16	5	5	5	5
96	14	15	5	5	5	5

Tab 7.7: Comparison between the three different incentives (UK FIT of 2018, UK FIT of 2010, Italian Secondo Conto Energia of 2007) in case of the PV systems analyzed.

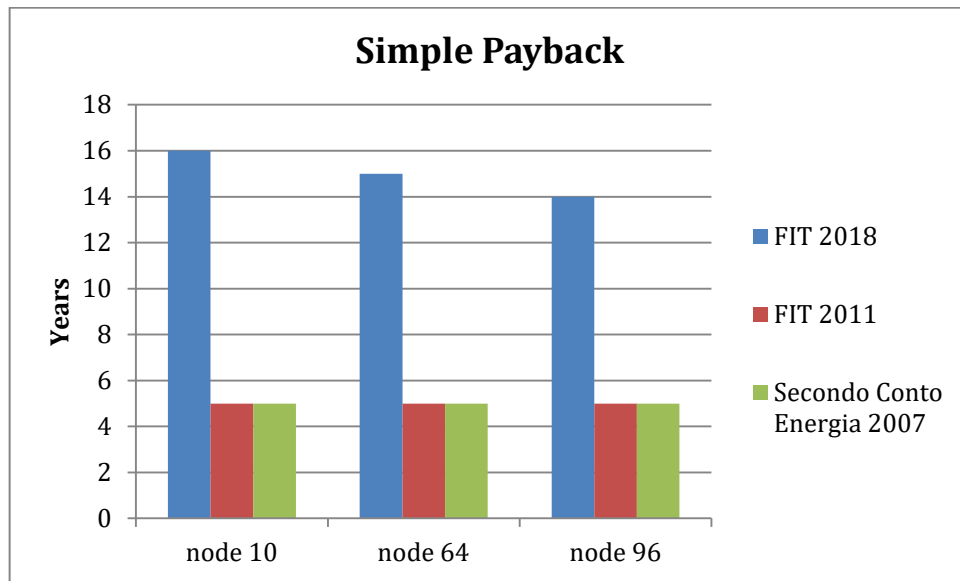


Fig 7.7: Chart of the different simple paybacks considering the three different incentives (UK FIT of 2018, UK FIT of 2010, Italian Secondo Conto Energia of 2007) in case of the PV systems analyzed.

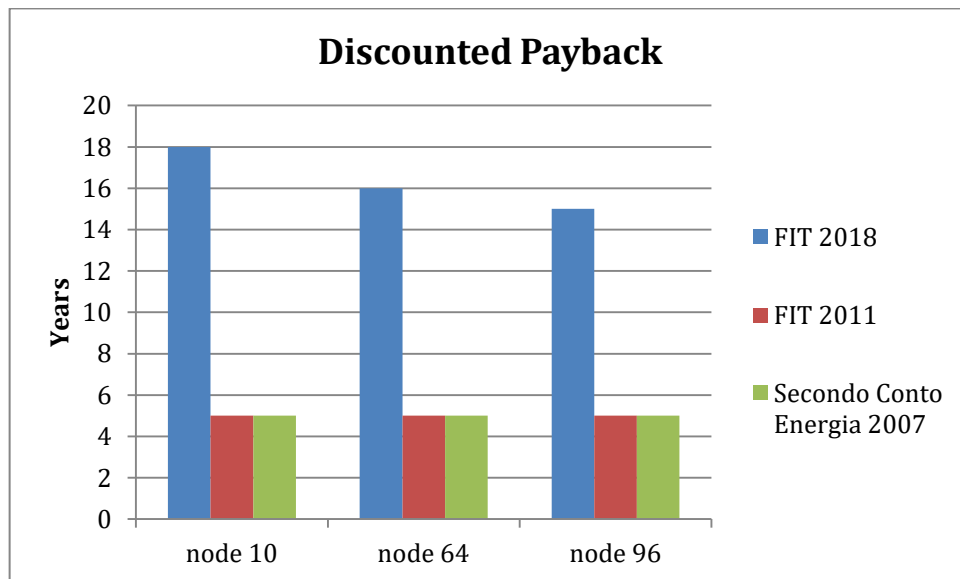


Fig 7.8: Chart of the different discounted paybacks considering the three different incentives (UK FIT of 2018, UK FIT of 2010, Italian Secondo Conto Energia of 2007) in case of the PV systems analyzed.

Criteria	Node	FIT 2018		FIT 2011		Second Energy Account 2007	
		Simple Payback [year]	Discounted Payback [year]	Simple Payback [year]	Discounted Payback [year]	Simple Payback [year]	Discounted Payback [year]
C1	10	40	54	12	12	11	12
C2	64	25	30	8	8	8	8
C4	67	65	126	18	21	18	20
C5	49	37	48	11	12	11	12
C6	96	27	32	9	9	9	9
C9	3	30	36	10	11	10	11

Tab 7.8: Comparison between the three different incentives (UK FIT of 2018, UK FIT of 2010, Italian Secondo Conto Energia of 2007) in case of the combined PV-BESS systems analyzed.

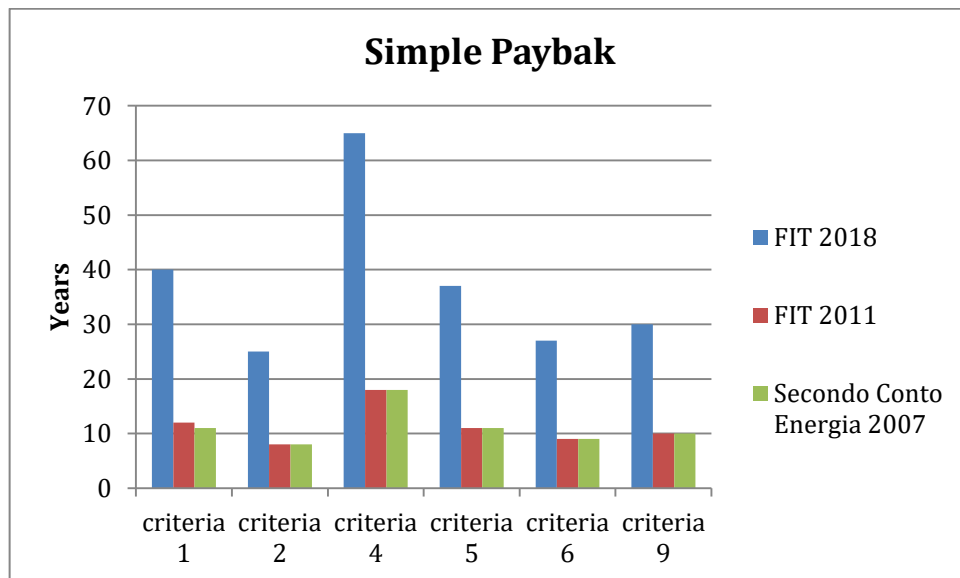


Fig 7.9: Chart of the different simple paybacks considering the three different incentives (UK FIT of 2018, UK FIT of 2010, Italian Secondo Conto Energia of 2007) in case of the combined PV-battery systems analyzed.

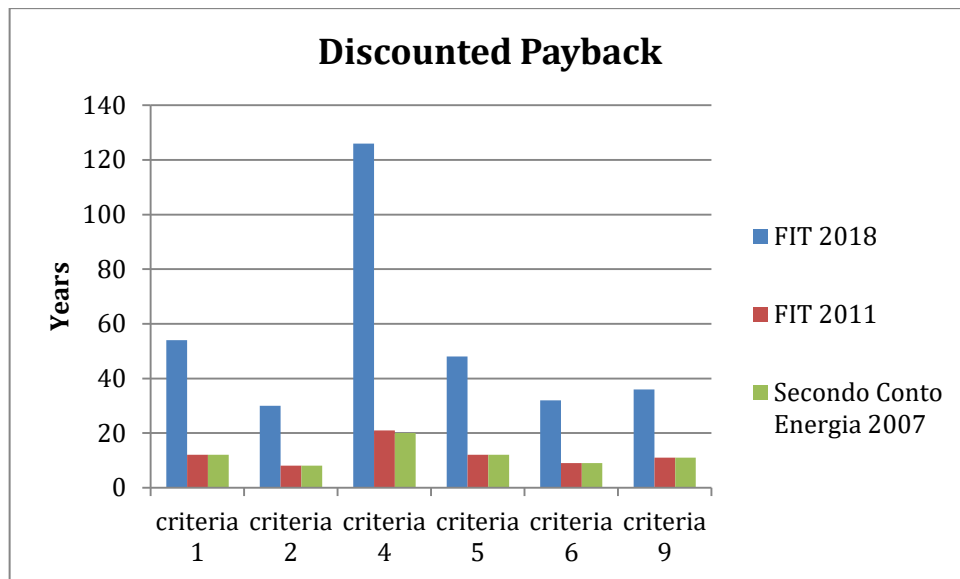


Fig 7.10: Chart of the different discounted paybacks considering the three different incentives (UK FIT of 2018, UK FIT of 2010, Italian Secondo Conto Energia of 2007) in case of the combined PV-battery systems analyzed.

In the two situations in which the old FIT of 2010 and the Secondo Conto Energia of 2007 rates are applied, the paybacks are lower. It is evident that an incentive for which the energy generated is paid about ten times more than the current values in Scotland would represent a huge economic advantage both in case of investment in a PV system and in case of investment in a combined PV-BESS system as for the gain in terms of self-consumption, the gain deriving from the energy sold and fed into the network and the income deriving from the remuneration of the generated energy are added. In other words, the beneficiary is paid for generating clean energy and paid twice for putting clean energy into the grid. Ultimately the payback values in both cases would be acceptable.

Increasing the incentives would be possible to greatly decrease the payback values both in the case of simple PV systems and in case of battery support. However, it would not be realistic to think of applying incentives whose tariffs are the same or otherwise similar to the old tariffs such as the 2011 FIT or the Secondo Conto Energia of 2007. The Secondo Conto Energia was applied in Italy at a time when the presence of photovoltaics on the territory it was relatively low compared to the major European countries. Precisely for this reason Italy was subject to heavy criticism regarding the high incentives that were applied at that time.

It is necessary to highlight how this comparison does not take into account numerous essential aspects such as a different capital cost, which certainly was much higher than the current one in 2007. This comparison has a purely numerical value and aims to show how the situation would change today if the FIT values were higher.

Considering the results of this work of thesis it is fair to conclude that investing in a photovoltaic system or in a combined PV-battery system in Scotland is not absolutely convenient in absence of incentives such as the FIT. However, it is not always convenient even if the incentives are taken into account because Scotland is in a low-irradiation zone where the amount of energy that can be produced is not sufficiently high.

8. REFERENCES

Abdallah, L., El-Shennawy, T., Nardini, S. (2013). Reducing carbon dioxide emissions from electricity sector using smart electric grid applications. *Journal of Engineering*, vol. 2013

Aguero, J.R., Chongfuangprinya, P., Shao, S. (2012). Integration of plug-in electric vehicles and distributed energy resources on power distribution systems. *IEEE*

Andreotti, M., Samorì, E. (2010). Centrali a biomassa e fotovoltaico – Sfruttamento dei terreni ed efficienze a confronto.

Ayodele, T.R., Ogunjuyigbe, A.S.O. (2015). Mitigation of wind power intermittency: storage technology approach. *Renewable and Sustainable Energy Reviews*, vol. 44, pp. 447-456

Beaudin, M., Zareipour, H., Schellenberglobe, A., Rosehart, W. (2010). Energy storage for mitigating the variability of renewable electricity sources: An updated review. *Energy for Sustainable Development*, vol. 14, issue 4, pp. 302-314

Bhandari, R., Stadler, I. (2009). Grid parity analysis of solar photovoltaic systems in Germany using experience curves. *Solar Energy*, vol 83, pp. 1634-1644

Bianchini, G., Paoletti, S., Vicino, A., Corti, F., Nebiacolombo, F. (2013). Model estimation of photovoltaic power generation using partial information. *IEEE PES*.

Cerino, G., Noussan, M. (2018). Electricity storage compared to net metering in residential PV applications. *Journal of Cleaner Production*, vol. 176, pp. 175-186

Chang, Y., Mao, X., Zhao, Y., Feng, S., Chen, H., Finlow, D. (2009). Lead-acid battery use in the development of renewable energy systems in China. *Journal of Power Sources*, vol. 191, pp. 176-183

Chau, K.T., Chan, C.C. (2007). Emerging energy-efficient technologies for hybrid electric vehicles. *IEEE*, vol. 95, n. 4, pp. 821-835

Chen, H., Ngoc Cong, T., Yang, W., Tan, C., Li, Y., Ding, Y. (2008). Progress in electrical energy storage system: A critical review. *Progress in Natural Science*, vol. 19, pp. 291-312.

Cherrington, R., Goodship, V., Longfield, A., Kirwan, K. (2012). The feed-in tariff in the UK: A case study focus on domestic photovoltaic systems. *Renewable Energy*, vol. 50, pp. 421-426

Corain, L. (2012). Modelli empirici. *Corso di laurea in Ingegneria Civile*. Università di Padova.

Corson, R., Regan, R., and Carlosn S., Triad Consulting Eng (2014). Implementing energy storage for peak-load shifting. *Consulting – Specifying Engineer*

Datta, M., Senjiyu, T., Yona, A., Funabashi, T., Kim, C.H. (2011). A frequency-control approach by photovoltaic generator in a PV-diesel hybrid power system. *IEEE*, vol. 26, n. 2, pp. 559-571

Davidson, C., Steinberg, D. (2013). Evaluating the impact of third-party price reporting and other drivers on residential photovoltaic price estimates. *Energy Policy*, vol. 62, pp. 752-761

De Azevedo Dias, C. L., Castelo Branco, D. A., Cardoso Arouca, M., Loureiro Legey, L. F. (2017). Performance estimation of photovoltaic technologies in Brazil. *Renewable Energy*, vol. 114, part B, pp. 367-375

Denholm, P., Margolis, R.M. (2007). Evaluating the limits of solar photovoltaics (PV) in electric power systems utilizing energy storage and other enabling technologies. *Energy Police*, vol. 35, n. 9, pp. 4424-4433

Elshurafa, A. M., Albardi, S. R., Bigerna, S., Bollino, C. A. (2018). Estimating the learning curve of solar PV balanceofesystem for over 20 countries: Implications and policy recommendations. *Journal of Cleaner Production*, vol. 196, pp. 122-134

Elshurafa, A. M., Albardi, S. R., Bollino, C. A., Bigerna, S. (2017). Estimating the Learning Curve of Solar PV Balance-of-Systems for Over 20 Countries. *KAPSARC*.

Gray, E.MacA., Webb, C.J., Andrews, J., Shabani, B., Tsai, P.J., Chan, S.L.I. (2011). Hydrogen storage for off-grid power supply. *International Journal of Hydrogen Energy*, vol. 36, n. 1, pp. 654-663

Hammou, Z.A., Lacroix, M. (2006). A hybrid thermal energy storage system for managing simultaneously solar and electric energy. *Energy Conversion and Management*, vol. 47, n. 3, pp. 273-288

Hill, C.A., Such, M.C., Chen, D., Gonzales, J., Grady, W.M. (2012). Battery energy storage for enabling integration of distributed solar power generation. *IEEE*, vol. 3, n. 2, pp. 850-857

Hoff, T.E., Perez, R. (2010). Quantifying PV power output variability. *Solar Energy*, vol. 84, n. 10, pp. 1782-1793

IRENA, International Renewable Energy Agency. (2017). Electricity storage and renewables: costs and markets to 2030.

Jabir, M., Illias, H.A., Raza, S., Mokhlis, H. (2017). Intermittent smoothing approaches for wind power output: a review. *Energies*

Jankowski, N.R., McCluskey, F.P. (2014). A review of phase change materials for vehicle component thermal buffering. *Applied Energy*, vol. 113, pp. 1525-1561

Jung, H.Y., Kim, A.R., Park, M., Yu, I.K., Kim, S.H (2009). A Study on the operating characteristics of SMES for the dispersed power generation system. *IEEE*, vol. 19, n. 3, pp. 2028-2031

Kaldellis, J. K., Kapsali, M., Kavadias, K. A. (2014). Temperature and wind speed impact on the efficiency of PV installations. Experience obtained from outdoor measurements in Greece. *Renewable Energy*, vol. 66, pp. 612-624.

Karimi, M., Mokhlis, H., Naidu, K., Uddin, S., Bakar, A.H.A. (2016). Photovoltaic penetration issues and impacts in distribution network. *Renewable and Sustainable Energy Reviews*, vol. 53, pp. 594-605

Lanzini, A. (2015). Hydrogen storage technologies. Politecnico di Torino

Leewiraphan, C., Rakwichien, W., Ketjoy, N., Thanarak, P. (2012). Learning Curve Analysis of Photovoltaic System in Residential Building in Thailand. *Elsevier*, vol. 32, pp. 407-413

Martinez-Cesena, E. A., Azzopardi, B., Mutale, J. (2012). Assessment of domestic photovoltaic systems based on real options theory. *Progress in photovoltaics*, vol. 21, pp. 250-262

Mundada, A. S., Prehoda, E. W., Pearce, J. M. (2017). U.S. market for solar photovoltaic plug-and-play systems. *Renewable Energy*, vol. 103, pp. 255-264.

NREL, National Renewable Energy Laboratory. (2009). Evaluation of the Performance of the PVUSA Rating Methodology Applied to DUAL Junction PV Technology.

Pamparana, G., Kracht, W., Haas, J., Díaz-Ferrán, G., Palma-Behnke, R., Román, R. (2017). Integrating photovoltaic solar energy and a battery energy storage system to operate a semi-autogenous grinding mill. *Journal of Cleaner Production*, vol. 165, pp. 273-280

Pielichowska, K., Pielichowski, K. (2014). Phase change materials for thermal energy storage. *Progress in Materials Science*, vol. 65, pp. 67-123

Schmidt, O. (2018). Future cost of electricity storage and impact on competitiveness. Imperial College London.

Seel, J., Barbose, G. L., Wiser, R. H. (2014). An analysis of residential PV system price differences between the United States and Germany. *Energy Policy*, vol. 69, pp. 216-226

Seixas, J., Simões, S., Dias, L., Kanudia, A., Fortes, P., Gargiuo, M. (2015). Assessing the cost-effectiveness of electric vehicles in European countries using integrated modeling. *Energy Policy*, vol. 80, pp. 165-176

Shivashankar, S., Mekhilef, S., Mokhlis, H., Karimi, M. (2016). Mitigating methods of power fluctuation of photovoltaic (PV) sources. *Renewable and Sustainable Energy Reviews*, vol. 59, pp. 1170-1184

Squatrito, R., Sgroi, F., Tudisca, S., Di Trapani, A. M., Testa, R. (2014). Post Feed-in Scheme Photovoltaic System Feasibility Evaluation in Italy: Sicilian Case Studies. *Energies*, vol. 7, pp. 7147-7165

Thomson, M., Infield, D. (2017). Impact of widespread photovoltaics generation on distribution systems. *IET Renewable Power Generation*, vol. 1, n. 1, pp. 33-40

Trappey, A. J. C., Trappey, C. V., Tan, H., Liu, P. H. Y., Li, S., Lin, L. (2016). The determinants of photovoltaic system costs: an evaluation using a hierarchical learning curve model. *Journal of Cleaner Production*, vol. 112, pp. 1709-1716

Woyte, A., Bodach, M., Belmans, R., Nijs, J. (2003). Power fluctuation in micro-grids introduced by photovoltaics: analysis and solutions

Zheng, C., Kammen, D. M. (2014). An innovation-focused roadmap for a sustainable global photovoltaic industry. *Energy Policy*, vol. 67, pp. 159-169

9. WEBSITES

Ronchetti, M. (2008). Celle a combustibile – Stato di sviluppo e prospettive della tecnologia. *Enea – Ente per le Nuove tecnologie, l'Energia e l'Ambiente*. Available on: http://old.enea.it/produzione_scientifica/pdf_volumi/V2008_02CelleCombustibile.pdf

Goldman, J. (2014). Comparing Electric Vehicles: Hybrid vs. BEV vs. PHEV vs. FCEV. *Union of Concerned Scientists*. Available on: <http://blog.ucsusa.org/josh-goldman/comparing-electric-vehicles-hybrid-vs-bev-vs-phev-vs-fcev-411>

Sistemi di accumulo di energia elettrica – Classificazione, caratteristiche, vantaggi e svantaggi (2014). *Energy Hunters – Consulenze e misure per energie rinnovabili*. Available on: <http://www.energyhunters.it/content/sistemi-di-accumulo-di-energia-elettrica-%E2%80%93-classificazione-caratteristiche-vantaggi-e-svanta>

Energipedia – Tutto sull'Energia\Fonti per generazione elettrica\Idrogeno. Available on: http://orizzontenergia.it/testi.php?id_testi=137#null

Quanta energia solare arriva sulla Terra? (consulted on: 16th February 2017). *Enea – Ente per le Nuove tecnologie, l'Energia e l'Ambiente*. Available on: <http://www.enea.it/it/seguici/le-parole-dellenergia/radiazione-solare/quanta-energia-solare-arriva-sulla-terra>

The Earth's Centre in 1000 Degrees Hotter than Previously Thought (2013). *ESRF – The European Synchrotron*. Available on: <http://www.esrf.eu/news/general/Earth-Center-Hotter>

Lipsky, J. (2015). Battery Market Growth is Tricky Business. *EETimes*, available on: https://www.eetimes.com/document.asp?doc_id=1327895

Cory K., Couture T., Kreycik C., Williams E. (2010), *A Policymaker's Guide to Feed in Tariff Policy Design*, National Renewable Energy Laboratory (NREL), U.S. Department of State, p. 6. Available on: <http://www.nrel.gov/docs/fy10osti/44849.pdf>

Agora – Energiewende (2015). Current and Future Cost of Photovoltaics. Available on: http://www.fvee.de/fileadmin/publikationen/weitere_publikationen/15_AgoraEnergiewende-ISE_Current_and_Future_Cost_of_PV.pdf

GSE, Gestore Servizi Elettrici. Guida al Conto Energia (2009). Available on: <http://www.alessco.it/images/downloads/2009/02/guidacontoenergia1.pdf>

<http://smartfintry.org.uk/> visited on: 9th November 2017

<https://www.rbgrant.co.uk/renewables/solar-pv-panels/> visited on: 14th November 2017

<http://planetsave.com/2015/10/08/stationary-battery-energy-storage-systems-what-will-drive-their-growth/> visited on: 14th December 2017

www.unife.it visited on: 15th December 2017

[https://www.doccity.com/it/panel- PV-composition/705 450/](https://www.doccity.com/it/panel-PV-composition/705_450/) visited on: 4th January 2018

<https://www.fotovoltaiconorditalia.it/idee/dimensioni-pannelli-fotovoltaici-2> visited on: 15th January 2018

[https://www.doccity.com/en/alternator-and-transformer/624 227/](https://www.doccity.com/en/alternator-and-transformer/624_227/) visited on: 15th January 2018

<http://www.mpptsolar.com/it/schema-funzionamento-inverter.html> visited on: 15th January 2018

<https://residenziale.viessmannitalia.it/cosa-e-come-funziona-inverter-fotovoltaico> visited on: 27th January 2018

www.puntoenergiashop.it visited on: 27th January 2018

http://www.nextville.it/Solare_fotovoltaico/454/Il_dimensionamento_ottimale visited on: 2nd February 2018

<http://www.rinnovabili.biz/calcolo-potenza-fotovoltaico.htm> visited on: 7th February 2018

<https://www.fotovoltaiconorditalia.it/idee/impianto-fotovoltaico-3-kw-dimensioni-rendimenti> visited on: 10th February 2018

<http://www.rinnovabili.it/innovazione/storage-ibrido-batterie-supercondensatori-666/> visited on: 10th February 2018

<http://www.qualenergia.it/articoli/20170612-nuovi-studi-di-mercato-sonnen-il-leader-energy-storage-europa-germania-> visited on: 10th February 2018

<https://eur-lex.europa.eu/legal-content/IT/TXT/?uri=LEGISSUM%3A128060> visited on: 16th June 2018

[https://eur-lex.europa.eu/legal-content/IT/TXT/?uri=CELEX:22016A1019\(01\)](https://eur-lex.europa.eu/legal-content/IT/TXT/?uri=CELEX:22016A1019(01)) visited on: 16th June 2018

www.gov.uk visited on: 2nd July 2018

<https://sonnen.de/stromspeicher/sonnenbatterie-eco/#product-config> visited on: 2nd July 2018

<https://www.ofgem.gov.uk/environmental-programmes/fit/fit-tariff-rates> visited on: 2nd July 2018